Scientia (Annual)
Number 1
Jan - Dec 2013
Volume 9
ISSN: 0976-8289

SCIENTIA

A National Science Journal

PUBLISHED BY
MERCY COLLEGE
PALAKKAD - 678 006, KERALA, INDIA
Govt. Aided Arts and Science College
Affiliated to University of Calicut, Accredited with 'A' grade in 3rd cycle
by the National Assessment and Accreditation Council

SCIENTIA

A National Science Journal

Volume 9 ○ Number 1 ○ Jan - Dec 2013 ○ ISSN: 0976-8289

A NATIONAL SCIENCE JOURNAL
PUBLISHED BY

MERCY COLLEGE
PALAKKAD - 678 006, KERALA, INDIA

Telephone : 0491 2541149 Fax: 0491 - 2542681
Website: http//:www.mercycollegepalakkad.com
Email: principal@mercycollegepalakkad.com

SCIENTIA

A National Science Journal Published Annually in January

Volume 9 ❍ Number 1 ❍ Jan - Dec 2013 ❍ ISSN: 0976-8289

Editorial Board

Statement of ownership and other particulars

Place of publication : Mercy College Palakkad

Periodicity of publication : Annual

Printers Name and Address : Dr. Sr. Alice Thomas, Principal
Mercy College, Palakkad

Phone : 0491-2541149

Fax : 0491-254681

Website : http//:www.mercycollegepalakkad.com

Email : scientia.mercycollege@gmail.com

Editorial

Greetings to all our contributors and readers...

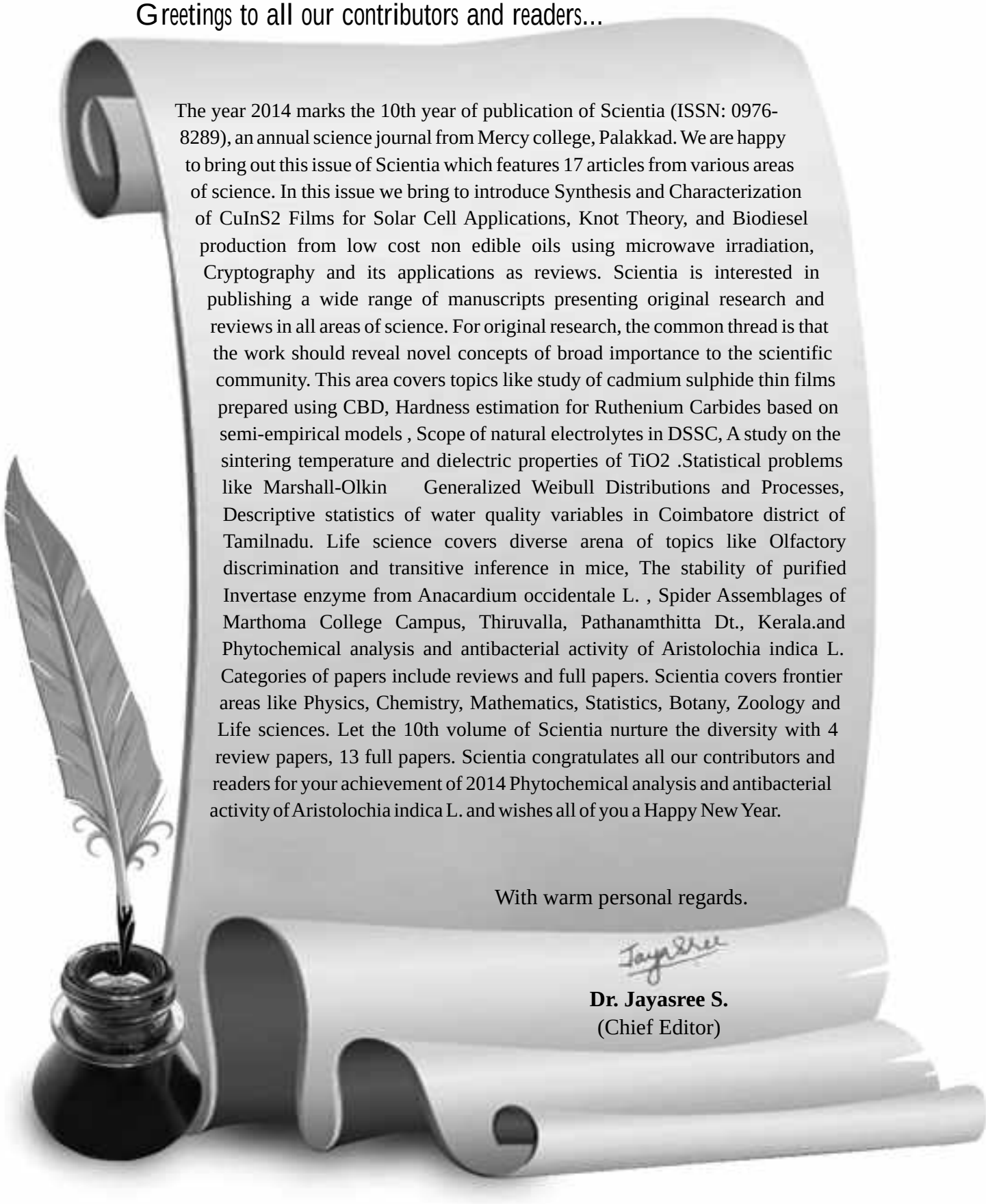

The year 2014 marks the 10th year of publication of Scientia (ISSN: 0976-8289), an annual science journal from Mercy college, Palakkad. We are happy to bring out this issue of Scientia which features 17 articles from various areas of science. In this issue we bring to introduce Synthesis and Characterization of CuInS2 Films for Solar Cell Applications, Knot Theory, and Biodiesel production from low cost non edible oils using microwave irradiation, Cryptography and its applications as reviews. Scientia is interested in publishing a wide range of manuscripts presenting original research and reviews in all areas of science. For original research, the common thread is that the work should reveal novel concepts of broad importance to the scientific community. This area covers topics like study of cadmium sulphide thin films prepared using CBD, Hardness estimation for Ruthenium Carbides based on semi-empirical models , Scope of natural electrolytes in DSSC, A study on the sintering temperature and dielectric properties of TiO2 .Statistical problems like Marshall-Olkin Generalized Weibull Distributions and Processes, Descriptive statistics of water quality variables in Coimbatore district of Tamilnadu. Life science covers diverse arena of topics like Olfactory discrimination and transitive inference in mice, The stability of purified Invertase enzyme from Anacardium occidentale L. , Spider Assemblages of Marthoma College Campus, Thiruvalla, Pathanamthitta Dt., Kerala.and Phytochemical analysis and antibacterial activity of Aristolochia indica L. Categories of papers include reviews and full papers. Scientia covers frontier areas like Physics, Chemistry, Mathematics, Statistics, Botany, Zoology and Life sciences. Let the 10th volume of Scientia nurture the diversity with 4 review papers, 13 full papers. Scientia congratulates all our contributors and readers for your achievement of 2014 Phytochemical analysis and antibacterial activity of Aristolochia indica L. and wishes all of you a Happy New Year.

With warm personal regards.

Jayasree

Dr. Jayasree S.
(Chief Editor)

SCIENTIA

A National Science Journal Published Annually in January

Volume 9 ○ Number 1 ○ Jan - Dec 2013 ○ ISSN: 0976-8289

CONTENTS

Scientia
Vol.9, No. 1, Jan - Dec. 2013, pp07-20
ISSN : 0976 - 8289

Ambily Jacob K.*, Anjaly Jacob K.[2], Anas S.[3] and S. Ananthakumar[3]

*1 Department of Chemistry, Mercy college, Palakkad-678006

2 Department of Pure and applied chemistry Cochin university

3 Materials DivisionNational Institute for Interdisciplinary Science and Technology,

CSIR Trivandrum-695019, Kerala, India

Abstract

As the environmental and energy resource concern, great efforts have been put in the development of renewable energy resources, among which photovoltaic solar power is the most desirable one and holds great potential and promise. The silicon supply shortage arising from the recent boom in the demand for photovoltaic modules, thin-film photovoltaic modules using $CuInS_2$ are entering the market in significant quantities. Thin-films have the potential to revolutionise the present cost structure of photovoltaics by completely eliminating the use of the expensive silicon wafers that alone account for 40-50% of total module manufacturing cost.

Key Words: Solar Cell; $CuInS_2$; Semiconductors; Optical properties; Thin film

Introduction

The fossil fuels and nuclear power are the main sources of energy in today's energy system and they supply about 78% of the energy demand. It has also been recognized that a massive consumption of fossil fuels in order to fulfil the present energy demands has a negative impact on the environment. They emit tons of harmful gases to the atmosphere every second. This many lead problems being faced today as ozone depletion. In addition, there has also been a great concern on the role of fossil fuels in global warming. Intergovernmental Panel on Climate Change observed that the global temperature is increasing since 20th century. This is due to the increasing concentrations of greenhouse gases in the atmosphere resulting from human activity, such as fossil fuel burning and deforestation. This is the reason why the attention is turning to the renewable energy sources.

Sun provides a reliable, sustainable and long-term supply of energy, in contrast to conventional resources such as coal and fossil fuels. All wind, fossil fuel, hydro and biomass energy have their origins in sunlight. Solar energy is rapidly becoming one of the most promising renewable energy sources available to us. Direct harvesting of the immense and never-ending power brought by the sun is not new, this was the elegant way of generating electricity in satellites and space stations. Today, Germany generates 50 % of its electric power from photovoltaic (PV) energy during mid-day hours on a sunny day[1].

First generation solar cell consist of high quality and single junction silicon solar cells. Silicon based solar cells have an 85 % market share and absolutely dominant technology in photovoltaic (PV) devices[2]. The

**Corresponding author, Email: taniyapalayoor@gmail.com*

ISSN : 0976 - 8289

manufacturing costs of single **Crystalline Silicon** based solar cell are still relatively high. Because they are cut from cylindrical ingots, do not completely cover a square solar cell module without a substantial waste of refined silicon[3]. Although single-crystalline Si-based solar cells are successfully used to harvest solar energy, inexpensive production of photovoltaic (PV) devices at a cost comparable to the energy production cost of fossil fuels has become a critical issue to meet the global energy crisis[4].

Low cost solar cells can be synthesized by reducing the production costs. Photovoltaic designs based on thin film nanostructure semiconducting materials offer an interesting route towards inexpensive, reliable, solar-based renewable power. These materials are applied in a thin film to a supporting substrate such as glass or ceramics reducing material. Now a days solar cells based on thin film semiconductors in the nano level are quite common[5]. **Figure 1.**shows the schematic drawing of the TiO_2/ $CuInS_2$ (CIS) nanostructure solar cell. It consist of nanostructured n-type TiO_2 and p-type $CuInS_2$ (CIS). n- type semiconductor was deposited on transparent conductive glass slides(TCO). Like most chalcopyrite solar cells, an interfacial monolayer is typically required between the n-type and p-type regions to control the effective charge separation at semiconductor/absorber interface. In the figure, a thin layer of In_2S_3 interface layer is used between the TiO_2 and CIS layers[6].

The operating principle of the nanostructured TiO_2/CIS solar cell is analogous to a traditional thin-film solar cell. Photons in sunlight hit the solar panel and are absorbed by semiconducting material. Electrons

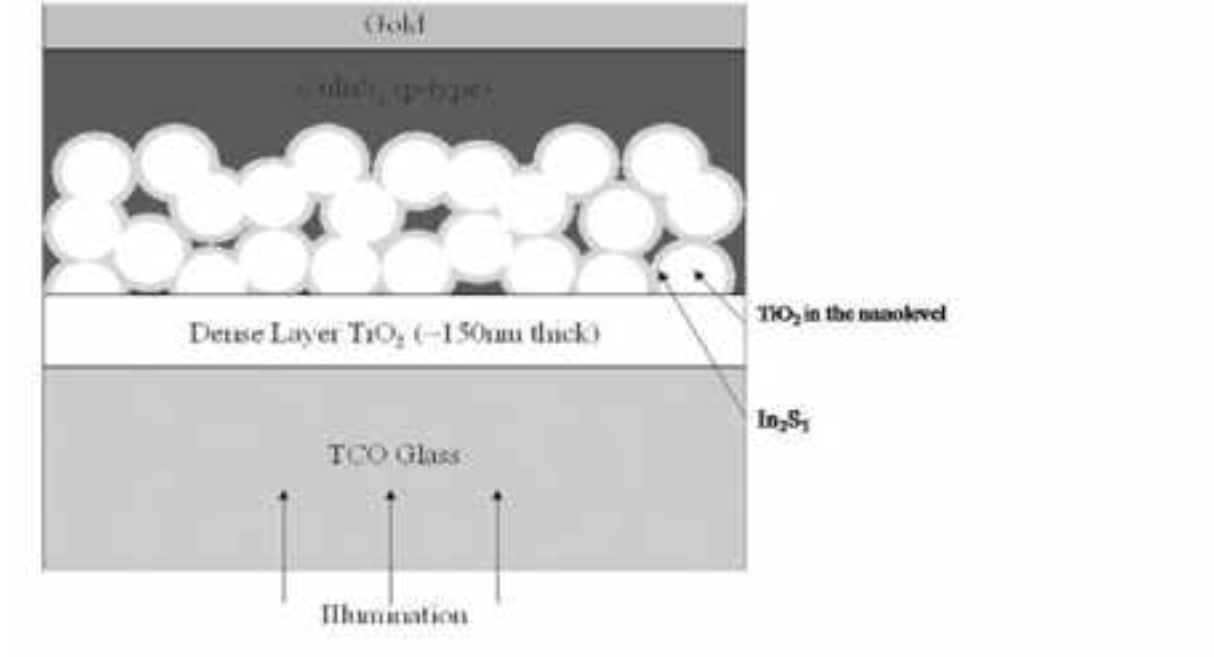

Fig. 1. Shows the schematic diagram of the TiO_2/CIS nanostructured solar cell

*Corresponding author,Email:ambilykj@gmail.com

are excited from their atom and allowing them to flow through the external circuit to produce electricity.

$CuInS_2$

Nanocrystalline inorganic semiconductor absorbers can be prepared in a relatively simple way and they have many other attractive advantages, such as tuneable band gaps, high extinction coefficients, large intrinsic dipole moments etc[7]. The most commonly used inorganic absorbers are II- VI, III- V, and I- III- IV semiconductors, such as CdSe, CdS, PbSe, PbS, InAs, Bi_2S_3, and $CuInS_2$ (copper indium sulfide, CIS). In particular, $CuInS_2$ is of great interest because of many attractive features including (i) nontoxicity (ii) a high absorption coefficient (6×10^5 cm- 1) and a direct band gap of 1.5eV well matched to the solar spectrum and (iii) appreciable photo electrochemical stability in polysulfide electrolytes, which are widely used as hole-transport materials. Several approaches have been employed to deposit inorganic photosensitizers on TiO_2 films, including chemical bath deposition, successive ionic layer absorption reaction (SILAR), electrophoresis deposition, electrochemical deposition, spray pyrolysis, sputtering method, and thermal decomposition etc [8, 9, 10].

Different methods for the preparation of $CuInS_2$ thin film

1. Preparation of $CuInS_2$-sensitized TiO_2 electrodes using SILAR process.

A dense film of anatase TiO_2 (100 nm thick) is deposited onto transparent conducting oxide (TCO) glass substrates. On the top of this compact layer, a transparent mesoporous TiO_2 film composed of 20 nm was prepared using the doctor blade method. The films were then sintered at 450°C for 30 minutes. The electrodes were sensitized with CIS via in situ deposition of In_xS followed by Cu_yS. The precursor solutions for In, Cu, and S were 0.01M CuCl, 0.075M Na_2S, and 0.1M $InCl_3$ aqueous solutions, respectively.TiO_2 electrodes were immersed in aqueous solution of $InCl_3$ followed by Na_2S solution .This process was repeated for several time to form In_xS. Cu_yS layer was deposited by immersing above slides into aqueous solution of CuCl followed by Na_2S solution.The sensitized electrodes were annealed at low pressure and 550°C in sulfur atmosphere .

2. Deposition of $CuInS_2$ sensitizers on TiO_2 photoanodes using dip coating

Mesoscopic TiO_2 films were prepared by screen printing of a TiO_2 slurry on the conducting glass slides. TiO_2 photoanodes was dipped in mixture of solution (1) 0.10M $In(NO_3)_3$, (2) 1.25×10- 3 M $Cu(NO_3)_2$, and (3) 0.135M Na_2S in a 50 mL solvent of methanol. Then electrodes were rinsed with pure methanol and dried with nitrogen gas. This procedure was repeated for six times until the desired $CuInS_2$-based TiO_2 photoanodes were created. The sensitized electrodes were annealed at 550°C in sulfur atmosphere.

3. Thin film deposition of $CuInS_2$ using spray pyrolysis.

A dense film of anatase TiO_2 (100 nm thick) is deposited onto transparent conducting oxide glass substrates by using spray pyrolysis. Nanocrystalline anatase-TiO_2 coating is applied using the doctor-

blade technique. After doctor blading, all samples are annealed at 450 ?C for 6 h in air.The samples are then coated with a spray-deposited n-type In_2S_3. All samples are spray coated with p-type $CuInS_2$.

4. Preparation of $CuInS_2$ thin film using chemical bath deposition

The syntheses of the CuInS2 thin films were performed with three steps. At the first step copper sulfide was deposited on the conducting glass substrates at 70 °C using 5mL of 0.5 mol/L $CuSO_4$ and 50 ml of 0.2 mol/L $Na_3C_6H_5O_7$. Then the indium sulfide thin film was deposited on the Cu_xS thin films at 85 °C using 20 ml of 0.2 mol/ L indium chloride solution and 100 ml of 0. 2 mol/ L thioacetamide solution. The deposition of Cu_xS and In_2S_3 Finally, the $CuInS_2$ thin films were synthesized by heating the Cu_xS andIn_2S_3 in sulfur atmosphere.

5. Preparation of $CuInS_2$ nanostructures using sonochemical method

The copper salicylate [$Cu(Hsal)_2$] precursor was prepared from reaction of 1 mmol of copper sulphate penta hydrate and 2mmol of sodium salicylate. $CuInS_2$ nanoparticles was prepared by the reaction of $Cu(Hsal)_2$ and $InCl_3$ with sulfur source in propylene glycol (PG) as solvent. 50 mg of $Cu(Hsal)_2$ and 20 mg of $InCl_3$ were dissolved in 60 mL of PG and was irradiated under ultrasound waves. Different sulphur sources (2mmol) such as ;sodium sulphite ($Na_2S_2O_3$), thiourea (Tu), thioacetamide (TAA), thiosemicarbazide (TSC), L cysteine (L-Cyst) and carbon disulfide (CS_2); were added dropwise to the solution. The black precipitate was washed with ethanol and deionized water. The product was dried at 60 °C for 3 h under vacuum. The precipitates were annealed under argon atmosphere at 450 °C for 2 h. The annealing converted mixture of In2S3 and CuS to $CuInS_2$.

6. Synthesis of $CuInS_2$ nanostructures using colloidal method

Copper (I) acetate (01. mmol), indium(III) acetate (0.1 mmol) and myristic acid (0.4 mmol), together with 6.2cm^3 of 1-octadecene (ODE) were introduced into a two-neck reaction flask. The flask was immersed in an oil bath at 170 °C and maintained at this temperature for 30 min under an Ar flow. Then, the flask was heated to 300 °C after attaining the temperature, 2 ml of ODE containing bis(tri- methylsilyl) sulphide TMS (0.30 mmol) was injected in order to obtain $CuInS_2$. The reaction mixtures were kept at 300 °C for 30 min and then allowed to cool spontaneously to room temperature. The obtained precipitates were washed three times with methanol and then dispersed in benzene.

Analysis of Some properties of CuInS2 thin film solar cell

The X-ray diffraction (XRD) pattern for the TiO_2/CIS film was recorded and analysed for the identification of the crystal structure. Figure 2 depicts XRD pattern of the TiO_2/CIS film obtained after annealing at 550 °C. Besides those existing interfacial monolayer peaks from SnO_2 (2θ: 26.6°, 33.8°, 37.8°,51.7°, 61.8°, 65.8°; from FTO substrate) and TiO_2 film (2θ:25.3°, 37.8°, 48.0°), the diffraction peaks at 27.8°,32.38°,46.5° and 55.1° are assigned to (112), (200), (204)/(220), and (312)/(116) planes of CIS,

respectively. The strong and sharp diffraction peaks confirm good crystallinity of the product. Pattern of the $CuInS_2$ show a pure tetragonal structure with suitable agreement to literature value Space group: 1-42d, lattice constants: *a*=5.5170, *b*=5.5170 and c=11.0600. The crystallite size **(*D*)** of the as-prepared $CuInS_2$, was calculated using the Debeye–Scherrer equation (1),

Where β is the breadth of the observed diffraction line at its half intensity maximum, K is the shape factor, which usually takes a value of abo [illegible] th of X-ray source used in XRD.

Morphology of the TiO_2 film was analysed by Scanning electron microscopy. Figure 3shows the SEM image of TiO_2 . SEM images confirm the formation of a dense TiO_2 layer on FTO glass, and this TiO_2 layer

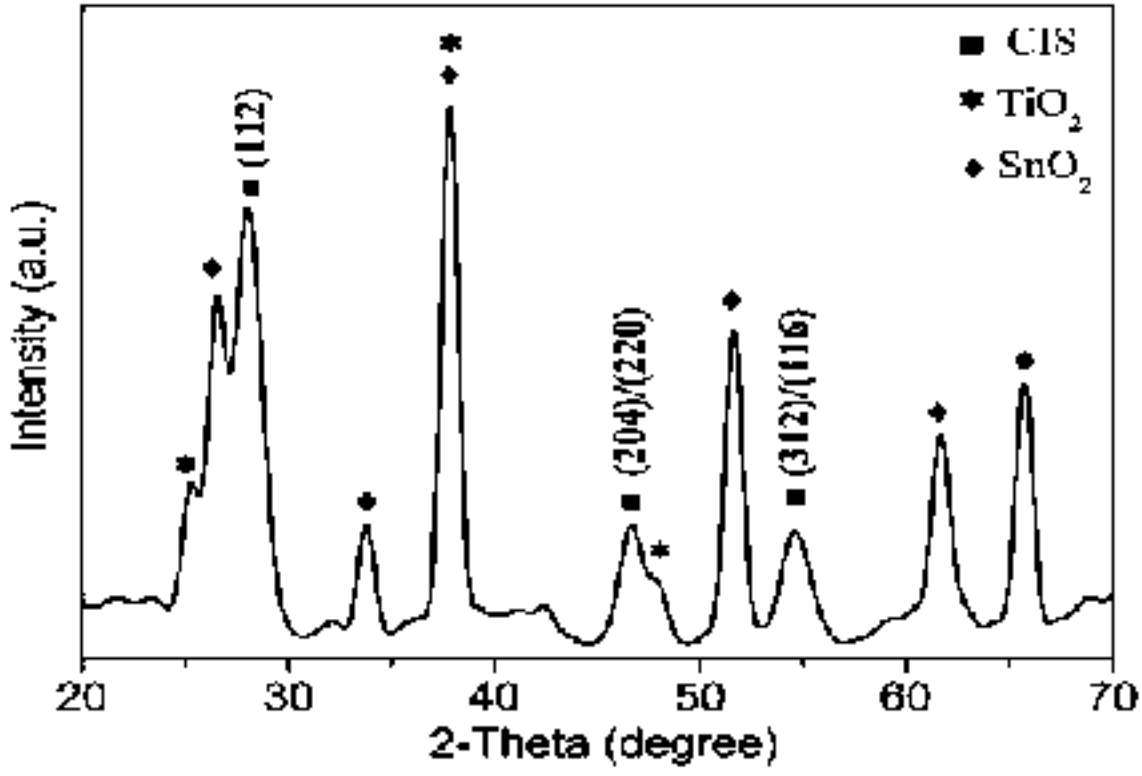

Fig. 2. XRD pattern of TiO_2/CIS film after annealing at 550 °C

has a thickness of about 300 nm. The particles are homogenously distributed in film. Figure 4 gives the typical morphologies of CIS films prepared with different $InCl_3$ concentration. When $InCl_3$ concentration is low, a large amount of high-ordered potato chip-shaped CIS nanosheet arrays are densely packed and uniformly covered over the entire surface of FTO/nanoporous-TiO_2 film (Figure 4a,c). More detailed nanostructure about CIS film can be observed using high-magnification SEM images (Figure 4b,d), where individual CIS nano sheet displays a crooked shape with a thickness of approximately 10 nm and length of approximately 2 μm. As $InCl_3$ concentration increased CIS flower-shaped superstructures with an average

diameter of 3 μm spread over the whole

FTO/compact-TiO2/nanoporous-TiO2 film (Figure 4e).

Fig. 3. SEM images of nanoporous TiO_2 film: (a) cross-sectional, (b) low-, and (c) high-magnification SEM images of the surface

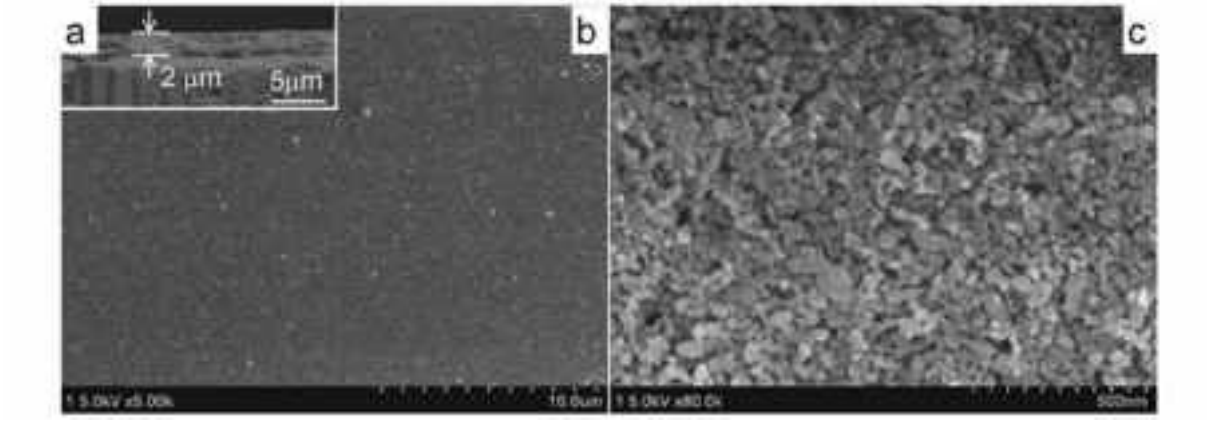

Fig. 4 SEM images of CIS layer on TiO_2 film with different $InCl_3$ concentration:
a,b at low; c,d Medium ; e,f high concentration .Photoluminescence (PL) measurement of $CuInS_2$

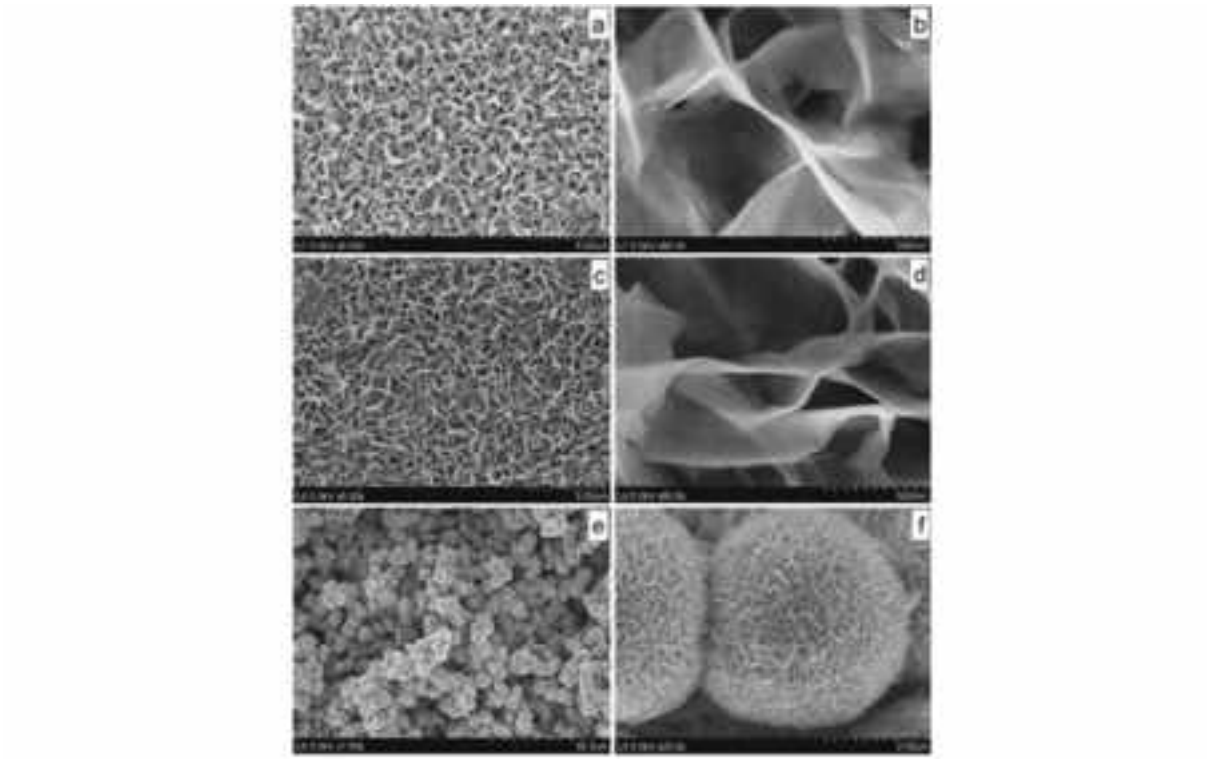

nanoparticles at room temperature with excitation wavelength at 418 nm was recorded. The PL spectrum consists of one strong peak at 554 nm that can be ascribed to a high level transition in $CuInS_2$

semiconductor crystallites. It is reported that this kind of band edge luminescence arises from recombination of trapped electron–hole pairs.

Mechanism

The In^{3+} and Cu^{2+} ions reacted with the S^{-2} ions to form the sulfide compounds of CuS and In_2S_3 according to Eq. (1) and (2). The reaction for the formation of stoichiometric $CuInS_2$ during annealing process might be given in Eq.(3).

$$Cu^{2+} + S^{2-} \rightarrow CuS \qquad \text{Eq. (1)}$$

$$2In^{+3} + 3S^{2-} \rightarrow In_2S_3 \qquad \text{Eq. (2)}$$

$$2CuS + In_2S_3 \rightarrow 2CuInS_2 + S \qquad \text{Eq. (3)}$$

Conclusion

In summary, an in situ growth of CIS nanocrystals on the mesoporous TiO_2 films has been demonstrated by various methods. Morphology of CIS was analysed by SEM image .crystalline nature was studied by using XRD analysis. Optical properties of CIS was analysed using PL spectra.

Acknowledgement

Anjaly Jacob K acknowledges Council of Scientific and Industrial Research (CSIR) for the financial support.The authors are also greateful to K.V. Mahesh, M.P. Prashanth ,S.Shankar for the fruitful discussion .

References

1. Ryan O'Hayre, Marian Nanu, Joop Schoonman and Albert Goossens, 2007. A parametric study of TiO_2/$CuInS_2$ nanocomposite solar cells: how cell thickness, buffer layer thickness, and TiO_2 particle size affect performance. *J. Nanotechnology*. 18, 55702-09.
2. Castro S.L, Bailey S.G, Raffaelle R.P, Banger K.K, Hepp A.F, 2003. *Chem. Mater* **15**, 3142.
3. Xueqing Xu, Qingcui Wan, Chunyan Luan and Fengjiao Mei Qian Zhao, 2013. Fabrication of $CuInS_2$-Sensitized Solar Cells via an Improved SILAR Process and Its Interface Electron Recombination. *Appl. Mater. Interfaces*. 5, 10605- 10613.
4. Jia-Yaw Chang, Jie-Mo Lin, Li-Fong Su, and Chia-Fu Chang, 2013. Improved Performance of CuInS2 Quantum Dot-Sensitized Solar Cells. *Appl. Mater. Interfaces*. 5, 8740- 8752.
5. Bonil Koo, Reken N. Patel and Brian A. Korgel, 2009. Wurtzite-Chalcopyrite Polytypism in $CuInS_2$ Nanodisks. *Chemistry of Materials* 21, 9, 1962-1966.
6. Fabrice M. Courtel, Royston W. Paynter, Benoıˆt Marsan and Mario Morin, 2009. Synthesis, Characterization, and Growth Mechanism of n-Type $CuInS_2$ Colloidal Particles. *Chem. Mater.* 21, 16, 3752 – 62.
7. Zhaohui Han, Yitai Qian, Shuhong Yu, Kaibin Tang, Huaqiao Zhao, and Neng Guo, 2000. Hydrothermal Evolution of the Thiourea-Cerium(III) Nitrate System:Formation of Cerium Hydroxycarbonate and Hydroxysulfate. *Inorg. Chem. 39*, 4380-

4382.

8. Stephanie L. Castro, Sheila G. Bailey, Ryne P. Raffaelle, Kulbinder K. Banger, and Aloysius F. Hepp. 2004. Synthesis and Characterization of Colloidal $CuInS_2$ Nanoparticles from a Molecular Single-Source Precursor. *J. Phys. Chem. 108*, 12429-12435.
9. *Ryan O'Hayre*, *Marian Nanu*, *Joop Schoonman*, *Albert Goossens*, *Qing Wang*, and *Michael Grätzel. 2006.* **The Influence of TiO_2 Particle Size in TiO_2/$CuInS_2$ Nanocomposite Solar Cells.** *Adv. Funct. Mater. 16*, 1566–1576.
10. Tang hui-x iang , Yan mi, Zhang hui, Ma xiang-y ang , Wang lei and Yang de-ren. 2004. Preparation and Characterization of $CuInS_2$ Thin Films for Solar Cells by Chemical Bath Deposition. *Chem. Res. Chinese u.* 21, 2, 236 239.

Introductory knot theory

Asha Sebastian*

Department of Mathematics, Mercy College, Palakkad- 678007

Abstract

Knots are subsets of R^3, homeomorphic to the circle. Some of the basic concepts in knot theory are introduced. A discussion on basic definitions of knots and links has been made along with the brief history of knots. Basic questions in knot theory are posed and a study on some of the available knot invariants is made. Applications of knot theory in physics, molecular biology and synthetic chemistry is quite interesting.

Keywords: Knot Theory, Knot Invariants

Introduction

Knots are familiar objects which are appearing in various forms throughout our daily life. From tying the shoe laces to wrapping the packages it shows up. Modern knot theory is the tale of a magnificent failure. To create an exact model for the elusive atomic theory, P.G.Tait created a table of knots on the request of Lord Kelvin. They proposed a model of atom which was knotted vortex tubes in ether in 1860. Their model was incorrect as Michaelson-Morley experiment denied the existence of ether. By the end of 19th century Mendeleev proposed the modern periodic table and knots lost its significance. By the mean time mathematicians were fascinated by knots and a century of work on mathematical theory of knots followed. The knots again caught the attention of vibrant researchers when Jones polynomial was introduced in 1985. Biochemists discovered knotting in DNA and chemists realised that it might be possible to create knotted particles. A mathematical field existing from Neolithic age and which lost its momentum many times throughout the history has turned out to have applications in quantum mechanics, molecular biology and chemistry. A study is made into the mysterious, aesthetic and vibrant theory of knots.

A knot, mathematically speaking, is a closed curve sitting in three dimensional space that does not intersect itself. Intuitively if we were to take a piece of string, cord, or the like, tie a knot in it and then glue the loose ends together, we would have a knot. It should be impossible to untangle the knot without cutting the string somewhere. The use of the word 'should' here is quite deliberate, however. The central problem of knot theory is to distinguish the equivalent and the non-equivalent knots from a collection of knots. Given any knot how do we tell that they are really knotted? What if, they are not even knotted and we have been asked to determine its properties? Is there any specific algorithm to help us?

**Corresponding author,Email: ashasebastian13@gmail.com*

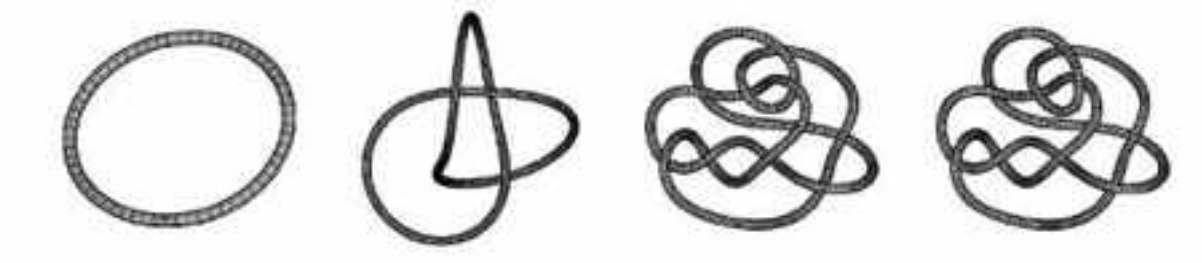

Fig. 1. Two different knots

It might be surprising to find out that the four images in Fig.1 only show two different knots. The question is which ones are the same? Are three of them the same and one different, or are there two pairs of identical knots? A better question is how can we work out which are the same and which are different? The biggest problem however, with both these methods and others as well, is that they are subject to circumstance. Maybe we can see the answer, or maybe we cannot. Maybe we are clever or lucky enough with the string to get an answer, or maybe we are not. There is no mathematical pattern to this, just circumstance. Furthermore, if we have two knots and, using whatever techniques we find appropriate, not succeed in turning one into the other, then we have no useful information. We have not shown that the two knots are different, but only that we cannot make them be the same. This puts a new light on our previous questions of telling knots apart. We at least have a chance of showing that two knots are the same, but how do we conclusively show that two tangled messes can never be manipulated to be the same?

We will formalize how we describe and present (i.e., draw) knots and how we manipulate them. But most importantly, we will introduce the tools that allows us to show that knots are different, the knot invariants, and will examine and discuss several of these.

Brief history of knot theory

Why should anyone be interested in knots? What is so important about being able to tell whether a tangled-up loop of strings is truly tangled or can in fact be untangled without cutting and gluing?

Much of the early interest in knot theory was motivated by chemistry. In the 1880s, it was believed that a substance called ether pervaded all of space. In an attempt to explain the different types of matter, Lord Kelvin hypothesized that atoms were merely knots in the fabric of this ether. Different knots would then correspond to different elements. This convinced the Scottish physicist Peter Guthrie Tait that if he could list all of the possible knots, he would be creating a table of the elements. He spent many years tabulating knots. At the same time an American mathematician named C.N.Little was working on tabulation for knots. Unfortunately Kelvin was wrong. In 1887, the Michelson-Morley experiment demonstrated that there was no ether to knot. A more accurate model of atomic structure appeared at the end of the nineteenth century and chemists lost interest in knots for the next 100 years. But, in the mean time, mathematicians

had become intrigued with knots. A century of work on the mathematical theory of knots followed. Interestingly enough, in the 1980s, biochemists discovered knotting in DNA molecules. Concurrently, synthetic chemists realized it might be possible to create knotted molecules, where the type of knot determined the properties of molecules. A mathematical field that was born out of a misguided model for atoms has turned out to have several significant applications to chemistry and biology.

Knots

Definition 1

A knot K $\subset$ R3 is a subset of points in R3 which is homeomorphic to circle

Examples

Fig.2. Unknot and Trefoil Knot

We know that knots are three dimensional objects and it is always difficult to model. So while looking at the knots we use a two dimensional image to model. Inorder to learn them, we have to replicate them to paper. One solution is that we can project them. But if there are multiple points it will put the learner into a dilemma. Let's restrict this multiple point being double, but not more than that. Such a projection is called regular projection. Here we rule out all the questions which may stop us from making an effective model on a two dimensional space. Knots have points where it crosses each other. Some strings go over the other and while some go under. Inorder to incorporate this information, we formulate knot projections.

Definition2: Let us denote by P the map that projects the point (x, y, z) in R 3 onto the point (x, y, 0) in the x-y plane, Fig.3

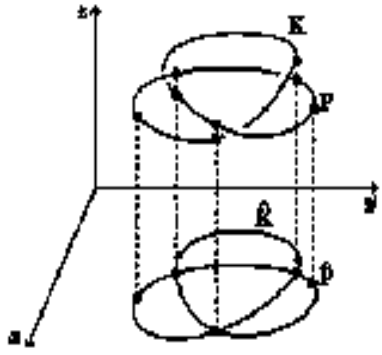

Fig.3. Knot Projection

If K is a knot (or link), we shall say that $P(K) = \hat{K}$ is the projection of K.

A projection $\hat{K}$ that satisfies the conditions below is said to be a regular projection:

(1) $\hat{K}$ has at most a finite number of points of intersection.

(2) If Q is a point of intersection of $\hat{K}$, then the inverse image, $P^{-1}(Q) \cap K$, in K has exactly two points. Fig. 4(a), it cannot be a multiple point of the kind shown in Fig.4(b).

(3) A vertex of K (the knot considered now as a polygon) is never mapped onto a double point of K. In the two examples in Fig.4(c) and (d), a polygonal line projected from K comes into contact with a vertex point(s) of K, so both of the cases are not permissible.

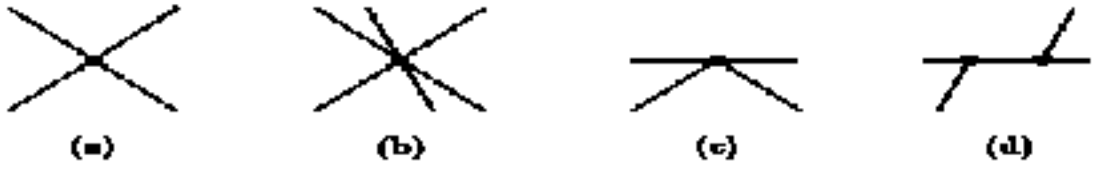

Fig.4. Crossings in a knot projection

Definition [2]:

A knot has an irregular projection if it has any edges parallel to the z-axis, if it has three or more points lying above each other, or any vertex lying above or below another point of K as in Fig.5. Thus, a regular projection of a knot consists of a polygonal circle drawn in the plane with only transverse double points as self-intersections.

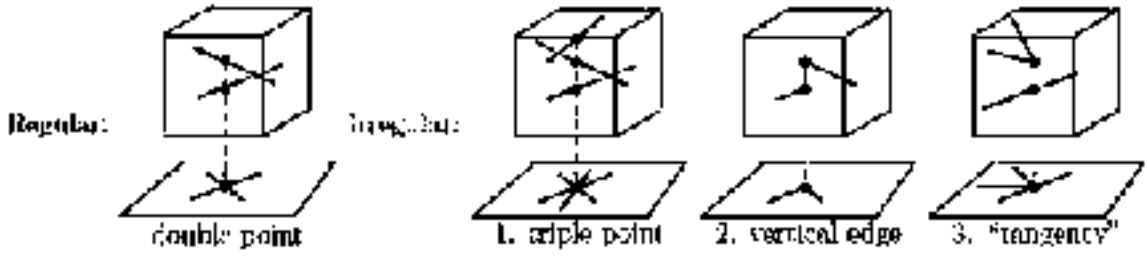

Fig.5. Regular and irregular projections

Crossings

Note the break in some of the lines in the trefoil projection in Fig.6. These are not, in fact, breaks in the string making up the knot, but a way of showing that the string goes under another string. This is how we differentiate between the string that is above and the string that is below. Such a point on the knot is known as a crossing. So the trefoil projection shown above has, as the name might have implied, three crossings. Each entire unbroken line of a projection is known as a strand of the knot projection.

Fig.6. Regular projection of unknot and trefoil knot

See Fig.7 for some examples of strands. The strands are marked in grey, but they are not the only strands of the projection in question.

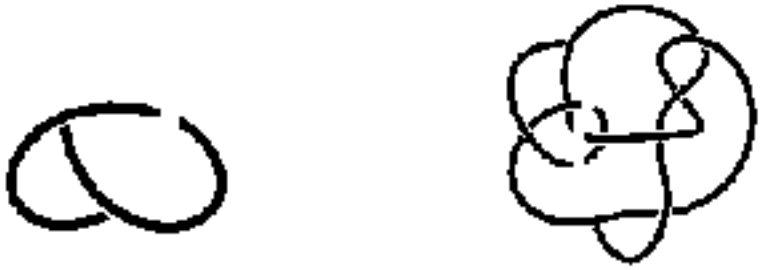

Fig.7. Strands in a regular projection

If we were to trace our finger around the projection in a single direction, we would pass through every crossing twice, once by tracing the uppermost string (the overstrand) and once, later on, when tracing the undermost string (the understrand). When tracing the knot this way, we call a crossing an overcrossing if we are traveling on the overstrand, and an undercrossing if we are traveling on the under strand.

Reidemeister moves

If we are given a ball of loops, how do we say that it is in fact knotted? A German mathematician, Kurt Reidemeister worked on it and found three basic moves which were named after him as Reidemeister moves. Any equivalent knots are obtained after applying Reidemeister moves on the other. One of the fundamental results in knot theory is that two equivalent knots are related by a sequence of Reidemeister moves i.e., when two knots are equivalent, one can be deformed to other using these moves. There are three moves- twist, poke and slide, Fig 8. In twist move, we twist the knot and it doesn't change the knot whereas in poke move we move one strand over/under the other. Poke move increases or decreases the number of crossings by 2. The slide move is to slide a strand completely over the other.

Definition [3]

I. Twist and untwist in either direction.

II. Move one strand completely over another.

III. Move a strand completely over or under a crossing.

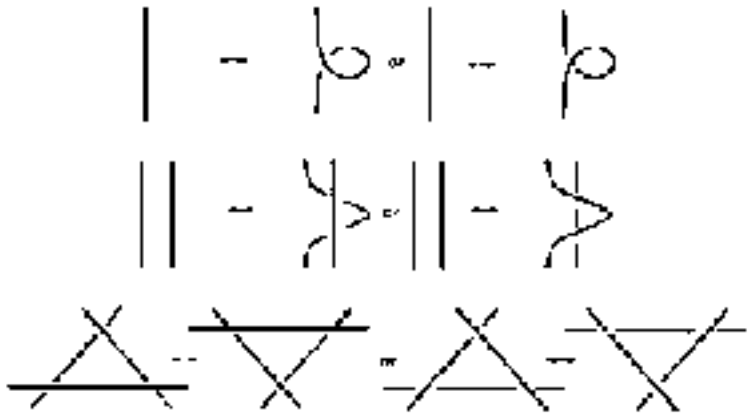

Fig. 8. Reidemeister moves

In each of these examples, it is assumed that the knot projection presented is only a small part of a larger projection, and that the rest of that projection remains unchanged. In 1926, the German mathematician Kurt Reidemeister proved that if we have two distinct projections of the same knot, we can get from one projection to the other by a series of Reidemeister moves and planar isotopies.

Links

Definition2: A link is a finite disjoint union of knots: $L=K_1 \cup K_2 \cup \ldots \cup K_n$ Each knot Ki is called a component of the link. The number of components of a link L is called the multiplicity of the link, and is denoted by μ

A link is trivial if all of its components are trivial knots and they are 'unlinked'. A knot will be considered a link of one component. Examples of hopf link with two components and Borromean link with three components are given in Fig.9.

Fig. 9. Hopf Link and Borromean Link

Knot invariants

Knot invariant is a property of a knot which does not change even if the knot is deformed. We know that equivalent knots are obtained only through these moves. So if we show that an invariant does not change on any Reidemeister move, it implies that the property remains invariant on all equivalent knots. If the property changes on any Reidemeister move, then it is not an invariant. This is the significance of Reidemeister moves.

Linking number

One of the simplest invariants that can actually be computed easily is the linking number of an oriented link. It is computed by using a diagram of the link, so we then have to use Reidemeister's theorem to prove that it is independent of this choice of diagram, and consequently really does depend only on the original link..

Definition2:

Assume that we have a link with k components. We assign the value ±1 at the crossing where the components cross each other ignoring the crossings of components with it. Linking number is half the total sum of values assigned at the crossings. The value +1 will be assigned if the under strand lines up with the over strand when rotated clockwise and -1 if it lines up only when it's rotated anticlockwise, Fig.10

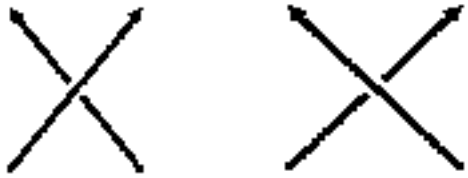

Fig.10. Positive crossing (+1) and Negative crossing(-1)

Example

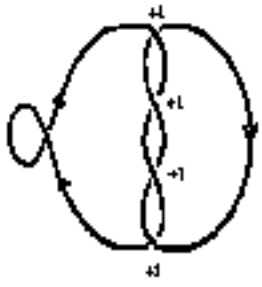

Fig. 11. Evaluation of linking nuber

Linking number= $\frac{|+1|-|+1|}{2}$ =2. (Fig.11)

We consider the effects of the three Reidemeister moves. Twist moves also do not contribute to the linking number, since they affect only self crossing of two components of the link, and these are not counted.

Tricolourability

Till now we have not proved that there is other knot besides unknot. To prove the existence of knots we use the concept of tricolouring. It is a combinatorial colouring method whose generalisation is p-colouring. Tricolouring is a method of colouring the strands in such a way that either there are three colours near the

crossing or only one colour is used. Any colouring of knot projection which meets these criteria is called valid tricolouring. This is illustrated below in Fig.12

Fig.12. Valid tricolouring

Any colouring of a knot projection that meets these criteria is called a valid tricolouring or just a tricolouring. An example of a tricolouring of the trefoil knot is shown below.

Fig. 13. A Tricolouring of Trefoil

Some thoughts should lead us to the conclusion that the definition given above allows any knot at all to be tricolourable, since we can colour every strand of a given knot the same colour and have a valid tricolouring. In order to prevent this, an extra stipulation is added that at least two colours must be used for a knot to be called tricolourable.

Applications

Ever since the late 20th century, knot theory has had many applications to the applied sciences. It was only in the 1980s, a century after Kelvin's hypothesis proved false, that scientists' interest in knot theory was renewed. Geneticists discovered that the structure of deoxyribonucleic acid (DNA) was that of a double helix, with the twists being the result of enzymes at work, and that the DNA structure could vary from one organism to another, resulting in a different type of knot altogether . Molecular biologists apply knot theory and other branches of mathematics in their studies. In 1990, Vaughan Jones established a relation between knot theory and statistical mechanics, which is a branch of physics mainly dealing with subatomic particles, specifically between knot invariants and quantum field theory. A 1989 New York Times article describes another application of knot theory: In July of 2009, Michael Atiyah, a mathematician at Oxford University in England, “asserts that the mathematics of the Jones polynomial is

exactly the mathematics of elementary particle physics". Edward Witten, a particle physicist at Princeton, investigated Atiyah's assertion and found the relation to be indeed true, meaning that "knot theory results can apply even when there is no knot at all". Judging from these recent applications of knot theory, it is logical to infer that there may be more applications waiting to be discovered[4].

Conclusions

Knot theory remains vibrant and mysterious till date. Effective classification of knots and an easily calculated complete invariant are the major questions occurring during the study of knots. Even though we have many braid invariants, topological invariants, numerical invariants and polynomial invariants, they are insufficient to meet the requirements. The journey of knots from knotted vortices in ether to Jones polynomial was with many sudden brainstorms, dazzling advances and dramatic failures, but still it was motivated by intellectual curiosity. The story of its development and the diversity of topics which came through its course is always a charm for the researchers around the globe.

Acknowledgement

I am thankful to my colleagues in Department of Mathematics, Mercy College, Palakkad. Let me extend gratitude to my supervisors Dr.Sunil Jacob John (NIT Calicut) and Dr.Rama Mishra (IISER Pune).

References

1. Cromwell P., 2004, *Knots and Links*, Cambridge University Press.
2. Crowell R.H. and Fox R.H., 1977, *Introduction to Knot Theory*, Springer-Verlag, NY.
3. Roberts J., 15 March 1999, *Knots Knotes*, Lecture notes from Edinburgh course Maths 415.
4. Adams C.C., 2012, *The knot book- An elementary introduction to the mathematical theory of knots*, American Mathematical Society.
5. Adams, Colin C. and Robert Franzosa., 2008, *Introduction to Topology: Pure and Applied. Upper Saddle River*, Pearson Prentice Hall.
6. Murasugi K.,1996, *Knot Theory and Its Applications*, translated by Bohdan Kurpita, Birkh¨auser Boston.
7. http://mathworld.wolfram.com/Knot.html
8. http://en.wikipedia.org/wiki/Knot_theory
9. A List of Approachable Open Problems in Knot Theory.
10. http://www.williams.edu/Mathematics/cadams/knotproblems.html

Scientia
Vol.10, No. 1, Jan - Dec. 2014, pp30-37
ISSN : 0976 - 8289

Biodiesel production from low cost non edible oils using microwave irradiation: A Review

Harsha Paul*and Taniya Antony

Dept of Chemistry, Mercy College, Palakkad-678006, Kerala.

Abstract

Due to rapid development, the worldwide demand for biodiesel as an alternative to the conventional transport fuel, petro diesel for diesel engines, is increasing because of the limited reserves of fossil fuels, increasing prices of crude oils and environmental concerns. The use of edible vegetable oils for biodiesel production is not feasible as the demand for edible vegetable oils is tremendously increasing. Prime importance is given to alternative biodiesel feed stocks like non-conventional seed oils as these oils will not cause food crisis leading to economic imbalance. In this review paper, an attempt is being taken to identify non-conventional oils with their oil contents for future biodiesel industries. Recent laboratory scale microwave applications in biodiesel production proved the potential of the technology to achieve superior results over conventional techniques. Short reaction time, cleaner reaction products, and reduced separation-purification times are the key observations reported by many researchers. This review also provides principles and practices of microwave energy technology as applied in biodiesel feedstock preparation and processing.

Key Words: Biodiesel; non edible-oils; transesterification; microwave irradiation.

Introduction

The worldwide worry about the protection of environment and the conservation ofnon-renewable natural resources, has given rise to alternate development of sources of energy as substitute for traditional fossil fuels. The major part of all energy consumed worldwidecomes from fossil sources (petroleum, coal and natural gas). However, these sources arelimited and will be exhausted in the near future. Thus, looking for alternative sources of newand renewable energy such as hydro, biomass (better sources of energy), wind, solar,geothermal, hydrogen and nuclear is of vital importance. Alternative new and renewable fuelshave the potential to solve many of the current social problems and concerns, from airpollution and global warming to other environmental improvements and sustainability issues[1].

Manufacturing biodiesel from used vegetable oils and non-edible is relatively easy and possesses many environmental benefits. The use of vegetable oils as frying oils produces significant amounts of used oils which may present a disposal problem. The use of waste cooking oils and non-edible oil for biodiesel production has the advantage of their low price. Used vegetable oil is described as a 'renewable fuel' as it does not add any extra carbon dioxide gas to the atmosphere, as opposed to fossil fuels, which cause changes in the atmosphere[2].

The application of biodiesel to our diesel engines for daily activities is advantageous for its environmental friendliness over petro-diesel which is currently in use. The main advantages of using biodiesel is that it is

**Corresponding author, Email: ambilykj@gmail.com*

biodegradable, can be used without modifying existing engines, and produces less harmful gas emissions such as sulfur oxide. Biodiesel reduces net carbon-dioxide emissions by 78% on a lifecycle basis when compared to conventional diesel fuel. [3]. Of the various alternate fuels under consideration, biodiesel, derived from vegetable oils, is the most promising alternative fuel to conventional diesel fuel [4].These biofuels are being looked to provide employment generation to rural people through plantation of plants which produce non-edible oils[2].

Recently, microwaves have received increased attention due to their ability to complete chemical reactions in very short times. Few advantages with microwave processing can be listed as: rapid heating and cooling; cost savings due to energy, time and work space savings; precise and controlled processing; selective heating; volumetric and uniform heating; reduced processing time; improved quality ("reportedly") and properties; and effects not achievable by conventional means of heating [5,6,7,8] .Due to these advantages, microwaves provide for tremendous opportunities to improve bio-diesel conversion processes from different feedstock and oils. The aim of this review paper is to assess biodiesel production from non-edible oil with a view to determine its performance in Internal Combustion engine and investigate the fuel properties of bio-diesel. Additionally, factors affecting biodiesel production were discussed. In this,we are also providing the basics of microwave energy applications specific to biodiesel preparation and processing, preliminary understanding and explanation of microwave effect on the chemical re-actions (extraction and transesterification), for biodiesel production[9,10,11] .

Biodiesel

Biodiesel is an alternative fuel made from renewable biological sources such as vegetable oils both (edible and non edible oil) and animal fats [12]. It can be defined as basically monoalkyl esters of fatty acids produced from animal fats or vegetable oils by transesterification or other methods with small chain alcohols, using different kinds of catalysts. Currently, more than 95% biodiesel are produced from edible oil feedstock (soya bean oil, sunflower oil, niger oil, rapeseed oil, palm oil, linseed oil and sesame oil), due to this there is a huge imbalance in the human nutrition chain versus fuel. This will make biodiesel economically unfeasible as compared to petroleum-derived fuels. To avoid these situations, non-edible oil seeds need to be used for commercial production of biodiesel. Many researchers have initiated work on the use of low cost non-edible oils as alternative feedstock for biodiesel production. Among non-edible oil feedstock, seeds of castor and jatropha, and microalgae oil are proved to be a one of the highly promising reliable source having high seed oil content [13]. Algae are an economical choice for biodiesel production, because of its availability and low cost [14].

Biodiesel, is advised for use as an alternative fuel for conventional petroleum-based diesel chiefly because it is a renewable, domestic resource with an environmentally friendly emission profile and is readily

biodegradable. Biodiesel, a promising substitute as an alternative fuel has gained significant attention due to the predicted shortness of conventional fuels and environmental concern. The amount of greenhouse gas emissions, generating energy from renewable resources is being possessed a high priority gradually to decrease both over-reliance on imported fossil fuels [15].

Production of biodiesel

Vegetable oils are chemically complex esters of fatty acids. These are the fats naturally present in oil seeds, and known as tri-glycerides of fatty acids. The molecular weight of these tri-glycerides would be of order of 800 kg/m^{3}or more. Because of their high molecularweights these fats have high viscosity causing major problems in their use as fuels in CI engines. These molecules have to be split into simpler molecules so that they have viscosity and other properties comparable to standard diesel oils. Modifying the vegetable oils (to make them lighter) can be achieved in many ways, including; Pyrolysis, Micro emulsification, Dilution and Transesterification. Among these, transesterification is the most commonly used commercial process to produce clean and environmentally friendly light vegetable oil fuel i.e. biodiesel [12].

Transesterification

Biodiesel, an alternative diesel fuel is derived from a chemical reaction called transesterifcation of plant-derived oil. It is the chemical conversion of oil to its corresponding fatty ester in the presence of a catalyst. The reaction converts esters from long chain fatty acids into mono alkyl esters. Chemically, biodiesel is a fatty acid methyl ester. Transesterification process helps reduce the viscosity of the oil. The process proceeds well in the presence of homogenous catalysts such as sodium hydroxide (NaOH), potassiumhydroxide (KOH), sulphuric acid [16]. The formation of fatty acid methylesters (FAME) through transesterification of seed oils requires raw oil, 15% of methanol & 5% of sodium hydroxide on mass basis. However, transesterification is an equilibrium reaction in which excess alcohol is required to drive the reaction very close to completion [17].

Transesterification transform the large branched molecule structure of the oils intosmaller, straight chained molecules similar to the standard diesel hydrocarbons. Transesterification is the process of exchanging the organic group R" of an ester with theorganic group R' of an alcohol. These reactions are often catalyzed by the addition of an acid or base. Transesterification is common and well-established chemical reaction in which alcohol reacts with triglycerides of fatty acids (non-edible oil) in the presence of catalyst. The transesterification reaction scheme is shown below [18].

Methanol and ethanol are used most frequently; especially methanol is preferred because of its low cost and its physical and chemical advantages (polar and shortest chain alcohol). It can quickly react with

triglycerides and NaOH gets easily dissolved in it. Ethyl ester and methyl ester almost has same heat content [18].The two methods preferred for the industrial production of biodiesel from non-edible oils are base catalyzed and acid catalyzed transesterification.

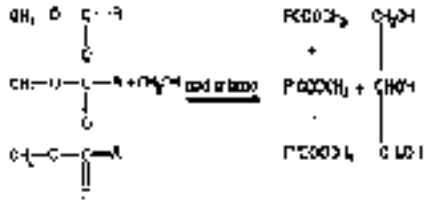

Fig.1. Transesterification Reaction Scheme[12]

Edible versus non-edible oils

There are two types of oils; edible and non-edible oils. Edible oils are the major sources to produce biodiesel fuel like sunflower, soybean, and palm oils. Due to higher prices of edible vegetable oils compared to diesel fuel, waste vegetable oils and non-edible crude vegetable oils are now being used as biodiesel sources. There are disadvantages of using edible oil such as: higher viscosity, lower volatility, the reactivity of unsaturated hydrocarbon chains. Due to these disadvantages, vegetable oils are not used directly as biodiesel, so there are methods to enhance the vegetable oil's characteristics for biodiesel production [19].

To evaluate for materials that are more suitable for biodiesel production, there are three important points to consider:

? Availability of these materials.

? Properties closer to the standard diesel.

? Economic value of biodiesel in comparison with fossil diesel.

Also, in comparing edible and non-edible materials, that is oil palm and soyabean oil as edible oil with jatropha and waste cooking oil as non-edible oil, it could be seen from the result that non edible oils are more suitable to produce biodiesel because they are not competitive with the food material, this will preserve the food sources alone even though biodiesel from edible oils have properties closer to standard diesel properties. Also, biodiesel from edible oils are not economical compared with non-edible oils. Jatropha oil and waste cooking oil are more readily available than edible oils. Jatropha appears to have

several advantages as a renewable diesel feedstock, because it is non-edible and can be grown on marginal lands; it is potentially a sustainable material for biofuel production. The high oil content of Jatrophacurcas indicates that Jatrophacurcas is suitable as non- edible plant oil feedstock in oleo chemical industries. Jatropha has been planted in several arid regions, in these regions it only yields about 0.5 ton per hectare. The seeds contain about 30% oil. Biodiesel from Jatrophacurcas so obtained is found to be comparable to those of fossil diesel conforming to the American and European standards [19].

Table.1. Annual Production of Non-edible Oil Seeds in India[20] .

Type	Production(Metric Ton)	Oil %
Neem	300	30
Karanja	200	25-39
Kusum	50	34
Pilu	50	33
Ratanjot	-	30-40
Jaoba	-	50
Shikai	-	7
Wild Walnut	-	60-70
Tung	4	50-75
Thumba	100	21

Major non-edible tree borne oilseeds (tbos)

Soapnut (*SapindusMukorossi*)

Soapnut is a fruit of the soapnut tree generally found in tropical and sub-tropical climate areas in various parts of the world including Asia, America and Europe. Two main varieties (S. mukorossi and S. trifoliatus) are widely available in India, Nepal, Bangladesh, Pakistan and many other countries. The oil content in S. trifoliatus which is very similar to S. mukorossi seed kernels, was on average 51.8% of seed weight. The oil from soapnut has been considered a nonedible oil having significant potential for biodiesel production from the material which otherwise is a waste material .A comprehensive study on the uses of various parts of the soapnut tree.Soapnut has several applications from medicinal treatments to soap and surfactant. Soapnut fruit shells have been in use as natural laundry detergents from ancient times for

washing fabrics, bathing and traditional medicines. The recorded external use of saponin does not cite any toxic effects on human skin and eyes .These application all make use of the pericarp shell and the seeds are usually waste. Hence, the use of soapnut seeds as a biodiesel source becomes the "waste-to-energy" scheme. Furthermore, planting soapnut trees in community forestry and in barren lands provides sink for carbon sequestration as well as feedstock for biodiesel production . The total value of exports of soapnut as medicinal use including other four species made up to 52% of the total non timber forest products export to India from Nepal. The totals of 32 non-timber forest products are exported with a total value of 8.1 million US dollar for the year 1997/1998. Recently it was reported that the glycerol, a by-product of biodiesel production, can be used to produce organic acids such succinic acids by bacterial fermentation .Hence, the economics of biodiesel from soapnut oil can easily be realized on community scale as it can be integrated in the community forestry plan[20].

Table.2. Fatty acid composition of Soapnut oil [20].

Fatty Acid	Structure	Amount %
Palmitic acid	16:0	4.67
Palmitoleic acid	16:1	0.37
Stearic acid	18:0	1.45
Oleic acid	18.1	53.64
Linoleic acid	18:2	4.73
Alpha or gamma-linolenic acid	18:3	1.54
Arachidic acid	20:0	7.02
Eicosenoic acid	20:1	23.35
Behenic acid	22:0	1.15
Erucic acid	22:1	1.05
Lignoceric acid	24:0	0.17
Others		0.39
Total		100.0

Mahua (*MadhucaIndica*)

Bio diesel from mahua seed is important it is found abundantly in tribal areas . The annual production of mahua is nearly 181Kt(Kilotonnes). Mahua is a nontraditional,& non edible oil also known as Indian butter tree. Mahua seed contain 30-40 percent fatty oil called mahua oil**.**Mahua is a medium to larger

tree.In India the mahua plant is found in most of the state e.g. Orissa, Chatishgada, Jharkhand, Bihar, Madhya Pradesh ,Tamilnadu. It can be sucessesfully grown in waste land & dry land. The tree is a strong light demander and gets readily suppressed under shade. The tree has potential of enhancing rural income. The tree may attain a height of upto 20 meters and is well adapted to varied weather conditions it has wide spreading branches and circular crown which presents a visually appealing structure. The tree has a large spreading root system, though many of them are superficial. The fruit is a kind of berry, egg shaped. Mature seeds can be obtained during June to July. The mahua tree starts bearing seeds from seventh years of planning. Commercial harvesting of seeds can be done only from the tenth year. Seed yield ranges from 20 -200 kg per tree every year, depending on its growth and development . As a plantation tree, Mahua is an important plant having vital socioeconomic value. This species can be planted on roadside and canal banks on commercial scale and in social forestry programs, particularly in tribal areas. Wood can be used as timber, making pulp and paper. Mahua flowers are rich in sugar, minerals, vitamins and calcium.

Table.3. Fatty acid composition of Mahuaoil[20] .

Fatty Acid	Structure	Amount %
Palmitic acid	16:0	15.0-28.2
Stearic acid	18:0	21.0-25.1
Oleic acid	18:1	41.0-51.0
Linoleic acid	18:2	8.0-13.7
Arachidic acid	20:0	0.6-3.1

Jatropha (*JatrophaCurcas*)

Jatrophacurcus is a drought-resistant perennial, growing well in marginal/poor soil. It produces seeds with an oil content of around 37%. The oil can be combusted as fuel without being refined. It burns with clear smoke-free flame, tested successfully as fuel for simple diesel engine. The by-products are press cake a good organic fertilizer, oil contains also insecticide. It is found to be growing in many parts of the country, rugged in nature and can survive with minimum inputs and easy to propagate .Medically it is used for diseases like cancer, piles, snakebite, paralysis, dropsy etc. Depending on soil quality and rainfall, oil can be extracted from the Jatropha nuts after two to five years. It grows on well drained soils with good aeration and is well adapted to marginal soils with low nutrient content. Jatrophacurcas grows almost anywhere, even on gravelly, sandy and saline soils. It can thrive on the poorest stony soil. The leaves shed during the winter months form mulch around the base of the plant. Its water requirement is extremely low and it can stand long periods of drought by shedding most of its leaves to reduce transpiration loss. Jatropha is also suitable for preventing soil erosion and shifting of sand dunes .

 ISSN : 0976 - 8289

Table.4. Fatty acid composition of Jatrophaoil[20] .

Fatty Acid	Structure	Amount %
Palmitic acid	16:0	15.98
Palmitoleic acid	16:1	0.85
Stearic acid	18:0	5.24
Oleic acid	18:1	45.59
Linoleic acid	18:2	32.27
Linolenic acid	12:0	0.51
Others		1.03
Total		100

Karanja (*PongamiaPinnata*)

The botanical name of Karanja seed Oil and is Pongamiaglabra of Leguminaceae family. Pongamia is widely distributed in tropical Asia and it is nonedible oil of Indian origin . It is found mainly in the Western Ghats in India, northern Australia, Fiji and in some regions of Eastern Asia. The plant is also said to be highly tolerant to salinity and can be grown in various soil textures viz. stony, sandy and clayey. Karanja can grow in humid as well as subtropical environments with annual rainfall ranging between 500 and 2500 mm. This is one of the reasons for wide availability of this plant species. The tree bears green pods which after some 10 months change to a tan colour. The pods are flat to elliptic, 5-7 cm long and contain 1 or 2 kidney shaped brownish red kernels. The yield of kernels per tree is reported between 8 and 24 kg. The kernels are white and covered by a thin reddish skin. The composition of typical air dried kernels is: Moisture 19%, Oil 27.5%, and Protein 17.4%. The present production of karanja oil approximately is 200 million tons per annum. The time needed by the tree to mature ranges from 4 to 7 years and depending on the size of the tree the yield of kernels per tree is between 8 and 24 kg. The oil content extracted by various authors ranges between 30.0 to 33% .The oil is used by common people due to its low cost and easy availability.

Table.5. Fatty acid composition of Karanjaoil[20]

Fatty Acid	Structure	Amount %
Palmitic acid	16:0	3.7-7.9
Stearic acid	18:0	2.4-8.9
Oleic acid	18:1	44.5-71.3
Linoleic acid	18:2	10.8-18.3
Lignoceric acid	24:0	1.1-3.5

Corresponding author, Email: ambilykj@gmail.com

Neem (*MelliaAzadirachta*)

Neem (Melliaazadirachta) is of Meliaceae family. The other names of neem are Margosa, Veppam, Vepun, Nimba and Vepa (Telugu) etc. It is one of the two species in the genus Azadirachta, and is native to India and Burma, growing in tropical and semi tropical regions. Neem is a fast growing tree and can reach upto a height of 15 – 20 to 35 – 40 m. It bears an ovoid fruit, 2cm by 1cm and each seed contains one kernel. The seed kernels, which weigh0.2g, constitute some 50-60% of the seed weight and 25% of the fruit. The fat content of the kernels ranges from 33-45% .The fruit yield per tree is 37-55 kg. Neem oil can be used as Soaps, medicinal and insecticide. Neem oil isusually opaque and bitter but it has recently been shown that it can be processed into non bitter edible oil with 50% oleic acid and 15% linoleum acid. The bitter cake after extraction of oil has no value for animal feeds although it has been reported that after solvent extraction with alcohol and hexane a meal suitable for animals is produced. Neem seeds are usually crushed prior to extraction in ghanis. Whole dried fruits may be directly passed to expellers. Good quality kernels (50% oil) yield 40% oil in ghanis. In expellers whole dried fruits, depulped seeds and kernels, yield 4-6%, 12-16% and 30-40% oil respectively (Bring). The cakes, which contain 7-12% oil are sold for solventextraction. Major fatty acid composition of oil are Palmitic acid 19.4%,Stearic acid 21.2%,Oleic acid 42.1%,Linoleic acid 14.9%,Arachidic acid 1.4% .

Neem oil is unusual in containing non-lipid associates often loosely termed as "bitters" and organic sulphur compounds that impart a pungent, disagreeable odour[20].

Table.6 . Fatty acid composition of Neemoil[20].

Fatty Acid	Structure	Amount %
Palmitic acid	16:0	17.8
Stearic acid	18:0	14.4
Oleic acid	18:1	51.3
Linoleic acid	18:2	14.7
Arachidic acid	20:0	1.6
Myristic acid	14:0	0.03

Microwave assisted biodiesel production

Microwave characteristics

Microwave irradiation is the electromagnetic irradiation with frequency range of 0.3-300 GHz. They lie in the electromagnetic spectrum between infrared waves and radio waves with wavelengths between 0.01 and 1 m. Commercial microwave ovens approved for domestic applications operate at a frequency of 2.45 GHz to avoid interference with telecommunication and cellular phone frequencies. Most of the reported microwave chemistry experiments are conducted at 2450 MHz (the corresponding wavelength is 12.24

cm) since this frequency is approved worldwide and used in currently available commercial microwave chemistry equipment. One reason is that near to this frequency, the microwave energy absorption by liquid water is maximal. Interaction of dielectric materials with microwaves leads to what is generally described as dielectric heating due to a net polarization of the substance [21,22,23,24].

Microwave energy

Energy associated with microwaves is lower than the energy of Brownian motion which is not strong enough to even break chemical bonds as such microwaves cannot induce chemical reactions. The influence of microwave energy on chemical or biochemical reactions is both thermal and non-thermal. The microwave energy quantum is given by the well-known equation, W = hν. Within the frequency domain of microwaves and hyper-frequencies (300 MHz - 300 GHz), the corresponding energies are 1.24×10^{-6} -1.24×10^{-3} eV, respectively. These energies are much lower than ionization energies of biological com-pounds (13.6 eV), of covalent bond energies such as OH-(5 eV), hydrogen bonds (2 eV), van der Waals inter-molecular interactions (lower than 2 eV) and even lower than the energy associated with Brownian motion at 37°C ($2.7\ 10^{-3}$eV) [25,26,27].Microwaves, as an energy source, produce heat by their interaction with the materials at molecular level without altering the molecular structure [28,29].Microwave heating offers several advantages over conventional heating such as non-contact heating (reduction of overheating of material surfaces), energy transfer instead of heat transfer (penetrative radiation), reduced thermal gradients, material selective and volumetric heating, fast start-up and stopping and reverse thermal effect, i.e. heat starts from the interior of material body. In terms of biodiesel production, the resultant value could include: more effective heating, fast heating of catalysts, reduced equipment size, faster response to process heating control, faster start-up, increased production, and elimination of process steps [27].

Microwave heat transfer mechanism

Microwave heating mechanism is complex.In conventional heating as well as supercritical methods, heat transferred to the sample volume is utilized to increase the temperature of the surface of the vessel followed by the internal materials. This is also called “wall heating”. Therefore, a large portion of energy supplied through conventional energy source is lost to the environment through conduction of materials and convection currents. Heating effect in the conventional method is heterogeneous and dependent on thermal conductivity of materials, specific heat, and density which result in higher surface temperatures causing heat transfer from the outer surface to the internal sample volume.

Microwave-enhanced transesterification

Microwave effect on the transesterification reaction can be two-fold: 1) enhancement of reaction by a thermal effect, and 2) evaporation of methanol due to the strong microwave interaction of the material [30,31] The microwave interaction with the reaction compounds (triglycerides and methanol) results in large

reduction of activation energy due to increased dipolar polarization phenomenon [32]. This is achieved due to molecular level interaction of the microwaves in the reaction mixture resulting in dipolar rotation and ionic conduction [33,34,35]. The amount, by which the activation energy is reduced, is essentially dependent on the medium and reaction mechanism Methanol is a strong microwave absorption material and in general, the presence of an -OH group attached to a large molecule behaves as though it were anchored to an immobile raft and the more localized rotations result in localized superheating which assists the reaction to complete faster[36]. For this reason, methanol is preferred over ethanol for microwave-assisted transesterification process[31].

Catalyst and alcohol-oil ratio

Among the most commonly used alkaline catalysts in the biodiesel industry are potassium hydroxide (KOH) and sodium hydroxide (NaOH) flakes which are inexpensive, easy to handle in transportation and storage, and are preferred by small producers. Alkyl oxide solutions of sodium methoxide or potassium methoxide in methanol, which are now commercially available, are the preferred catalysts for large continuous-flow production processes. However, both NaOH and KOH catalysts cause separation and purification a difficult process due to their high solubility in the both biodiesel and glycerin[37, 38, 39.] Biodiesel with the best properties was obtained using sodium hydroxide as catalyst in many studies. On the other hand, many other studies achieved best results using potassium hydroxide .Refaat used 500 mL reactor at a reaction temperature of 65°C with a microwave power of 500 W controlled by microprocessor. A methanol/oil molar ratio of 6:1 was employed, and potassium hydroxide (1%) was used as a catalyst. Barium hydroxide was also used a homogeneous catalyst. The range of homogeneous catalysts applied was between 0.1 and 5% (Table 7) [40]. Slightly higher concentrations of KOH will be required compared to NaOH catalyst due to its higher molecular weight. For feedstock containing high free fatty acid content such as animal fats and used vegetable oils, KOH proved to be a better performer [40]. Transesterification reaction depends on the type of oil and catalyst applied and the effects of catalysts vary with types of oils.

Although homogeneous catalysts are advantageous in terms of fast reaction rates, the drawback of this application is that the reaction products require longer separation and purification times. Use of heterogeneous catalysts can be advantageous in microwave-enhanced transesterification reactions since the catalyst can provide locations for hotspots for rapid heating. In addition, they are recyclable and reusable with acceptable performance. Patil et al. employed heterogeneous catalysts such as BaO, CaO, MgO, and SrO for transesterification of CamelinaSativa oil into biodiesel. They reported the kinetic rate constants for different catalysts. Two orders of magnitude of difference in the kinetic rate constants between the conventional heating method and micro-wave heating methods were reported in their study[40]. Sol gel type catalysts were also developed and tested by the same group of researchers.

Table.7.Summary of microwave enhanced bio-diesel production studies40.

Sample	Reaction time (min)	Reaction temp. (°c)	Catalyst	Oil to alcohol ratio	FAEE/FAME conv. (%)	Equipment	Mode
Waste vegetable oil (domestic)	1	65	KOH	1:9 Methanol	96	Start S Milestone	Batch
Waste vegetable oil restaurant)	1	65	KOH	1:9 Methanol	94.5	Start S Milestone	Batch
Used vegetable oil	0.5	-	NaOH (1%)	1:9 Ethanol	100	Domestic Microwave	Continuous
Used Palm oil	0.5	77.5	NaOH	1:9 Ethanol	82.5	Domestic Microwave	Continuous
Waste vegetable oil	6	50	KOH	1:6 Methanol	96	CEM Explorer	Batch
Macauba	15	30	Novozym 435 (2.5%)	1:9 Ethanol	45.2	CEM Explorer	Batch
Jatropha	2	65	KOH (1.5%)	1:75 Methanol	97.4	70W	
Castor	60	338	H2SO4	1:12 Methanol	94	200W	-
Maize	-	-	NaOH (1.5%)	1:10 Methanol	98	-	-

Note: FAEE/FAME-Fatty Acid Ethyl Ester/Fatty Acid Methyl Ester

Table.8. Comparison between microwave irradiation and conventional techniques39.

System	Reaction time (min)	Separation time (min)
Conventional	60 to 180	480
Microwave irradiation	5 to 9	5

Conclusion

The high consumption of diesel fuels and limited sources of the others are reasons for an enormous rise in price of petroleum fuels. The Vegetable oils hold special promise in this regard since they can be produced from plants grown in waste lands like Jatropha, Mahua, Neem. These are clean burning, renewable, non-toxic, biodegradable and environmentally friendly transportation fuels that can be used in neat form or in blends with petroleum derived diesel in diesel engines. The production of biodiesel from edible oil is currently much more expensive than diesel fuels due to relatively high cost of edible oil. Utilization of edible oil like vegetable oils as fuel actualized the competition between human needs in food and non -

food applications. There is a need to explore non-edible oils as alternative feed stock for the production of biodiesel from non-edible oils like Karanja, Neem, Jatropha, Mahua, Soapnut etc. owing to big climatic diversity, there are numerous oil bearing seed plants/trees available. Extraction of the oil from these plants and its conversion to bio-diesel involves energy consumption at various stages starting from the plantation to the end use in the compression ignition engine. In addition, slow and relatively inefficient heating in conventional heating methods bring the production cost of biodiesel higher, thus an alternative method, "microwave irradiation" was applied for the production of this alternative fuel source. The results showed that microwave assisted irradiation is one of the best methods to reduce the reaction time and separation time as well.

Acknowledgement

Author acknowledges University Grant Commission(UGC) for the financial support.The authors are also greateful to Ms Mercy Leena Paul for the fruitful discussion .

References

1. Anitha A., Dawn S.S.,2010. Performance Characteristics of Biodiesel Produced from Waste Groundnut Oil using Supported Heteropolyacids.*International Journal of Chemical Engineering and Applications*. 1(3), 261-265.
2. Mulimani.H.,Hebbal O.D., Navindgi M.C.,2012. Extraction of Biodiesel from Vegetable Oils and their Comparisons. *International Journal of Advanced Scientific Research And Technology*. 2(2), 242-250.
3. CarvalhoJ.,Ribeiro A., Castro J., Vilarinho C., Castro F.,2011. Biodiesel Production By Microalgae and Macroalgae from North Littoral Portuguese Coast. *1St International Conference*.
4. Jaichandar S., Annamalai K., 2011. The Status of Biodiesel as an alternative fuel for Diesel Engine – An Overview. *Journal of Sustainable Energy & Environment*. 2, 71-75.
5. Clark D.E., Sutton W.H.,1996. Microwave processing of materials. *Annual Review of Materials Science*. 26:299–331.
6. Caddick S., Fitzmaurice R., 2009. Microwave enhanced synthesis. *Tetrahedron*. 65:3325–3355.
7. Ku H.S., Siores E., Taube A., Ball J.A.R., 2002. Productivity improvements through the use of industrial microwave technologies. *Computers & Industrial Engineering*. 42, 281–290.
8. de la Hoz A., Diaz-Ortiz A., Moreno A.,2005. Microwaves in organic synthesis. Thermal and non-thermal microwave effects. *ChemSoc Rev*. 34,164–178.
9. Roberts B., Strauss C.R., 2005. Toward rapid, "green", predictable microwave-assisted synthesis. *AccChem Res*. 38, 653–661.
10. Varma R.S.,1999. Solvent- free organic syntheses using supported reagents and microwave irradiation. *Green Chem*. 1, 43–55.
11. Giguere R.J., Bray T.L., Duncan S.M., Majetich G.,1986. Application of commercial microwave ovens to organic

synthesis.*Tetrahedron Lett*. 27, 4945–4948.

12. Antony Raja S.,Robinson D.S., Robert Lee C. 2011. Biodiesel production from jatropha oil and its characterization. *Research Journal of Chemical Sciences*. 1, 81-85
13. SruthiK., Kumar R., ShirishaG., 2013. Determination of physico-chemical properties of Castor Biodiesel: A potential alternate to Conventional Diesel. *International Journal of Advanced Research in Engineering and Technology*, 4(3), 101-107.
14. BasumataryS., 2013. Biodiesel Production: *Journal of Chemical, Biological and Physical Sciences.* 3(1), 551-558.
15. Hossain A.B.M.S., Boyce A.N., 2009. Biodiesel production from Waste Sunflower Cooking oil as an Environmental Recycling Process and Renewable Energy. *Bulgarian Journal of Agricultural Science*, 15 (4), 312-317.
16. Demirbas A., 2002. Biodiesel from vegetable oils via transesterification in supercritical methanol. *Energy conversion management.* 43(23), 49–56.
17. Ahmad M., Khan M., Zafar M., Sultana S., 2011. Biodiesel from Non Edible Oil Seeds: a Renewable Source of Bioenergy. *Economic Effects of Biofuel Production*. http://www.intechopen.com/books/economic-effects-of-biofuel-production/biodiesel-from-non-edible-oil-seedsa-renewable-source-of-bioenergy
18. Ojolo S.J., Ogunsina B.S., Adelaja, A.O., OgbonnayaM. 2011. Study of an EffectiveTechnique for the Production of Biodiesel from Jatropha Oil. *Journal of Emerging Trends in Engineering and Applied Sciences*. 2 (1), 79-86.
19. Alnuami W., Buthainah A., EttiC.J., Jassim L.I., Gomes, G.A., 2014. Evaluation of Different Materials for Biodiesel Production.*International Journal of Innovative Technology and Exploring Engineering*. 3, (8), 1-8.
20. Khandelwal S., Chauhan.Y.R.,2012. Biodiesel production from non edile-oils-A Review.*J.Chem.Pharm.Res*. 4(9), 4219-4230.
21. Baghurst D.R., Mingos D.M.P., 1991. Applications of microwave dielectric heating effects to the synthetic problems in chemistry. *ChemSoc Rev*. 20,1–47.
22. Gabriel C., Gabriel S., Grant E.H., Halstead B.S., MingosD.M.P,1998. Dielectric parameters relevant to microwave dielectric heating. *ChemSoc Rev*. 27, 213–223.
23. Peterson E.R., 1994. Microwave chemical processing. *Res ChemIntermed*. 1,93–96.
24. Chemat-Djenni Z., Hamada B., Chemat F., 2007. Atmospheric pressure microwave assisted heterogeneous catalytic reactions. *Molecules*. 12, 1399–1409.
25. Varma R.S., 2001. Solvent-free accelerated organic syntheses using microwaves. *Pure and Applied Chemistry*. 73(1), 193–198.
26. Refaat A.A.,2010. Different techniques for the production of biodiesel from waste vegetable oil. *Int J Environ Sci Tech*. 7(1),183–213.
27. Loupy A., Petit A., Ramdani M., Yvanaeff C., 1993.The synthesis of esters under microwave irradiation using dry-

media conditions. *Can J Chem*, 71,90–95.

28. Yuan H., Yang B.L., Zhu G.L.,2009. Synthesis of biodiesel using microwave absorption catalysts. *Energy & Fuels*, 23,548–552.
29. Perreux L., Loupy A.,2001.A tentative rationalization of microwave effects in organic synthesis according to the reaction medium and mechanistic considerations. *Tetrahedron*. 57,9199–9223.
30. Boldor D., Kanitkar A., Terigar B.G., Leonardi C., Lima M., Breintenbeck G.A., 2010.Microwave assisted extraction of biodiesel feedstock from the seeds of the invasive Chinese tallow tree. *Environ Sci Technol*. 44, 4019–4025.
31. Lidstrom P, Tierney JP, Wathey B, Westman J,2001.Microwave assisted organic synthesis – a review. *Tetrahedron*, 57:9225–9283.
32. Terigar B.G., Balasubramanian S., Boldor D., Xu Z., Lima M., Sabliov C.M., 2010.Continuous microwave-assisted isoflavone extraction system-design and performance evaluation. BioresourTechnol.101(7), 2466–2471.
33. Demirbas A., 2007. Biodiesel from sunflower oil in supercritical methanol with calcium oxide. *Energy Conversion and Management*. 48, 937–941.
34. Chai F., Cao F.H., Zhai F.Y., Chen Y., Wang X.H., Su Z.M.,2007. Transesterification of vegetable oil to biodiesel using a heteropolyacid solid catalyst. *Adv Synth Catal*. 349, 1057–1065.
35. Shibasaki-Kitakawa N., Honda H., Kuribayashi H., Toda T., Fukumura T., Yonemoto T.,2007. Biodiesel production using anionic ion-exchange resin as heterogeneous catalyst. *Bioresource Technol*. 98, 416–421.
36. Refaat A., Attia N.K., SibakH.A., El Sheltawy S.T., ElDiwani G.I.,2008.Production optimization and quality assessment of biodiesel from waste vegetable oil. *Int J Environ Sci Tech*. 5(1),75–82.
37. Brunschwig C., Moussavou W., Blin J., 2012. Use of bioethanol for biodiesel production. *Progress in Energy and Combustion Science*. 38, 283–301.
38. Patil P.D., Gude V.G., Pinappu S., Deng S., 2011. Transesterification kinetics of Camelinasativa oil on metal oxide catalysts under conventional and microwave heating conditions. *ChemEng J*. 168(3),1296–1300.
39. FaroughMotasemi., Farid N.A., 2011. The production of biodiesel from waste cooking oil using microwave irradiation. *JurnalMekanikal*. 32,61-72.
40. Veera G.G., Prafulla P., Martinez-Guerra E., Deng S., 2012.Microwave energy potential for biodiesl production.*Sustainable Chemical Processes*. 1, 5,1-31.

Scientia
Vol.9, No. 1, Jan - Dec. 2013, pp38-41
ISSN : 0976 - 8289

Sucharitha R S

Dept of Mathematics ,Mercy College, Palakkad-678006, Kerala.

Abstract

Today's world , for secure data transmission via internet or any public network , there is no alternative to cryptography. The role of cryptography is most important in the field of network security. The main goal of cryptography is Confidentiality, Integrity, Authentication, Non repudiation. Cryptography is widely used by governmental and intelligence agencies around the world to safe transmission of any format of messages online or offline. In this the basic idea of cryptography , its classification, usage of mathematics in encryption and decryption, and its application in every day life are dealt.

Key words: Cryptography, plain text, cipher text, encryption, decryption.

Introduction

Cryptography[1] is the science of using Mathematics to encrypt and decrypt data. Cryptography enables you to store sensitive information or transmit it across insecure networks (like internet) so that it can be read by anyone except the intended recipient. Cryptography is the science and art of transforming message to make them secure and immune to attack.

Fig.1. Encryption and decryption

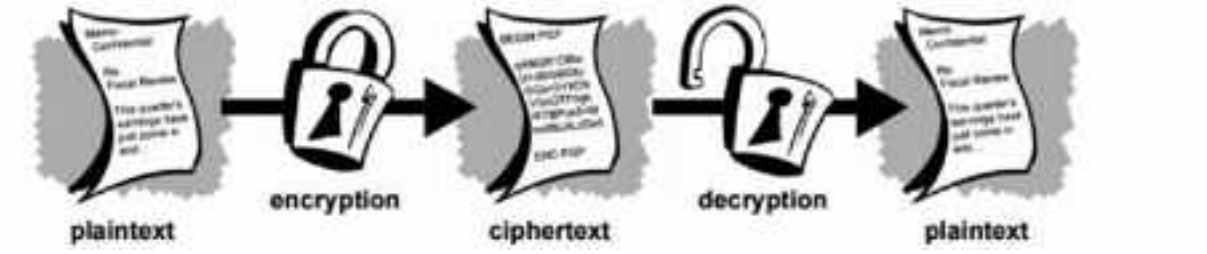

From past to present

The history of Cryptography begins where many old tales do in ancient Egypt with hieroglyphics. These were not meant to hide messages so much as to give a formal and ceremonial touch to stories of everyday events. The earliest form of cryptography was the simple writing of a message, as most people could not read . In fact, the very word cryptography comes from the Greek words kryptos and graphein, which mean hidden and writing, respectively.

As early as 1900 B.C., Egyptian scribes used hieroglyphs in a non-standard fashion, presumably to hide the meaning from those who did not know the meaning. The Greek's idea was to wrap a tape around a stick, and then write the message on the wound tape. When the tape was unwound, the writing would be

Corresponding author, Email: saruthurs@gmail.com

meaningless. The receiver of the message would of course have a stick of the same diameter and use it to decipher the message. The Roman method of cryptography was known as the Caesar Shift Cipher. It utilized the idea of shifting letters by an agreed upon number (three was a common historical choice), and thus writing the message using the letter-shift. The receiving group would then shift the letters back by the same number and decipher the message.

Fig. 2. Old era techniques to encrypt message

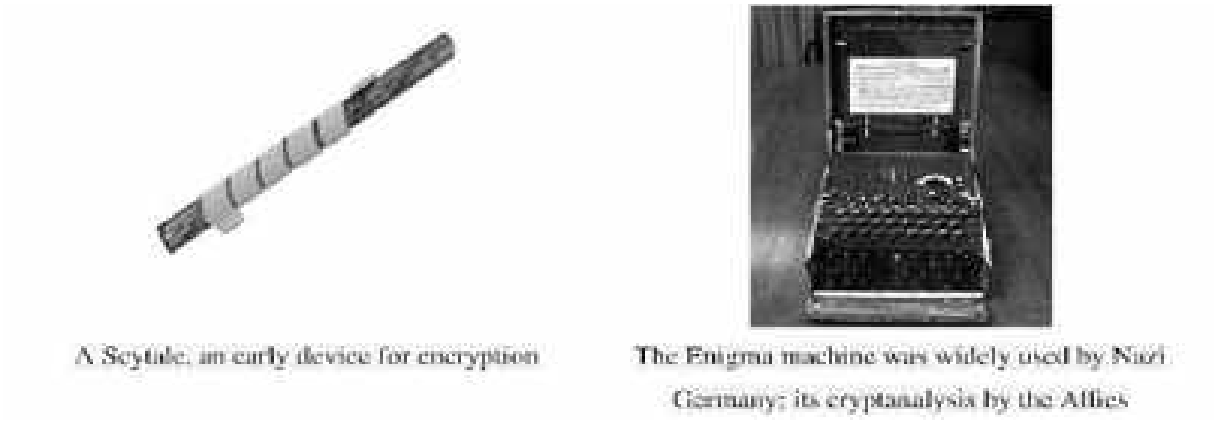

A Scytale, an early device for encryption

The Enigma machine was widely used by Nazi Germany; its cryptanalysis by the Allies

The art and science of cryptography showed no major changes or advancements until the Middle Ages. By that time, all of the western European governments were utilizing cryptography in one form or another. Keeping in touch with ambassadors was the major use of cryptography. One Leon Battista Alberti was known as “The Father of Western Cryptology,” most notably due to his development of polyalphabetic substitution. His method was to use two copper disks that fit together. Each one of them had the alphabet inscribed on it. After every few words, the disks were rotated to change the encryption logic, thereby limiting the use of frequency analysis to crack the cipher. Polyalphabetic substitution went through a variety of changes and is most notably attributed to Vigenere, although Rubin claims that he in fact had nothing to do with its creation. Rubin further points out that the use of the cipher disks continued in the Civil War, with the South using brass cipher disks, although the North regularly cracked the messages

Modern computing gave Cryptographers vast resources for improving the complexity of cryptosystems1 as well as for attacking them.And with the spread of personal computing,electronic commerce,and personal privacy concerns ,use of encryption has spread beyond its traditional use in military and government applications.Modern Cryptography is heavily based on mathematical theory and computerscience practice.

Cryptanalysis

While cryptography is the science of securing data , cryptanalysis is the science of analyzing and breaking

secure communication. Classical cryptanalysis involves an interesting combination of analytical reasoning, application of mathematical tools, pattern finding, patience, determination and luck.

Strength of Cryptography

Cryptography can be strong or weak. Cryptography's strength is measured in the time and resources it would require to recover the plain text. The result of strong Cryptography is cipher text that is very difficult to decipher without possession of the appropriate decoding tool.

Key

In cryptography , a key is a variable value that is applied using an algorithm to a string or block of unencrypted text to produce encrypted text, or to decrypt encrypted text. The length of the key is a factor in considering how difficult it will be to decrypt the text in a given message.

Working of Cryptography

A Cryptographic algorithm ,or cipher, is a mathematical function used in the encryption and decryption process. A cryptographic algorithm works in combination with a key (which can be a word, number or phrase) to encrypt the plain text. The same plain text encrypts to different cipher text with different keys. The security of encrypted data depends on:

I. The strength of cryptographic algorithm.

II. The security of the key.

Cryptosystem

A cryptographic algorithm with all possible keys and all the protocols that make it work comprise a cryptosystem.

Types of Cryptography

Cryptography is classified in to two as :

1. Conventional cryptography (or symmetric cryptography)
2. Public key Cryptography (or asymmetric cryptography)

Conventional Cryptography

In conventional cryptography one key is used both for encryption and decryption.

Fig.3. Conventional cryptography

Fig.3. Conventional cryptography

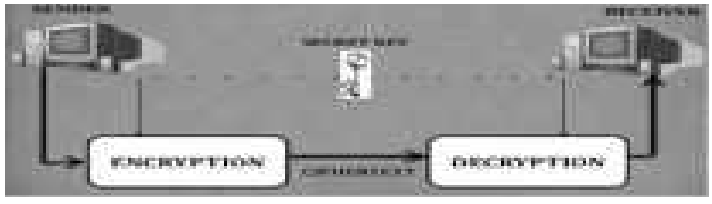

The Data Encryption Standard (DES) is an example of a conventional cryptosystem that is widely

employed by the Federal government. Simple example of conventional cryptography is a substitution cipher. Asubstitution cipher substitutes one piece of information for another. For example ,if we encode the word "SECRET " using Caesar's key value of 3 , we offset the alphabet so that the third letter down (ie D) begins the alphabet.So starting with "ABCDEFGHIJKLMNOPQRSTUVWXYZ"
and sliding everything up by 3, we get "DEFGHIJKLMNOPQRSTUVWXYZABC", where "D=A", "E=B", "F=C" and so on. Using this scheme, the plain text "SECRET" encrypts as "VHFUHW". To allow someone else to read this cipher text you tell them that the key is 3.

Advantage of conventional encryption

? It is very fast.

Disadvantage of conventional encryption

? It is expensive, due to the difficulty of secure key distribution.

Public key Cryptography

The problems of key distribution are solved by Public key cryptography , the concept of which was introduced by Whitfield Diffie and Martin Hellman in 1975. Public key cryptography is an asymmetric scheme that uses a pair of keys for encryption,a public key which encrypts data ,and a corresponding private or secret key for decryption.

Fig.4. Public key Cryptography

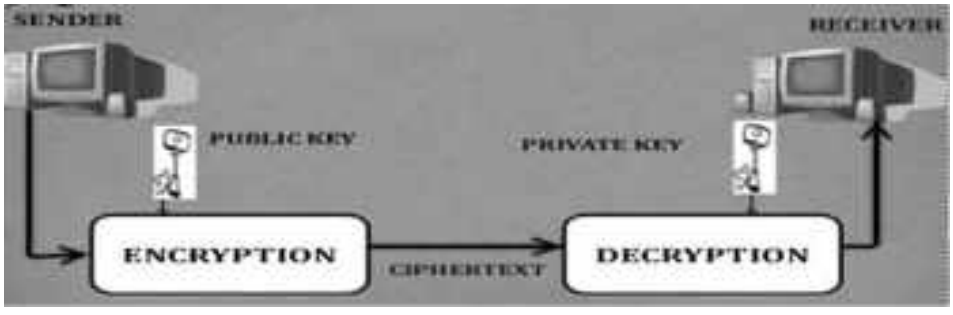

The public key is kept published to the world while the private key is kept secret. Anyone with a copy of the public key can then encrypt information that only the sender can read. It is computationally infeasible to deduce the private key from the public key. Anyone who has a public key can encrypt information but cannot decrypt it. Only the person who has the corresponding private key can decrypt the information. The primary benefit of public key cryptography is that it allows people, who have no preexisting security arrangement to exchange messages securely. The need for sender and receiver to share secret keys via some secure channel is eliminated; all communications involve only public keys, and no private key is ever transmitted or shared. Example of public key cryptosystems are Elgamel[1], RSA[1], Diffie –Helman[1] and DSA(Digital Signal Algorithm).

- ***Advantages of public key cryptography***
  - Increased security and convenience.
  - They can provide a method for digital signatures.

Disadvantages of public key cryptography

- The speed for encryption using public key is slow.

Methods

Mathematics and cryptography

An early use of modular arithmetic in encryption was the Caesar Cipher, in which, each letter of a message is encrypted by replacing it with the letter three places further along in the alphabet. So "IBC" would be encrypted as "LEF".

Modular arithmetic as a one-to-one mapping

We do not want encryption to have a big effect on the size of a message. Making a message smaller is the domain of compression, while making it bigger is the domain of error protection. In encryption, we would like a reversible mapping between the message (plaintext) and its encrypted version(ciphertext) and we don't want to add too much redundant information. When we come to multiplication and exponentiation using integers, the problem with ordinary arithmetic is that the range of outputs from fairly small inputnumbers can be huge. The nice thing about modular arithmetic[7] is that everything is kept within the range of the chosen modulus.

Modular multiplication

Again, modular multiplication[2] is just like ordinary multiplication with the added step of dividing the result by the modulus and taking the remainder. For example, in modulo-7 arithmetic, 3 x 6 = 4, because 4 is the remainder on dividing 18 by 7.

Modular multiplication could be the basis of a slightly more sophisticated version of the Caesar cipher in which we modulo- 26 multiply the numbers by a key. But we have to be careful when we consider how this is decoded. Just as the inverse of modular addition is modular subtraction, so the inverse of modular multiplication is modular division. Unfortunately, modular division does not always work.

Modular division

Dividing an even number by 2 has two possible results, while dividing an odd number by 2 isn't possible. This does not fit our need for a one-to-one mapping. We need a unique result for every division, and we

don't want to start introducing fractions to deal with the odd numbers. It turns out that we don't get this problem if the divisor and the modulus are relatively prime[2] . It's even better if the modulus is prime, because then the condition will be met for all divisors. When we meet this condition, we can do modular division. This is one reason why modular arithmetic for encryption is done using prime or relatively prime numbers.

We are now in a position to see how the maths we have looked at so far can be used in a public-key encryption system. The goal of a public-key system is to find a pair of functions, represented by numerical keys, that are inverses of each other and where the second function (decryption) cannot easily be deduced from the first function. The most celebrated and practically useful public key encryption system so far developed is the RSA algorithm, named after its inventors Rivest, Shamir and Adelman.

The RSA algorithm

The RSA algorithm[1] works in modulo-pq arithmetic, where p and q are large prime numbers. If Alice is sending a message to Bob[2] , Alice[2] uses Bob's public key e (and pq, which is actually part of Bob's public key) to encrypt her message which has been expressed as a number m < pq. The encryption is very simple; it's just raising m to the power e (modulo pq,). When Bob receives the message m^e, he raises it to the power of his private decryption key d to obtain a result "m^{ed}". In order for this to work as an encryption system, two conditions have to be met. First, it must be "very difficult" to calculate the private decryption key d from knowledge of the public encryption key e and pq. Second, the decrypted result m^{ed} must of course be equal to the original message m. The public key e is selected so that it is relatively prime to (p- 1)(q-1). This makes it possible to find a private key d which is the "reciprocal" of e, i.e. ed = 1 in modulo-(p- 1)(q-1) arithmetic. The actual calculation of this reciprocal can be done using a version of Euclid's algorithm, and is easy provided that p and q are known. However, it is very difficult if only the product pq is known; this number would first have to be factorized and we are working on the assumption that it is very difficult to factorize large numbers. So we have met our first condition. It remains to show that $m^{ed} = m$. Choosing d as the reciprocal of e means that there must be an integer t with ed = 1 + t(p - 1)(q - 1) (in normal arithmetic). So "$m^{ed} = m^{1+t(p-1)(q-1)} = m(m^t)^{(p-1)(q-1)}$".

Now in modulo-p arithmetic, Fermat's Little[2] Theorem says that$(m^t)^{(p-1)(q-1)} = 1$, so $m(m^t)^{(p-1)(q-1)} = m$. This will also be true in modulo-q arithmetic, and it is then not hard to show that it will be true in modulo-pq arithmetic. So we have shown that decryption is the inverse of encryption.

Here's a simple example using ridiculously small numbers. Suppose p = 5, q = 11, so pq = 55. We just have to pretend that 55 is hard to factorize! Then (p-1)(q-1) = 40. The public key e must be selected to be relatively prime to 40, for example 27. Then the private key d will be equal to 3 (because 27 x 3 = 81 which

gives a remainder of 1 when divided by 40).

Suppose the message is represented by a number m = 6. By the repeated squaring process, we can encrypt this "message" in our modulo-55 arithmetic:

62 = 36

64 = 362 = 1,296, remainder = 31

68 = 312 = 961, remainder = 26

616 = 262 = 676, remainder = 16

So 627 = 616+8+2+1 = ((16 x 26) x 36) x 6) = (31 x 36) x 6 = 16 x 6 = 41, taking remainders whenever we need to. So the ciphertext is the number 41, and we decrypt it by raising it to the power of 3, again in modulo-55 arithmetic: (41 x 41) x 41 = 31 x 41 = 6. This is our original message. Not only the modular arithmetic and prime numbers but also the probability theory is used in cryptography.

Discussions

Applications in daily life

Authentication/Digital Signatures

Authentication and digital signatures are a very important application of public-key cryptography. For example, If a message has to be sent from the sender to the receiver, then the sender will encrypt the message using the private key and if the receiver is able to decrypt the message then he/she will understand that the message has come from the right source. The only requirement is that public keys are associated with their users by a trusted manner, for example a trusted directory. To address this weakness, the standards community has invented an object called a Certificate. A certificate contains, the certificate issuer's name, the name of the subject for whom the certificate is being issued, the public key of the subject, and some time stamps. You know the public key is good, because the certificate issuer has a certificate too.

Pretty Good Privacy (PGP) is a software package originally developed by Phil Zimmerman that provides encryption and authentication for e-mail and file storage applications. Zimmerman developed his freeware program using existing encryption techniques, and made it available on multiple platforms. It provides message encryption, digital signatures, data compression, and e-mail compatibility. PGP uses RSA for key transport and IDEA for bulk encryption of messages. Zimmerman ran into legal problems with RSA over his use of the RSA algorithm in his program. PGP is now available in a couple of legal forms: MIT PGP versions 2.6 and later are legal freeware for non-commercial use, and Viacrypt PGP versions 2.7 and later are legal commercial versions of the same software.

Time Stamping

Time stamping[6] is a technique that can certify that a certain electronic document or communication existed or was delivered at a certain time. Time stamping uses an encryption model called a Blind Signature Scheme. Blind signature schemes allow the sender to get a message receipted by another party without revealing any information about the message to the other party.

Time stamping is very similar to sending a registered letter through the U.S. mail, but provides an additional level of proof. It can prove that a recipient received a specific document. Possible applications include patent applications, copyright archives, and contracts. Time stamping is a critical application that will help make the transition to electronic legal documents possible.

Electronic Money/ Electronic Cash/ Digital Cash

It includes transactions carried out electronically with a net transfer of funds from one party to another, which may be either debit or credit and can be either anonymous or identified. There are both hardware and software implementations.

Anonymous applications do not reveal the identity of the customer and are based on blind signature schemes. Digicash's Ecash, Identified spending schemes reveal the identity of the customer and are based on more general forms of signature schemes. Anonymous schemes are the electronic analog of cash, while identified schemes are the electronic analog of a debit or credit card. There are also some hybrid approaches where payments can be anonymous with respect to the merchant but not the bank (CyberCash credit card transactions) ; or anonymous to everyone, but traceable (a sequence of purchases can be related, but not linked directly to the spender's identity).

Encryption is used in electronic money schemes to protect conventional transaction data like account numbers and transaction amounts, digital signatures can replace handwritten signatures or a credit-card authorizations, and public-key encryption can provide confidentiality. There are several systems that cover this range of applications, from transactions mimicking conventional paper transactions with values of several dollars and up, to various micropayment schemes that batch extremely low cost transactions into amounts that will bear the overhead of encryption and clearing the bank.

Secure Network Communications

Secure Socket Layer (SSL)

Netscape has developed a public-key protocol called Secure Socket Layer [6](SSL) for providing data security layered between TCP/IP (the foundation of Internet-based communications) and application

protocols (such as HTTP, Telnet, NNTP, or FTP). SSL supports data encryption, server authentication, message integrity, and client authentication for TCP/IP connections.

The SSL Handshake Protocol authenticates each end of the connection (server and client), with the second or client authentication being optional. In phase 1, the client requests the server's certificate and its cipher preferences. When the client receives this information, it generates a master key and encrypts it with the server's public key, then sends the encrypted master key to the server. The server decrypts the master key with its private key, then authenticates itself to the client by returning a message encrypted with the master key. Following data is encrypted with keys derived from the master key. Phase 2, client authentication, is optional. The server challenges the client, and the client responds by returning the client's digital signature on the challenge with its public-key certificate.

SSL uses the RSA public-key cryptosystem for the authentication steps. After the exchange of keys, a number of different cryptosystems are used, including RC2, RC4, IDEA, DES and triple-DES.

Kerberos

Kerberos[6] is an authentication service developed by MIT which uses secret-key ciphers for encryption and authentication. Kerberos was designed to authenticate requests for network resources and does not authenticate authorship of documents.

In a Kerberos system, there is a site on the network, called the Kerberos server, to perform centralized key management and administrative functions. The server maintains a key database with the secret keys of all users, authenticates the identities of users, and distributes session keys to users and servers who need to authenticate one another. Kerberos depends on a trusted third party, the Kerberos server, and if the server were compromised, the integrity of the whole system would be lost. Kerberos is generally used within an administrative domain (for example across a companies closed network); across domains (e.g., the Internet), the more robust functions and properties of public-key systems are often preferred.

Disk Encryption

Disk encryption [6] programs encrypt the entire hard disk so that there in no worry about leaving any traces of the unencrypted data on your disk. PGP can also be used to encrypt files. In this case, PGP uses the user's private key along with a user-supplied password to encrypt the file using IDEA. The same password and key are used to unlock the file. Thus cryptography plays a major role in everyday life and scientists are still trying to invent new techniques so that the messages could be read only by the intended recipient.

References

1. *Neal Koblitz., 1994. A Course in Number Theory and Cryptography*, second *ed*. *Springer*
2. David Burton., 1997. *Elementary Number Theory* fourth ed. Mcgraw-Hill Companies.
3. *Oded Goldreich., 2001. Foundations of Cryptography – Vol. 1,* Cambridge University Press.
4. http://en.m.wikipedia. org/wiki/History_of_cryptography
5. http://fisher.osu.edu/~muhanna.1/pdf/crypto.pdf
6. http://www.laits.utexas. edu/~anorman/...life.htm. http://www.ti89.com/crypto tut/mod_arithmetic.htm.

Scientia
Vol.9, No. 1, Jan - Dec. 2013, pp30-37
ISSN : 0976 - 8289

Alice Thomas*

Department of Statistics, Mercy College, Palakkad-678006.

Abstract

This paper generalizes the Weibull distributions to obtain a wider class of distributions using Marshall-Olkin method by introducing a new parameter. We consider the reliability properties and obtain various characterizations. We extend it to develop a more general class called Marshall-Olkin semi-weibull distributions and construct a first order autoregressive model with these stationary marginal distributions. Applications are also discussed along with simulation studies.

Key words: regressive process, bivariate case, hazard rate functions, reliability properties, Weibull distribution.

Introduction

The need for developing time series models having non–Gaussian marginal distributions has been long felt from the fact that many naturally occurring time series are non–Gaussian with Markovian structure. In recent years Tavares[1], Arnold[2], Arnold and Robertson[3], Anderson and Arnold[4], Sim[5], Yeh et al.[6], Pillai et al[7], Jose and Alice[8], Alice and Jose[9], [10,11,12,13,14,15] and others have developed various autoregressive models with minification structure. Jose et al[16], Krishna et al[17] introduced and discussed various forms of Marshall-Olkin distributions. Dewald et al[18] introduced an additive first order autoregressive bivariate exponential process. The Weibull distributions, including exponential distributions play a central role in the modeling of survival or lifetime data and time series data of non-negative random variables such as hydrological data and wind velocity magnitudes. Johnson and Kotz[19], Galmbos and Kotz[20] discussed various properties of Weibull distributions and Hanagal[21] deals with estimation of reliability. Lewis and McKenzie[22], Brown et al[23] note that although studies have shown that Weibull marginal distribution have been found adequate for wind velocity magnitudes, unfortunately 'no time series models have been rigorously developed for random variables possessing a Weibull distribution'. Wind power data are even more likely to need very long tailed marginal distributions. Again in reliability studies, sequences of times between failures are correlated and models with non-constant marginal hazard rate are needed to model them adequately.

In the present chapter we generalize the family of semi-Weibull distributions to obtain a wider class of distributions using the method of Marshall and Olkin[24] by adding a parameter. In section 2, we derive the probability density function of the new generalized family of distributions. The hazard rate function is also obtained. Some properties of Marshall-Olkin semi-Weibull (MO-SW) distributions are considered. In section 3, we construct an AR (1) model with the new generalized Weibull family as the stationary marginal distribution and innovations distributed as semi-Weibull. We also extend it to kth order In section

**Corresponding author, Email: ambilykj@gmail.com*

4, we derive the probability density function and hazard rate function. Graphs of the probability density function and hazard rate function are obtained with respect to different combinations of the parameters. The hazard rate function is increasing, decreasing and constant with respect to different parameter values showing that this distribution has wider scope for modeling in reliability contexts with respect to different types of reliability data. Also it is shown that this distribution is geometrically extreme stable so that the geometric maximum and geometric minimums are belonging to the same family. In section 5, we construct an AR (1) model with new generalized Weibull family as the stationary marginal distribution and innovations distributed as Weibull and study the sample path behaviour of the process in detail. It is evident from the graphs that the new process is capable to model different types of time series data from reliability, hydrology and financial contexts.

2. Marshall-Olkin semi-Weibull distributions and properties

The Weibull distribution is named after the Swedish physicist Waloddi Weibull. He used this distribution to model the breaking strength of the materials, fatigue life of steel etc. This distribution includes the exponential and the Rayleigh distributions as special cases. This distribution offers wide scope in reliability studies as it can model constant, increasing as well as decreasing hazard rates. Now we consider the generalization of the Weibull distribution namely semi-Weibull distribution.

References

We say that a random variable X with positive support follows the semi Weibull distributions and write $X \sim SW(\beta, \rho)$ if its survival function is given by

$$\bar{F}_X(x) = P(X > x) = \exp(-\psi(x)) \qquad (2.1)$$

where $\psi(x)$ satisfies the functional equation

$$\rho\,\psi(x) = \psi(\rho^{1/\beta}x);\ \beta > 0,\ 0 < \rho < 1. \qquad (2.2)$$

Consider a survival function $\bar{F}$. Then a new family of survival functions is constructed as

$$\bar{G}(x;\alpha) = \frac{\alpha \bar{F}(x)}{1-(1-\alpha)\bar{F}(x)};\ -\infty < x < \infty,\ 0 < \alpha < \infty \qquad (2.3)$$

Clearly when $\alpha = 1$, we get $\bar{G} = \bar{F}$.

Whenever F has a density, the survival function G given by (2.3) have easily computed densities. In particular, if F has a density f and hazard rate η, then G has the density g given by

$$g(x;\alpha) = \frac{\alpha f(x)}{\left(1-(1-\alpha)\bar{F}(x)\right)^2};\ -\infty < x < \infty,\ 0 < \alpha < \infty.$$

and hazard rate

$$r(x;\alpha) = \frac{f_1(x)}{\left[1-(1-\alpha)F(x)\right]}, \quad -\infty < x < \infty, \ 0 < \alpha < \infty.$$

Substituting (2.1) in (2.3) we get another family of distributions, which we shall refer to as Marshall Olkin Semi Weibull (MO-SW) distributions whose survival function is given by

$$\bar{G}(x;\alpha) = \frac{\alpha}{e^{\beta x^{\gamma}}(1-\bar{\alpha})}; \ x > 0, \alpha > 0$$

The probability density function corresponding to G is given by

$$g(x;\alpha) = \frac{\alpha\beta\gamma x^{\gamma-1}e^{\beta x^{\gamma}}}{\left[e^{\beta x^{\gamma}}-(1-\alpha)\right]^2}; \ x > 0, \alpha > 0.$$

The hazard rate is given by

$$r(x;\alpha) = \frac{\beta\gamma x^{\gamma-1}}{1-(1-\alpha)e^{-\beta x^{\gamma}}}; \ x > 0, \alpha > 0.$$

If $\{X_i, i = 1,2, \ldots n\}$ are independent and identically distributed random variables having the survival function of MO-SW $\bar{G}(x)$, then $U_{1:n} = \min(X_1, X_2, \ldots, X_n)$ has the survival function

$$\bar{G}_{1:n}(x) = \left[\frac{\alpha}{\exp(\beta x^{\gamma}) - (1-\alpha)}\right]^n.$$

Theorem 2.1

Let N be an integer valued random variable independent of the X_i's such that $P[N \geq 2] = 1$ where $\{X_n\}, n = 1,2, \ldots$ is a sequence of independent and identically distributed MO-SW random variables. Then $Y = (N/\alpha)^{1/\gamma} \min(X_1, X_2, \ldots, X_N); N > 0, \alpha > 1$ is distributed as semi-Weibull.

Proof

We have

$$F_Y(x) = P[Y > x] = \sum_{n=2}^{\infty} P[N = n]P[Y > x / N = n]$$

$$= \sum_{n=2}^{\infty} P[N = n]\bar{F}_V((n/\alpha)^{-1/\gamma}x)^n$$

$$= \sum_{n=2}^{\infty} P[N = n]\left[\frac{1}{1+(1/\alpha)(e^{\beta(n/\alpha)^{-1/\gamma}x^{\gamma}}-1)}\right]^n = e^{-\beta x^{\gamma}}.$$

Hence Y is distributed as semi Weibull.

Theorem 2.2

Let $\{X_i, i \geq 1\}$ be a sequence of independent and identically distributed random variables with common survival function $\bar{F}(x)$ and N be a geometric random variable with parameter p and $P(N = n) = pq^{n-1}$, $n = 1,2, \ldots$, $0 < p < 1$, $q = 1-p$, which is independent of $\{X_i\}$ for all $i \geq 1$. Let $U_N = \min_{1 \leq i \leq N} X_i$. Then U_N is distributed as MO-SW if and only if X_i is distributed as semi Weibull

Proof

Now we have

$$\bar{F}(x) = \frac{p\bar{F}(x)}{1-(1-p)\bar{F}(x)}.$$

Suppose $\bar{F}(x) = \exp\{-\psi(x)\}$,

Then $\bar{F}(x) = \frac{1}{1-(1-p)(e^{\psi(x)}-1)}$, which is MO-SW.

This proves the necessary part of the theorem.

Conversely suppose $\bar{F}(x) = \frac{1}{1-(1-p)(e^{\psi(x)}-1)}$,

Then we get $F(x) = 1 - \exp\{-\psi(x)\}$,

which is the survival function of semi – Weibull

3. An AR(1) model with MO-SW marginal distributions

Theorem 3.1

Consider the AR (1) structure

$$X_n = \begin{cases} \varepsilon_n & \text{with probability } p \\ \min\{X_{n-1}, \varepsilon_n\} & \text{with probability } (1-p) \end{cases} \qquad (3.1)$$

$0 \leq p \leq 1$, where $\{\varepsilon_n\}$ is a sequence of i.i.d random variables independent of $\{X_{n-1}, X_{n-2}, \ldots\}$, then $\{X_n\}$ is a stationary Markovian AR(1) process with MO-SW marginals if and only if $\{\varepsilon_n\}$ is distributed as semi-Weibull distributions.

Proof

Here we proceed by taking $\bar{F}_{\varepsilon}(x) = e^{-\psi(x)}$,

then it easily follows that $\bar{F}_X(x) = \frac{p}{e^{\psi(x)} - (1-p)}$, which is the survival function of MO-SW.

Conversely if we take $F_X(x) = \frac{p}{e^{\psi(x)} - (1-p)}$, it is easy to show that $\{\varepsilon_n\}$ is distributed as semi-Weibull and the process is stationary. In order to establish stationarity we proceed as follows

Assume that $X_1 \sim$ MO-SW with $\alpha = \alpha^*$ and $\beta = \beta^*$ where α^* and β^* are known. We have

Then $\bar{F}_{X_1}(x) = \dfrac{\alpha^* e^{-\lambda^* x^{\beta^*}}}{1-(1-\alpha^*)e^{-\lambda^* x^{\beta^*}}}$

This establishes that $\{X_n\}$ is distributed as MO-SW. Even if X_0 is not known it is easy to establish that $\{X_n\}$ is stationary and is asymptotically equivalent to MO-SW.

It can be seen that the semi-Weibull distribution is a more general class of distributions which includes Weibull distribution in the sense that for $b(x) = 1$, we have $\omega(x) = x^{\beta}$.

Theorem 3.2

Consider an autoregressive model of order k as follows

$$X_n = \begin{cases} \in_n^{*} & \text{with prob.} \quad p_0 \\ \min(X_{n-1}, \in_n) & \text{with prob.} \quad p_1 \\ \min(X_{n-2}, \in_n) & \text{with prob.} \quad p_2 \\ \vdots & \\ \min(X_{n-k}, \in_n) & \text{with prob.} \quad p_k \end{cases} \qquad (3.2)$$

where $0 < p_i < 1$, $\sum_{i=0}^{k} p_i = 1$ and $\{\in_n^{*}\}$ is a sequence of iid random variables.

Then $\{X_n\}$ has stationary marginal distribution as MO-SW if and only if $\{\in_n^{*}\}$ is distributed as semi-Weibull.

4. Marshall-Olkin generalized Weibull distribution

Consider the two parameter Weibull distribution with survival function $\bar{F}(x) = \exp(-\lambda x^{\beta})$; $x > 0, \lambda > 0, \beta > 0$.

Substituting this in (2.3) we get a new family of distributions, which we shall refer to as the Marshall–Olkin Generalized Weibull (MO-GW) family, whose survival function is given by

$$\bar{G}(x;\alpha,\lambda,\beta) = \frac{\alpha \exp[-(\lambda x)^{\beta}]}{1-(1-\alpha)\exp[-(\lambda x)^{\beta}]}; \quad x > 0, \lambda, \beta, \alpha > 0.$$

Table 5.1 gives the cumulative distribution function of MO-GW distribution.

The probability density function corresponding to $\bar{G}$ is given by

$$g(x;\alpha,\lambda,\beta) = \frac{\alpha\beta\lambda^{\beta}x^{\beta-1}\exp(\lambda x)^{\beta}}{\{\exp(\lambda x)^{\beta} - (1-\alpha)\}^2}, \quad x > 0, \lambda, \beta, \alpha > 0.$$

The hazard rate is given by

$$r(x;\alpha,\lambda,\beta) = \frac{\lambda^{\beta}\beta(\alpha)x^{\beta-1}\exp(\lambda x)^{\beta}}{\{\exp(\lambda x)^{\beta} - (1-\alpha)\}}, \quad x > 0, \lambda, \beta, \alpha > 0.$$

Figure (4.1) gives the graphs of the probability density functions $g(x)$ for $\alpha = .05, 1, 5, 10$; $\lambda = 1$ and $\beta = 1$. It is clear that for values of α close to 1, the curve resembles the standard Weibull distribution, while as $\alpha \to \infty$, the curve tends to be symmetric with close resemblance to the normal distribution.

We also explore the nature of the hazard rate $r(x)$. It is increasing if $\alpha \geq 1$, $\beta \geq 1$ and decreasing if $\alpha \leq 1$, $\beta \leq 1$. If $\beta > 1$ then $r(x)$ is initially increasing and eventually increasing but there may be an interval where it is decreasing. Similarly if $\beta < 1$, then $r(x)$ is initially decreasing and eventually decreasing but there is an interval where it is increasing. When $\alpha = 1$, it coincides with the Weibull distribution. The graphs are depicted in figure 3.2a, 3.2b and figure 3.2c. This point out the wide applicability of the MO-GW distribution in modeling various types of reliability data.

Theorem 4.1

Marshall-Olkin generalized Weibull distribution is geometric maximum stable.

Proof

Let $X_1, X_2, \ldots$ be a sequence of independent, identically distributed random variables. Suppose N is independent of the X_i's with a geometric (p) distribution, $P(N = n) = (1-p)^{n-1} p$, $n = 1, 2, \ldots$ and let $U_N = \min(X_1, X_2, \ldots, X_N)$, $V_N = \max(X_1, X_2, \ldots, X_N)$.

$$\bar{G}(x) = P(U_N > x) = P(X_1 > x, X_2 > x, \ldots, X_N > x)$$

$$= \sum_{n=1}^{\infty} \bar{F}^n(x)(1-p)^{n-1} p = \frac{p\bar{F}(x)}{1-(1-p)\bar{F}(x)}, \quad -\infty < x < \infty$$

Suppose $\bar{F}(x) = \dfrac{\alpha \exp[-(\lambda x)^{\beta}]}{1-(1-\alpha)\exp[-(\lambda x)^{\beta}]}$, which is the survival function of Marshall-Olkin Generalised Weibull (MO-GW). Then

$$\bar{G}(x) = \frac{1}{1-\dfrac{1}{p+\alpha}\left(e^{\lambda x^{\beta}} - \alpha\right)}$$

Hence U_N is geometric minimum stable.

Let $V_N = \max(X_1, X_2, \ldots, X_N)$. Then

$$H(x) = P(V_N \leq x) = P(X_1 \leq x, X_2 \leq x, \ldots, X_N \leq x)$$

$$= \sum_{n=1}^{\infty} F^n(x)(1-p)^{n-1} = \frac{pF(x)}{1-(1-p)F(x)},$$

so that $h(x) = \dfrac{\bar{F}(x)}{p + (1-p)F(x)}$, $-\infty < x < \infty$.

Suppose $\bar{F}(x) = \frac{\alpha \exp[-(\lambda x)^{\beta}]}{1-(1-\alpha)\exp[-(\lambda x)^{\beta}]}$, which is the survival function of MO-GW distribution.

Then $\bar{H}(x) = \frac{1}{1-(\rho/\alpha)(\exp[(\alpha x)^{\beta}]-1)}$. Hence V_n is geometric extreme stable. Hence the sum of

of MO-GW distribution with the survival function of the form $\bar{F}(x) = \frac{\alpha \exp[-(\lambda x)^{\beta}]}{1-(1-\alpha)\exp[-(\lambda x)^{\beta}]}$ is

geometric extreme stable.

Theorem 4.3

Let $\{X_i, i \geq 1\}$ be a sequence of independent and identically distributed random variables with common survival function $\bar{F}(x)$ and

N be a geometric random variable with probability mass function $P(N = n) = pq^{n-1}$, $n = 1, 2, \ldots$, $0 < p < 1$, $q = 1 - p$, which is independent of $\{X_i\}$ for $i \geq 1$. Let $U_N = \min_{1 \leq i \leq N} X_i$. Then U_N is distributed as MO-GW if and only if X_i is distributed as Weibull.

Proof

Proceeding as in Theorem 2.2 we have $\bar{H}(x) = \frac{p\bar{F}(x)}{1-(1-p)\bar{F}(x)}$.

Suppose $\bar{F}(x) = \exp(-\lambda x)^{\beta}$, the survival function of Weibull distribution, then $\bar{H}(x) = \frac{\bar{F}}{1-(1/p)(e^{(\lambda x)^{\beta}}-1)}$, which is the survival function of MO-GW. This proves the sufficiency part of the theorem.

To prove the converse, assume $\bar{H}(x) = \frac{1}{1+(1/p)(e^{(\lambda x)^{\beta}}-1)}$

Then we get $\bar{F}(x) = \exp(-\lambda x)^{\beta}$, which is the survival function of Weibull. Hence the proof is complete.

5. An AR (1) model with MO-GW marginal distribution

Theorem 5.1

Consider the AR (1) scheme given by (3.1), where $\{\varepsilon_n\}$ is a sequence of independent and identically distributed random variables independent of $\{X_1, X_2, \ldots\}$; then $\{X_n\}$ is a stationary Markovian AR(1) process with MO-GW marginals if and only if $\{\varepsilon_n\}$ is distributed as Weibull distribution with parameters λ and β.

Proof

Proceeding as in the case of Theorem 3.1, if we take

$\bar{F}_{\varepsilon}(x) = \exp(-\lambda x)^{\beta}$, then it easily follows that

$$\overline{F}_{\epsilon}(x) = p \exp(-\lambda x)^{\beta} / [1-(1-p)\exp(-\lambda x)^{\beta}]$$
$$= p / [\exp(\lambda x)^{\beta} - (1-p)]$$

which is the survival function of MO-GW

Conversely if we take $F_{\epsilon_n}(x) = p / [\exp(\lambda x)^{\beta} - (1-p)]$, it is easy to show that $1-\epsilon_n(x)$ is distributed as Weibull with parameter λ, β and the process is stationary. In order to establish stationarity we proceed as follows.

Assume $X_0 \overset{d}{=}$ MO-GW (p,λ,β) and $\{\epsilon_n\} \overset{d}{=}$ Weibull(λ,β).

Then $F_{X_1}(x) = p[\exp(-\lambda x)^{\beta}]/[1-(1-p)\exp(-\lambda x)^{\beta}]$.

Thus establishes that $\{X_n\}$ is distributed as MO-GW(p, λ,β). Even if X_0 is arbitrary, it is easy to establish that $\{X_n\}$ is stationary and is asymptotically marginally distributed as MO-GW.

Theorem 5.2

Consider an autoregressive model X_n of order k with structure (3.2). Then $\{X_n\}$ has stationary marginal distribution as MO-GW if and only if $\{\epsilon_n\}$ is distributed as Weibull.

Proof is similar to Theorem 5.1.

5.1 Sample path behaviour

The sample path behaviour of the MO-GWAR (1) process for different values of p and β are given in figure 3.3. These observations can be verified by referring to the Table 3.2 showing $P(X_n < X_{n-1})$. These probabilities are obtained through a Monte Carlo simulation procedure. Sequences of 100, 300, 500, 700, 900 observations from MO-GWAR (1) process are generated repeatedly for ten times and for each sequence the probability is estimated. A table of such probabilities is provided with the average from ten trials along with an estimate of standard error given in brackets (See Table 3.2).

Table 3.1. c.d.f. **Table of MOCW distribution for $\lambda = 1, \beta = 0.5$**

x \ α	0.1	0.2	0.3	0.4	0.5	0.6	0.7	0.8
0.005	0.02442	0.012361	0.008275	0.006219	0.004981	0.004155	0.003563	0.003119
0.01	0.047933	0.02445	0.016134	0.012376	0.009926	0.008283	0.00711	0.006227
0.03	0.121259	0.070256	0.047961	0.036407	0.029339	0.02457	0.021134	0.018541
0.05	[illegible]	0.112334	0.077317	0.059521	0.047319	0.040181	0.034902	0.030673
0.1	0.328925	0.204047	0.145059	0.113615	0.093006	0.078715	0.068246	0.060227
0.15	0.437535	0.280276	0.206196	0.162977	0.134775	0.114853	0.100123	0.088716
0.2	0.512601	0.34463	0.259572	0.208189	0.173787	0.149142	0.130619	0.116159
0.25	0.571959	0.399667	0.307447	0.24974	0.209496	0.181612	0.159814	0.142657
0.3	0.618079	0.447261	0.350416	0.288046	0.244524	0.212427	0.187779	0.168255
0.35	0.656515	0.488813	0.389308	0.323163	0.275569	0.241763	0.214283	0.192655
0.4	0.688564	0.525395	0.424529	0.356295	0.306306	0.269542	0.240289	0.216763
0.45	0.716149	0.557838	0.456339	0.386807	0.335392	0.296641	0.264955	0.239977
0.5	0.739601	0.586799	0.486324	0.415226	0.362266	0.321285	0.288636	0.26201
0.55	0.759932	0.612801	0.513106	0.441753	0.387653	0.345957	0.311383	0.283495
0.6	0.777708	0.63627	0.538351	0.466566	0.411567	0.368277	0.333244	0.304252
0.65	0.793452	0.657552	0.561123	0.489816	0.434109	0.390363	0.354262	0.324312
0.7	0.807247	0.676933	0.582795	0.51164	0.45597	0.411226	0.374479	0.343761
0.75	0.819517	0.694652	0.602544	0.532139	0.476435	0.431277	0.393935	0.362345
0.8	0.831021	0.710909	0.621128	0.551481	0.495879	0.450461	0.412065	0.380721
0.85	0.841167	0.725874	0.638576	0.569703	0.51437	0.468821	0.430705	0.399311
0.9	0.850759	0.739689	0.654592	0.58691	0.531972	0.486472	0.448085	0.415739
0.95	0.85975	0.75218	0.669599	0.60318	0.548712	0.503317	0.464838	0.431924
	0.866439	0.764351	0.683785	0.618583	0.564733	0.519506	0.48099	0.447799
1.	0.879988	0.785696	0.709555	0.647034	0.594568	0.549677	0.511601	0.479321
1.2	0.891554	0.804326	0.733549	0.6727	0.621819	0.578054	0.540115	0.506618
1.4	0.916319	0.835222	0.771547	0.717063	0.669595	0.628155	0.59154	0.558525
1.6	0.924559	0.859702	0.803348	0.753928	0.710236	0.67127	0.636466	0.605044
1.8	0.935991	0.879489	0.829597	0.7849	0.744346	0.708682	0.675866	0.645555
2	0.945003	0.89574	0.851159	0.81165	0.7746	0.741156	0.710638	0.682123
2.5	0.961395	0.92566	0.892456	0.861602	0.832795	0.805847	0.780588	0.756654
3	0.97209	0.945677	0.92057	0.896952	0.874425	0.853064	0.832604	0.813154

3.5	0.979401	0.959633	0.940648	0.922399	0.904845	0.887947	0.871668	0.855975
4	0.984589	0.969647	0.955151	0.941082	0.927421	0.914151	0.901256	0.88872
5	0.991137	0.982439	0.973873	0.965465	0.957201	0.949077	0.94109	0.933236
6	0.994788	0.98963	0.984525	0.979472	0.974471	0.969521	0.964621	0.95977
7	0.996806	0.993811	0.990745	0.987608	0.98467	0.98166	0.978669	0.975695
8	0.998138	0.996282	0.994434	0.992592	0.990758	0.98893	0.987108	0.985294
9	0.998878	0.997758	0.996641	0.995527	0.994414	0.993305	0.992198	0.991093
10	0.999322	0.998645	0.997969	0.997294	0.99662	0.995946	0.995274	0.994602
12	0.999752	0.999503	0.999255	0.999007	0.998759	0.998511	0.998264	0.998016
16	0.999966	0.999933	0.999899	0.999866	0.999832	0.999799	0.999765	0.999732
20	0.999995	0.999991	0.999986	0.999982	0.999977	0.999973	0.999968	0.999964
25	1	0.999999	0.999999	0.999999	0.999998	0.999998	0.999997	0.999997
30	1	1	1	1	1	1	1	1

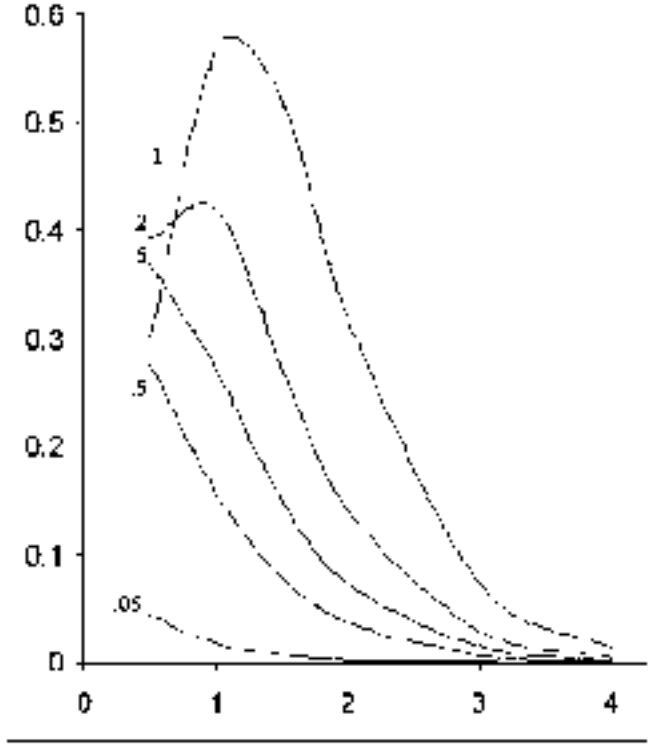

Fig.3.1.p.d.f of MOGW for various values of $\alpha, \lambda = 1, \beta = 2$

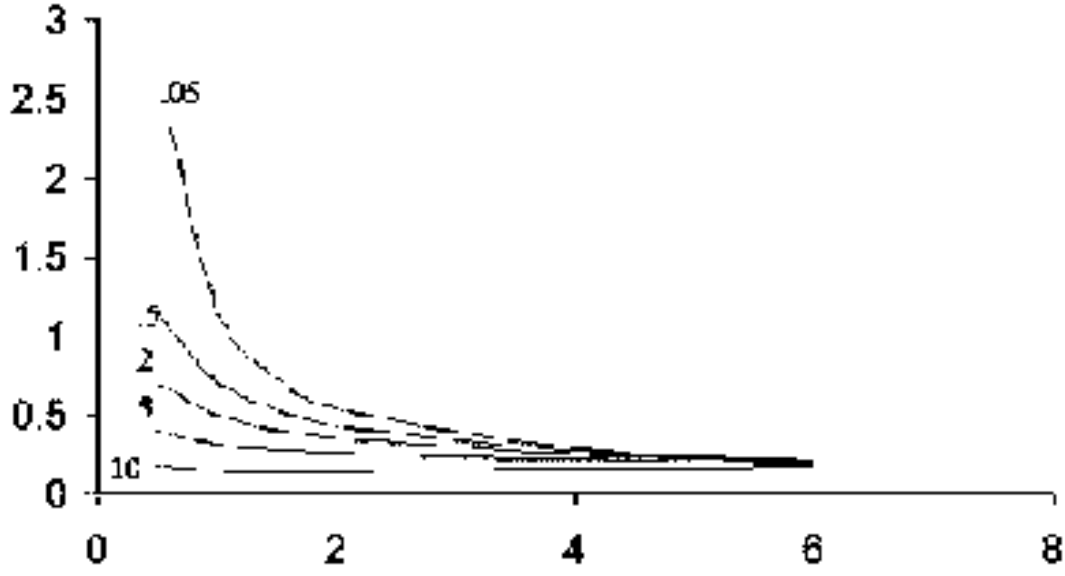

Fig.3.2a. Hazard rate function of MOGW for various values of α and $\lambda = 1$, $\beta = 0.5$

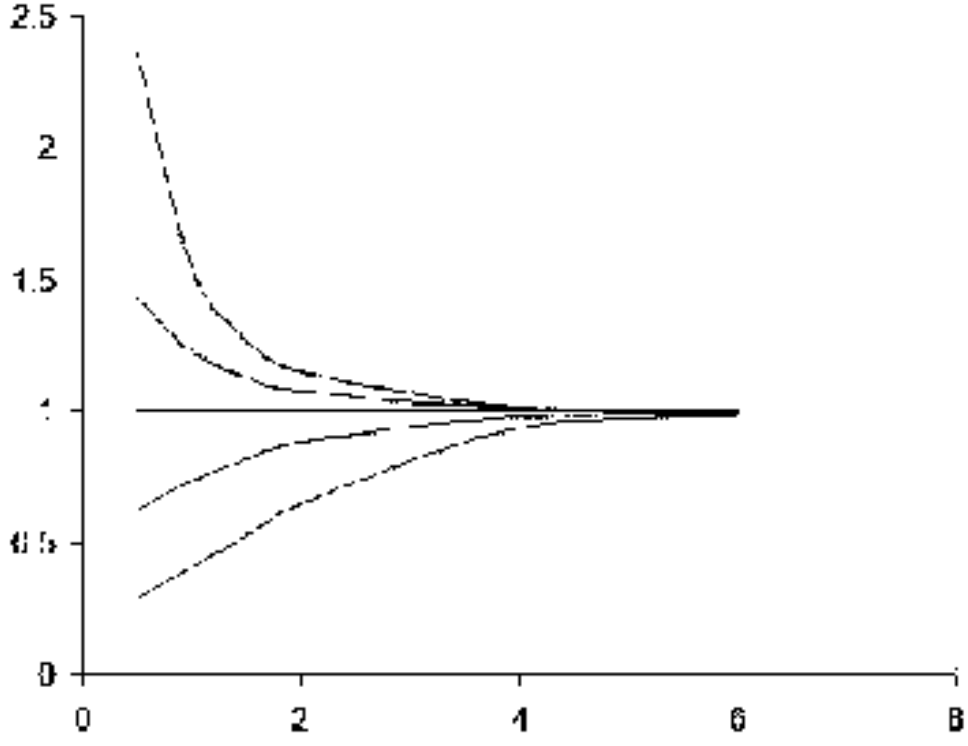

Fig.3.2b. Hazard rate function of MOGW for various values of α and $\lambda = .$, $\beta = .$

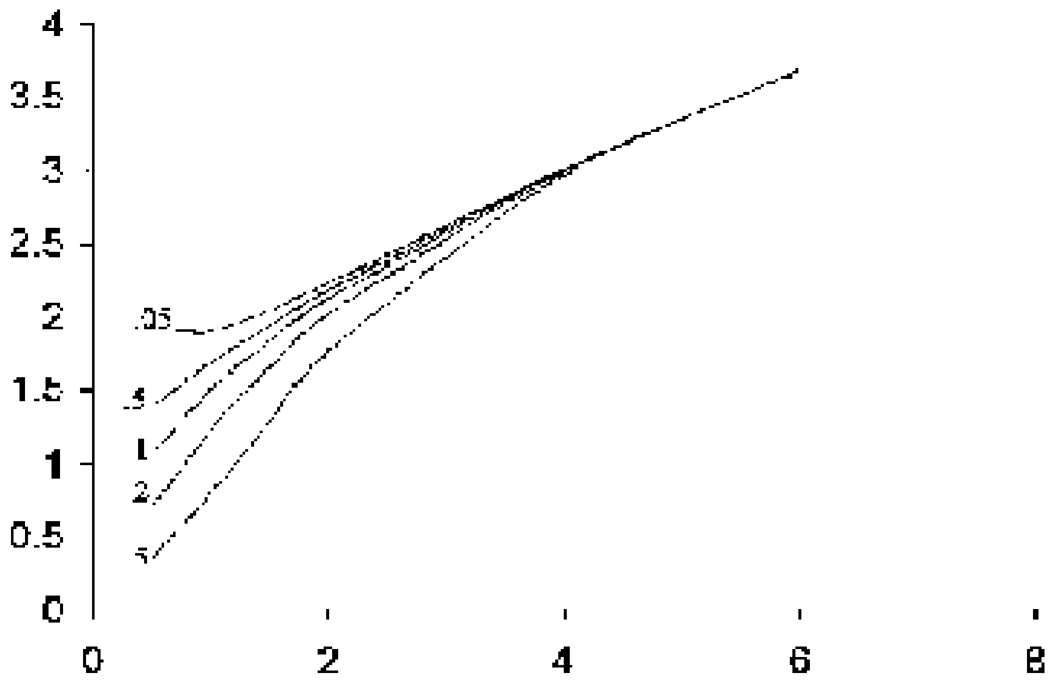

Fig.3.2c. Hazard rate function of MOGW for various values of α and λ = 1, β = 2.

Table 3.2 $P(X_n < X_{n+1})$ for the MOGWAR(1) process when λ = 1, β = 5

(Standard error given in brackets)

p/n	200	400	600	800	1000
0.1	0.7705171 (0.0029001358)	0.7523951 (0.0036614558)	0.7573606 (0.002599518)	0.745249 (0.0032595377)	0.7585128 (0.0021389177)
0.2	0.6740114 (0.0026064845)	0.6557776 (0.0034481987)	0.6564568 (0.0032624489)	0.6621319 (0.0024557129)	0.6651536 (0.0017652571)
0.3	0.5253240 (0.0551365)	0.5697756 (0.0022648813)	0.5930808 (0.0299573)	0.554139 (0.002407355)	0.5913163 (0.0030541616)
0.4	0.5027496 (0.0036997938)	0.4852535 (0.0043944413)	0.5230972 (0.0034650777)	0.5237219 (0.001724345)	0.5153204 (0.002951751)
0.5	0.4097892 (0.0024180096)	0.4350949 (0.0031213511)	0.4486389 (0.0034257733)	0.4265552 (0.0030871083)	0.4378709 (0.0018939821)
0.6	0.3229861 (0.003857560)	0.3545796 (0.0050020925)	0.3573585 (0.003365153)	0.3421062 (0.0024212807)	0.337975 (0.003009082)
0.7	0.2695293 (0.0050095901)	0.2676158 (0.0031685013)	0.2516377 (0.003340412)	0.2775244 (0.0034590137)	0.2731059 (0.003440734)
0.8	0.1874956 (0.0035806508)	0.2107357 (0.0055069411)	0.1766628 (0.002695997)	0.1861547 (0.0023855325)	0.2006061 (0.0033087591)
0.9	0.1175264 (0.0029446155)	0.1154025 (0.0052529862)	0.1119517 (0.0018494928)	0.1012818 (0.0024789095)	0.1120154 (0.0035103906)

1. Tavares, L. V. ,1980. An exponential Markovian stationary process, *J. Appl. Prob*. 17, 1117- 1120.
2. Arnold, B. C. ,1993. Logistic processes involving Markovian minimization. *Commun. Statist.-Theory Meth*., 22(6), 1699-1707.
3. Arnold, B. C. and Robertson, C. A.,1989. Autoregressive logistic processes, *J. Appl. Prob.*, 26, 524-531.
4. Anderson, D. N. and Arnold, B. C.,1993. Linnik distributions and processes, *J. Appl. Prob.*, 30, 330-340.
5. Sim, C. H.,1986. Simulation of Weibull and gamma autoregressive stationary Process, *Commun. Statist.-Simul. Comput*., B 15, 1141-1146.
6. Yeh, H. C., Arnold, B. C. and Robertson, C. A.,1988. Pareto processes, *J. Appl. Prob*., 25, 291-301.
7. Pillai, R.N., Jose, K. K. and Jayakumar, K.,1995. Autoregressive minification processes and the class of distributions of universal geometric minima, *J. Indian Stat. Assoc*, 33,53-61.
8. Jose, K. K. and Alice, T.,2001. Marshall-Olkin generalized Weibull Distributions and Applications, *STARS Int. Journal* 2, 1, 1-8.
9. Alice, T. and Jose, K. K.,2002. Multivariate Minification Processes, *STARS*: *Int. Journal*, Vol. 3, 1-9.
10. Alice, T. and Jose, K.K., 2003. Marshall-Olkin Pareto Processes, *Far East Journal of Theoretical Statistics* 9, 2,117-132.
11. Alice, T. and Jose, K. K.,2004a. Bivariate semi-Pareto minification Processes, *Metrika* 59, 305-313.
12. Alice, T. and Jose, K. K.,2004b. Marshall-Olkin Pareto distributions and its reliability applications, *IAPQR Transactions*, 29,1,1-9.
13. Alice, T. and Jose, K. K.,2004c. Marshall-Olkin Exponential Time series modelling *STARS: Int. Journal* 5,1,12-22.
14. Alice, T. and Jose, K.K.,2005a. Bivariate Marshall-Olkin semi-Weibull distributions and autoregressive Processes, *J.Statistical Studies.*
15. Alice, T. and Jose, K. K.,2005b. Logistic Processes, *STARS* : *Int. Journal*, Vol. 6, 1-9.
16. Jose KK, Ristic MM, Ancy J., 2011. Marshall Olkin Weibull distributions and minification processes. *Stat. Pap*. 52,789–798.
17. Krishna, Jose, Alice, Ristic ., 2013.The Marshall-Olkin Frechet Distribution, *Communication in Statistics-Theory and Methods*,42:22,4091-4107.
18. Dewald, L. S. and Lewis, P. A. W. ,1985. A new Laplace second order autoregressive time series model NLAR(2), *IEEE Trans. Infor. Theor.*, Vol. IT. 31, 5, 645-651.
19. Johnson, N. L., and Kotz, S.,1970. *Continuous Univariate Distributions –1*, John Wiley and Sons, New York.
20. Galambos, J. and Kotz, S.,1978. *Characterizations of Probability Distributions*, Springer-Verlag, New York.
21. Hanagal, D.D.,1996. Estimation of system reliability from stress-strength relationship, *Communication in Statistics:*

Theory and Methods 25,1783– 1797.

22. Lewis, P. A. W. and McKenzie, E.,1991. Minification process and their Transformations, *J. Appl. Prob*., 28, 45-57.
23. Brown, B. G., Katz, R. W. and Murphy, A. H.,1984. Time series models to Simulate and forecast wind speed and wind power. *J. Climate Appl. Meteorol*. 23, 1184-1195.
24. Marshall, A. W. and Olkin, I.,1997. A new method for adding a parameter to a family of distributions with application to the exponential and Weibull families. *Biometrica*, 84, 3, 641-652.

Bhuvaneshwari. N[1], Kavitha. S[2] and Lakshmi. M[1]

[1]Department Of Physics, Mercy College, Calicut University, Palakkad, Kerala, India.

[2]Departmkent of Physics, Christ College, Calicut University, Irrinjalakkuda, Kerala, India.

Abstract

Cadmium sulphide (CdS) is a wide band gap semiconductor which has emerged as an important material due to its applications in optical filters , multilayer light emitting diodes, photo detectors, thin film field effect transistors and photovoltaic cell as window layers. CdS is naturally an n-type material with an optical band gap of 2.41 eV. In the present work cadmium sulphide thin films were prepared by chemical bath deposition technique (CBD) on Fluorine doped tin oxide (FTO) glass and plain glass substrates. To get good CdS films we have chosen two methods of preparations. In first method a chemical bath containing cadmium chloride (CdCl_2), triethanol amine (TEA), ammonium hydroxide (NH_4 OH) and thiourea was used. The deposition was carried out at 70? for 15min. In the second method TEA was avoided under altered deposition condition. The morphological study of the film was done with scanning electron microscopy (SEM) and elemental analysis was done with Energy dispersive X- ray spectrometer (EDS/EDX). The absorption spectra were recorded using a UV-visible double beam spectrophotometer and structural characterization was done by X-ray diffraction spectrometer (XRD). Using Keithley source measuring unit electrical resistance of CdS thin films was measured. Modification of morphology, structural, and optical properties of these thin films were achieved by annealing. It was found that the first method maintains cadmium to sulphur ratio near to unity both before and after annealing. But the stoichiometry is poor in second method. Comparison of CdS film prepared by these two different procedures reveal that first method will be more appropriate for solar cell fabrication. Solar cell was tried by using FTO/TiO_2/CdS as photo anode and platinum as cathode .The efficiency of these cells were found to be very less and it may be due to high resistance of CdS layer.

Key words: CdS, Chemical bath deposition, DSSC.

Introduction

Cadmium sulphide (CdS) is a II–VI compound semiconductor which has gained attention due to its various applications and capability of large-area deposition in the form of thin films[1,2] . Different techniques for the deposition of CdS thin film includes electrostatic deposition, spray pyrolysis, pulsed laser deposition, chemical bath deposition (CBD), etc[3] . Among these techniques, CBD process is more attractive due to simplicity and low cost. This technique can yield homogeneous, adherent, transparent and highly stoichiometric CdS films[4]. One of the interesting properties of this material is its photoconductivity[5] and the polycrystalline CdS films have been used to produce thin film solar cells[6]. Other applications of CdS films include various photoconductive devices[7], image intensifiers [6] and

electroluminescent devices. CdS was also one of the first semiconductor materials to be used for thin-film transistors (TFTs)[8]. In the present work, CdS thin films are prepared using two slightly different chemical bath deposition methods. The structural, surface morphological, compositional, electrical and optical properties of as-deposited and annealed thin films prepared through both methods are studied.

Materials and methods

Cadmium sulphide thin films are prepared by chemical bath deposition technique (CBD) on plain glass substrate and Fluorine doped tin oxide (FTO) coated glass substrate. Two slightly different methods of preparation is adopted which is hereby referred to as 'method a' and 'method b'. In 'method a' chemical bath containing

Fig .1 Experimental set up for chemical bath deposition of CdS thin film

The crystallographic nature of these thin films was studied using X-ray diffractometer. The diffraction

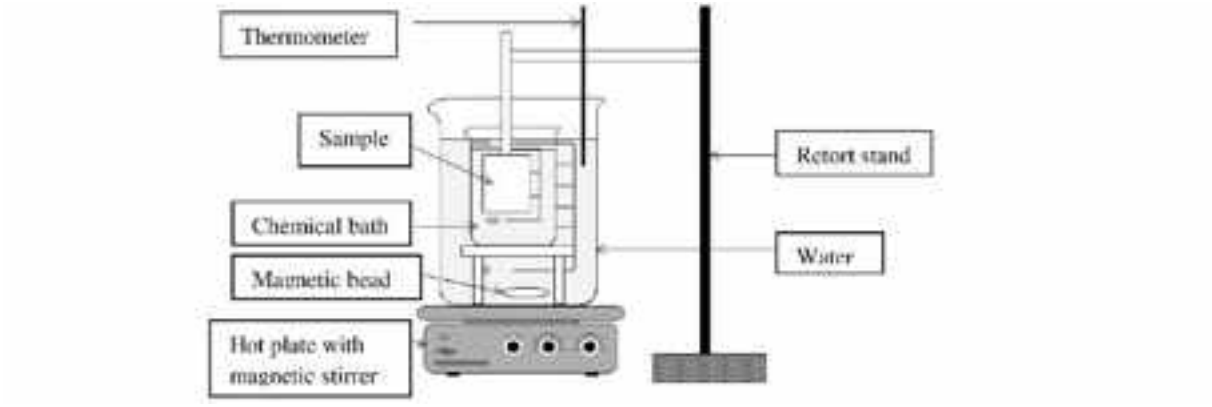

spectra were obtained for 2θ in the range of 20-80°. SEM pictures were taken to view the surface morphology of the films. The elemental analysis were done using Energy dispersive X-ray spectrum (EDAX). A double beam UV-visible spectrometer was used to study absorption spectrum. Resistance measurements were done using Keithley source measuring unit.

Results and Discussion

Structural Studies

The XRD spectra of as-deposited and annealed CdS films prepared by the two methods are shown in Fig: 2, Fig: 3, Fig: 4 and Fig: 5 respectively. Fig: 2 shows the XRD pattern for as-deposited CdS film prepared by 'method a'. Here the diffraction peaks corresponds to the (002) and (110) lattice plane of hexagonal phase. When this CdS film was annealed at 200 in air for 40 minutes, XRD spectrum revealed improvement in crystallinity with new preferred planes of (101) and (201) of hexagonal structure [Fig: 3].

This was confirmed with the standard data card (JCPDS 80-0006). Similarly XRD spectra of as-deposited CdS thin film prepared by 'method b' [Fig: 4], shows strong lines of (002), (101) and (201) orientations of hexagonal structure. Fig: 5 shows annealed CdS film prepared by 'method b'. The diffraction peaks in Fig: 4 completely disappeared and new orientations (102), (200), (103) and (220) are found to appear. Formation of new phase of CdO with (200) and (220) planes were confirmed (standard JCPDS data (75-1529)). In both methods annealed films show well resolved peaks and also their peak widths are found to decrease slightly when compared with that of the as prepared CdS films, justifying improvement in crystalline nature.

Fig. 2 XRD pattern of as-deposited CdS film prepared by method a

Fig. 3 XRD pattern of annealed CdS film prepared by method a

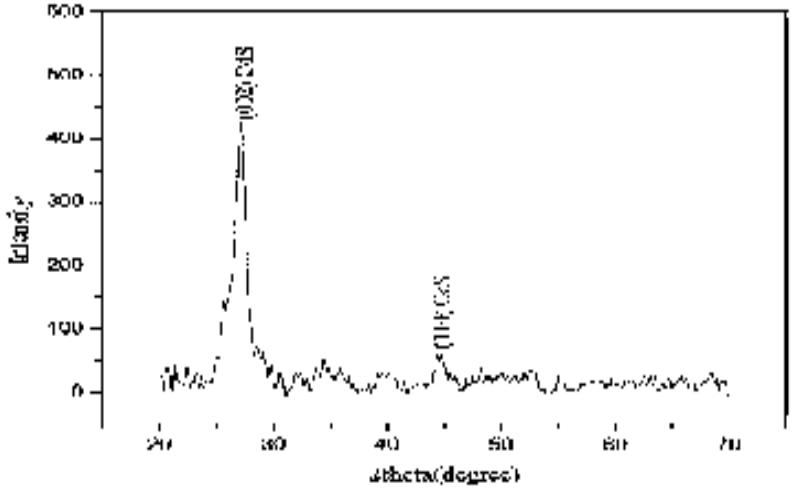

Fig. 4 XRD pattern of as-deposited CdS film prepared by method b

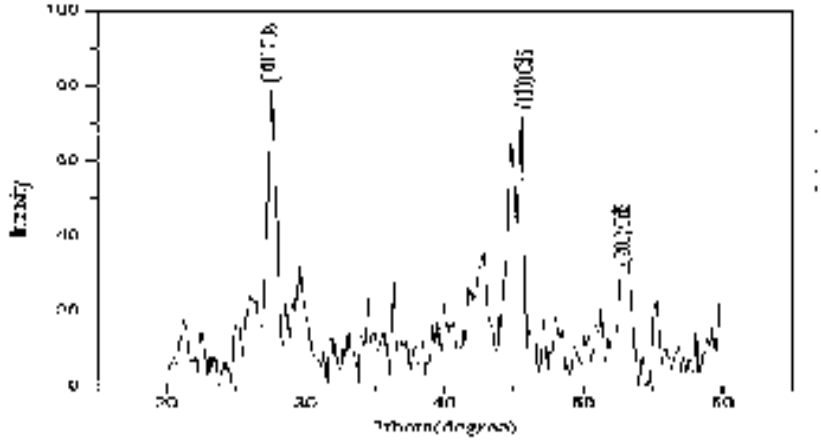

Fig. 5 XRD pattern of annealed CdS film prepared by method b

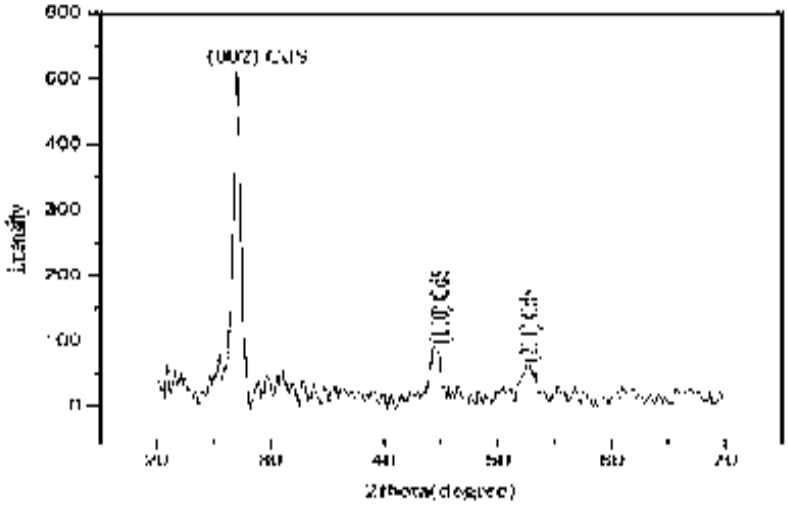

The average crystallite size has been calculated by using Scherer's equation, **D=Kλ／βcosθ** where, the

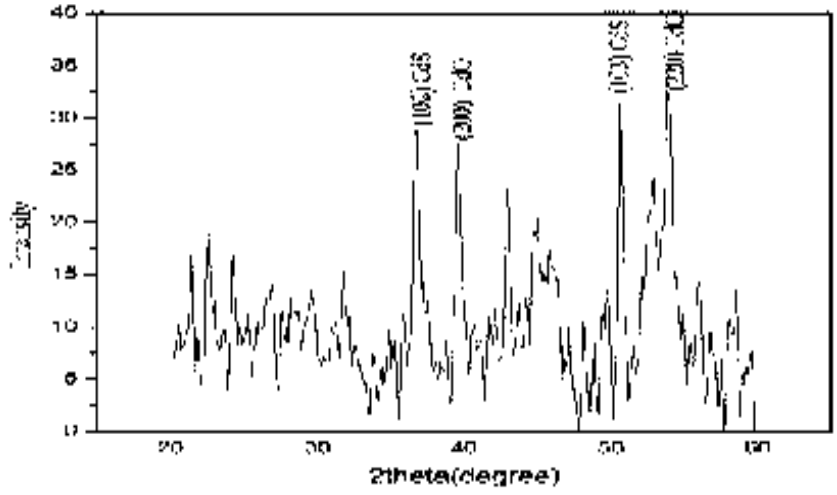

constant *K* is the shape factor (0.94), λ the wave length of X-ray (0.15418 nm), β the FWHM in radians and θ is the Bragg's angle. It has been observed that the grain size of the CdS film prepared by 'method a' increases from 28 nm to 50 nm and 'method b' from 50 nm to around 58 nm when annealed at 200°C.

Surface morphology

SEM yields microscopic information of the surface. This technique is helpful to identify the growth mode, determining the effect of complexing agent on the film morphology. Here the micrographs reveal the homogeneity of film prepared through both methods.

Fig. 6 SEM images of CdS films prepared by 'method a' (a) as-deposited (5000 magnification) (b) as-deposited (10000 magnifications) (c) annealed (5000 magnification)

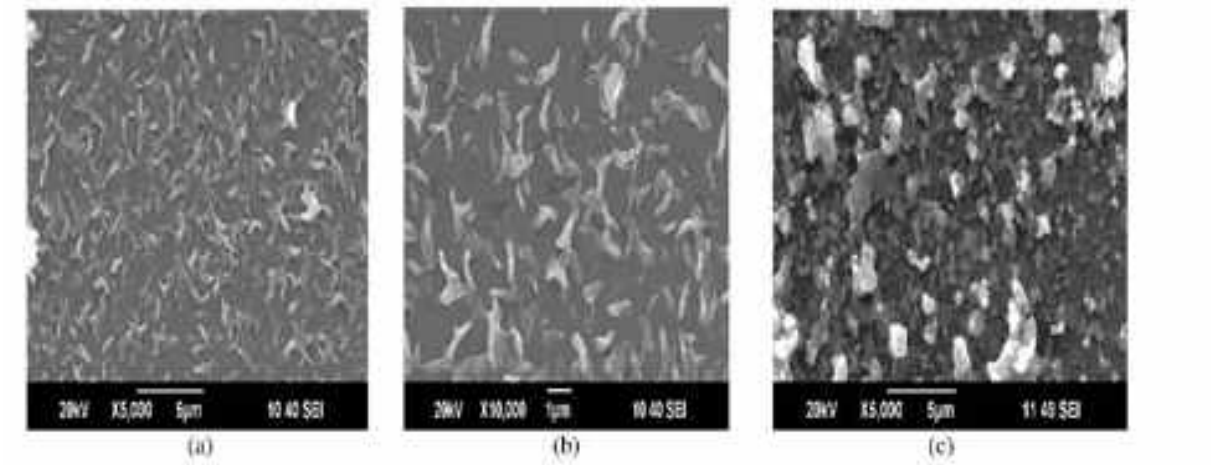

Fig.7 (a) & Fig. 7(b) shows SEM image of as-deposited CdS film prepared by 'method b' of different magnifications. They are having granular structure. Gaps seen in-between the grains suggest that this film

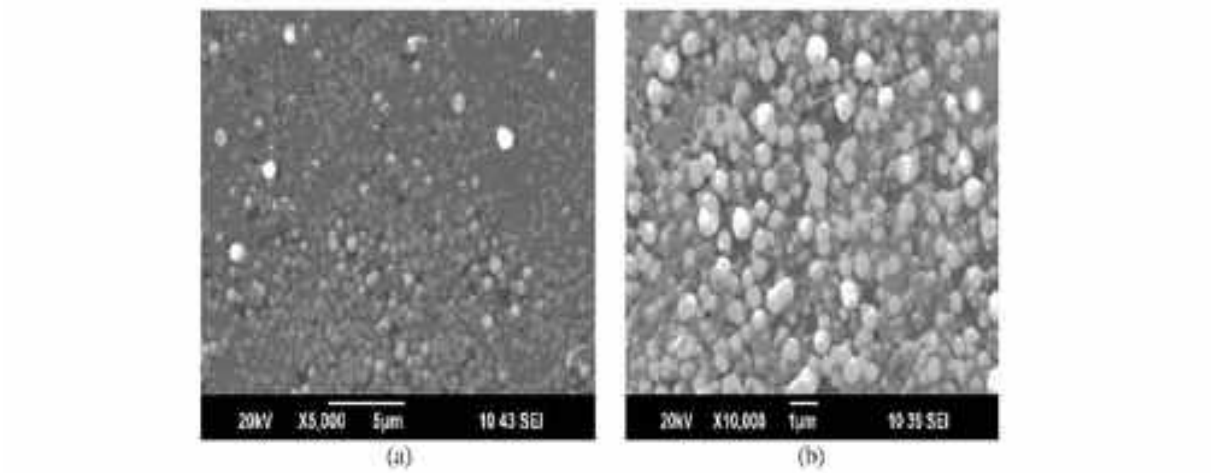

is not so continuous in nature. Fig. 7 (c) Fig.7 (d) and F

Energy Dispersive X-ray analysis (E-DAX)

In material characterization, it is important to determine the stoichiometry. Here this was performed with EDAX analysis where a focused probe of x-rays is scanned over a small surface area and the characteristic elemental signals are used to produce an elemental map of the surface. The presence of cadmium, sulphur and other elements of substrate (silicon, sodium, calcium etc…) were detected in the E-DAX spectrum.

To understand the composition between cadmium and sulphur, Cd/S ratio was calculated.

Table .1 Composition of CdS thin filmsig.7 (e) shows the SEM image of annealed CdS films prepared by 'method b'. They develop flowery structure.

From the above tabulation it is observed that, CdS film prepared by 'method a' maintains Cd: S ratio near to unity in both as-deposited and annealed films. Whereas in 'method b' the annealed sample has very low

Method of preparation	As-deposited /annealed	Cd : S
method a	as-deposited	1:0.83
	annealed	1:0.77
method b	as deposited	1:0.71
	annealed	1:0.16

sulphur content when compared to cadmium. This indicates poor stoichiometry of 'method b'.

Optical Studies

The optical properties of CdS films were determined from absorbance measurement in the range 300-900 nm. For a direct band-gap material like CdS the absorption coefficient has the relationship

where, K is a constant of proportionality and E_gis the band-gap energy.The energy gap values depend on the crystal structure and composition. The energy gap value is calculated by extrapolation of the straight

$$\alpha = A(h\nu - E_g)^n$$

line portion of the plot of square of absorbance versus photon energy for CdS films prepared by two methods. The energy band gap of CdS films prepared by 'method a' and 'method b' was observed to be 2.41 eV and 2.28 eV respectively and these values reduced to 2.37 eV and 2.08 eV when the films were annealed.

Fig: 8 Plot of (ah?)^2 versus (hv) of film from method a (a) asdeposited film with band gap 2.41 eV (b) annealed film with band gap 2.37 eV

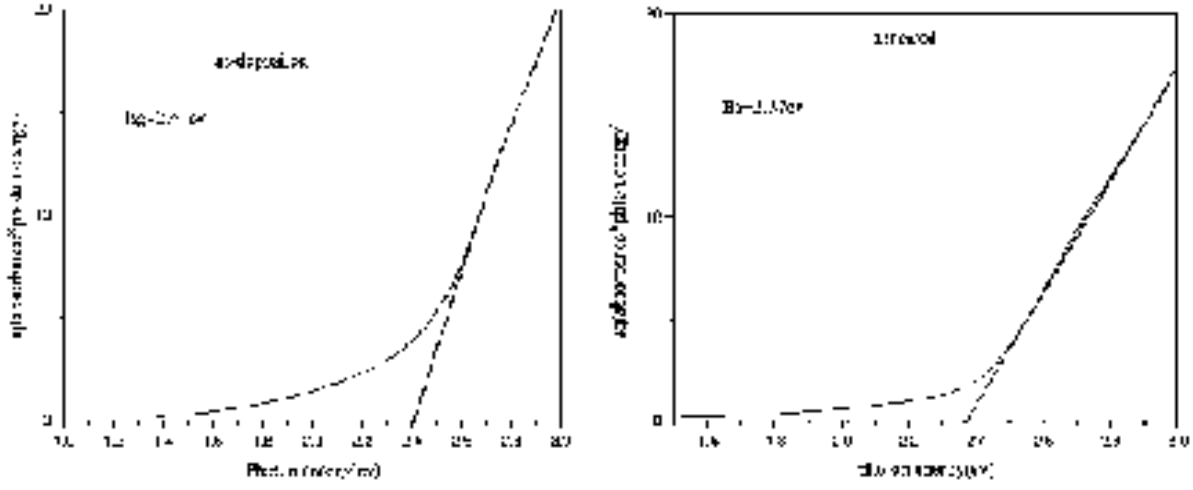

Fig. 9 Plot of (ah?)^2 versus (hv) prepared by method b (a) as-deposited film with band gap 2.28 eV (b) annealed film with band gap 2.08 eV

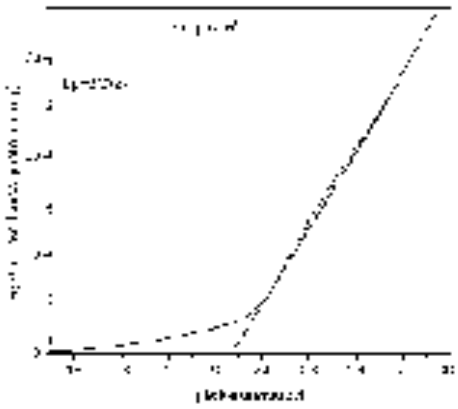

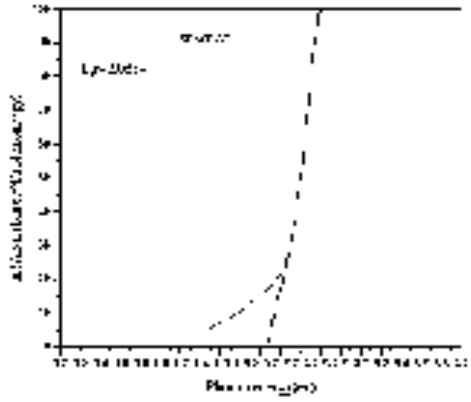

The decrease in band gap due to annealing may be due to increase in grain size on annealing and this can be attributed to the improvement in crystallites size

Resistance measurement

The electrical resistivity of CdS films was measured using Keithley source measuring unit. The electrical resistance was calculated for as-deposited and annealed CdS film deposited on glass and FTO substrate. Good ohmic contact was achieved by using silver.

Table 2.Resistance of CdS film prepared by 'method a' and 'method b'

Resistance of CdS film deposited on glass substrate is many orders greater than the film deposited on FTO. Hence CdS film grown on TCO (transparent conducting oxide) can be chosen for photovoltaic

Method of preparation	Substrate	Resistance (ohms)	
		as-deposited	annealed
Method a	Glass	1.7 * E+04 Ω	4* E+02 Ω
	ITO	40Ω	30Ω
Method b	Glass	0.64 * E+02Ω	1.31 * E+01Ω
	ITO	50Ω	70Ω

applications. It is found that resistance of film prepared by 'method a' decreases on annealing, while film from 'method b' shows an increase in resistance due to annealing. This can be interrupted as a result of formation on impurity phase of cadmium oxide in the film from second method.

Table 3. Comparative study between 'method a' and 'method b'

From the above table it can be concluded that film prepared by 'method a' is superior to that prepared by

'method b'

As-prepared sample

Properties	***method a***	***method b***
Structure	Hexagonal	Hexagonal
Grain size	28 nm	50nm
Continuity of film	Continuous	Not Continuous
Cd:S ratio	1:0.83	1:0.71
Annealed sample		
Structure	Hexagonal	Hexagonal
Phase	Single (CdS)	Mixed (CdS &CdO)
Grain size	50 nm	58 nm
Cd:S ratio	1:0.77	1:0.16
Application	More suitable for device application	Less suitable for device application

I-V characteristics

I-V characteristics of dye sensitized solar cell of the structure FTO/CdS/Dye/electrolyte/Pt/FTO were studied. Here FTO/CdS act as photo anode and platinum/FTO act as cathode. Pomegranate and eosin are the two types of photo sensitizer used in this study. Iodine redox system is used as electrolyte. Efficiency, short circuited current, open circuit voltage and fill factor are the some important parameters that are tabulated below.

Table.4 Parameters of solar cell

Fig. 10 and Fig: 11 show the I-V curve of ITO/TiO_2/CdS –Pt solar cell with Pomegranate and Eosin as photo sensitizer. All the solar cells are having fill factor in the range of 0.35-0.37.The efficiency of cells

Photo sensitizer	Fill factor	Open circuit voltage	Close circuit current	Efficiency	Series resistance
Eosin	0.3314	0.309	1.26 * E-05	2.21 * E-02	1.89 * E+04
Pomegranate	0.2520	0.352	1.09 * E-05	1.43 * E-02	1.5 * E+04

Corresponding author, Email: rafiqkhanmd.k@gmail.com

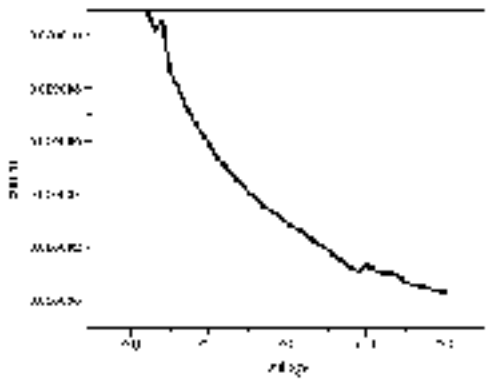

Fig. 10 I-V characterstics of solar cell with pomegranate as a photosensitizer

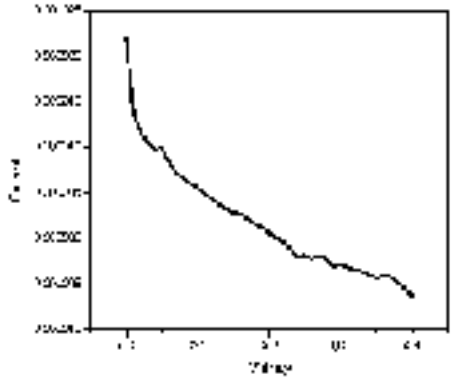

Fig. 11 I-V characteristic of solar cell with Eosin as a photosensitizer

based on both dyes are found to be more or less of the same order .but it was observed that eosin based cells had poor photo stability.

Conclusions

CdS film was prepared by chemical bath deposition technique using cadmium chloride as source of cadmium and thiourea as the source of sulphur. CdS film was deposited on FTO and plain glass substrates. Two slightly different methods of preparation was adopted, where the main difference between the two methods is the presence of additional complexing agent in first method. Moreover the concentration of cadmium is 10 times greater than sulphur in the reaction bath of first method, while in second method they are equimolar in ratio. From XRD spectra it is observed that CdS films exhibits hexagonal structure and the grain size of the CdS film prepared by 'method a' was found to increase from 28nm to 50nm on annealing, whereas in 'method b' the increase was from 50nm to 58nm. XRD spectrum reveals that 'method a' maintains its pure phase both in as-deposited and annealed film, while 'method b' incorporates cadmium oxide (CdO) impurity on annealing. This may be one of the reasons for the transfer of granular morphology to flowery structure as well as variation in band gap energy on annealing. From the elemental analysis it is observed that CdS film prepared by 'method a' maintains Cd: S ratio near to unity in both as-deposited and annealed films. But in 'method b' the annealed sample has very low sulphur content compared with cadmium. This hints to the formation of cadmium oxide impurity, leading to poor stoichiometry of 'method b'. From all above results it can be inferred that CdS prepared by 'method a' is much suitable for solar cell fabrication. Using FTO/ TiO2 /CdS as a photo anode, and platinum/FTO as cathode, Dye sensitized solar cell was constructed and cell parameters was measured.

Acknowledgment

The authors gratefully acknowledge BRNS, Department of Atomic Energy, Government of India for

funding the project No: 2010/34/43/BRNS. Authors are also thankful to STIC, Cochin University of Science and Technology for extending SEM and XRD facility.

Reference

1. Shodhanganga.inflibnet.ac.in/bitstream/10603/../08_chapter/202.pdf
2. Quazi Galib Samdami, Hameed A.Naseem and W.D. Brown., 1995. Characterization of Cadmium Sulfide Films Deposited By Chemical Bath Method. Proceedings Arkansas Academy of Science, Vol.49.
3. Selma M.H, Al-Jawad Zahra'a, S. Ahmed Wessal ,A. Taha., 2009. Optical Properties of Annealed Cadmium Sulfide Thin Films Prepared by Chemical Bath Deposition Iraqi. Journal of Applied Physics Letters. 2(2), 19-22.
4. Fajimi G.R and JSA Adelabu., 2009. Preparation and characterization of chemically deposited cadmium sulphide thin films .The Pacific Journal of Science and Technology. 10, 817-821.
5. Fthenakis V. M. and H. C. Kim., 2007. "CdTe photovoltaics: Life cycle environmental profile and comparisons," Thin Solid Films. 515, 5961-5963.
6. The shodhganga inflibnet.ac.in/bit stream/10603/4025/…/08-chapter%202.pdf.
7. Nair P. K et al,1998. Solar Energy Materials and Solar Cells Thin Solid Films. 52-313.
8. Ebookbrowse.net/79e41502833098efc7pdf.

Hardness estimation for Ruthenium Carbides based on semi-empirical

Harikrishnan G[1] and Ajith K.M[2]

[1]Department of Physics, Govt. College Madappally, Vatakara, Kerala – 673102, India.

[2]Department of Physics, National Institute of Technology Karnataka (NITK), Surathkal, Karnataka -575025, India.

Abstract

For the three dynamically stable structures of Ruthenium Carbides yielded by computational structure search, hardness values are estimated using semi-empirical macroscopic models based on Debye temperature and on Pugh's ratio, both derived from elastic constants. The values obtained are contrasted with the ones from a semi-empirical microscopic model based on bond strength. The hardness model based on Pugh's ratio is able to predict the decrease in hardness with the increase in metallic components in Ruthenium Carbides. Both macroscopic hardness models based on elastic properties fail to predict the high hardness of one predominantly covalent system RuC-Zinc blende. It is established that the microscopic model based on bond strength is more comprehensive and reliable in estimating the hardness of Ruthenium Carbides..

Keywords: Density Functional Theory, Evolutionary algorithm, Debye temperature, Pugh's ratio, Hardness

Introduction

A major class of potentially hard materials consists of the compounds formed by the transition metal atoms with atoms of B, C or N1-3. There are two reasons for the potential high hardness of borides, carbides and nitrides of transition metals. One is the p–d hybridized strong covalent bonds formed between B, C or N atom and transition metal atom and the other is the high charge density of valence electrons supplied by the transition metal atom. Transition metal carbides and nitrides have many industrial applications such as cutting and polishing tools, wear-resistant coatings etc. because of their high melting point, high hardness, good thermal conductivity and high resistance to wear and corrosion4. Their strategic importance has motivated various electronic structure studies to investigate their stability and structural properties5-11.

Two reported synthesis of Ruthenium Carbide gave tungsten carbide (WC) type hexagonal structure with the space group $P\bar{6}m2$ (187) in RuC stoichiometry12 and Fe2N type hexagonal structure with the space group $P\bar{3}m1$ (164) in Ru2C stoichiometry13. The computational studies on Ruthenium Carbide had so far been concentrating exclusively on RuC stoichiometry14-19. Only the zinc blende structure of RuC was found to be dynamically as well as mechanically stable17,18. Though tungsten carbide structure was mechanically stable, it lacked dynamical stability. From the electronic energy band calculation, RuC–zinc blende system was found to be a semiconductor and it was estimated to have a Vickers hardness of 42.8 GPa17,18. Z.M. Guang et al.19 made a structure search for RuC stoichiometry using particle swarm

optimization algorithm and they reported R3 ¯m structure as the lowest energy one, with mechanical and dynamical stability and metallic in nature. We undertook an exhaustive structure search of Ruthenium Carbides using evolutionary algorithm with no assumptions about the possible outcomes20. We investigated the possible structures of three stoichiometry, Ru1C1, Ru2C1 and Ru3C1. For the five distinct structures yielded by our structure search, we analyzed the mechanical stability through the computation of elastic constants and the dynamical stability through the phonon spectra. Consequently we got three dynamically stable systems. For these three stable systems we also calculated electronic energy bands and density of states, hardness and thermodynamic properties, these estimates being the first attempt for the systems belonging to Ru2C1 and Ru3C1 stoichiometries20.

With the growth of interest on novel super hard materials over the past several decades, it has become necessary to understand the microscopic features that control the hardness of materials. Many empirical models have been developed that aim to correlate hardness with different properties of materials. Some of these, which can be classified as macroscopic models, attempt to correlate hardness with different combinations of elastic properties. One such macroscopic model of hardness in terms of Debye temperature has been proposed by Abrahams and Hsu21 and modified by Deuss and Schneider22. Another model by Chen et al.23 that was subsequently modified by Tian et al.24 expresses hardness in terms of Pugh's ratio G/B. In the present work, we undertake to calculate the hardness of the three stable systems yielded by the structure search using these two semi-empirical macroscopic models of hardness and compare the results with those previously obtained20 from a semi-empirical microscopic model of hardness based on bond strength25-27 to investigate the applicability of these models to transition metal carbides.

Materials and Methods

Computational Methods

The evolutionary algorithm based tool USPEX (Universal Structure Predictor: Evolutionary Xtallography)28,29 was used to investigate the possible crystal structures of Ruthenium Carbides. Vienna Ab initio Simulation Package (VASP)30,31, employing electronic density functional theory, was used along with USPEX for the local optimization and energy calculation. Further stages of relaxation and the calculation of properties were done using VASP. Charge density and other quantities were evaluated by integrating over the Brillouin Zone (BZ) and the integrals were approximated by sums over a suitable discrete k–grid. Projector augmented wave (PAW) pseudopotentials32,33 as supplied with VASP were used, with 4p, 4d and 5s as the valence states for Ru, and 2s and 2p for C. They were tested for convergence of both ENCUT and the k-grid. Monkhorst–Pack k–point meshes34 were used except for hexagonal systems for which Gamma centered k-meshes were used. The Perdew–Burke–Ernzerhof (PBE)35

generalized gradient approximation (GGA) to the exchange–correlation functional was used. The states were smeared using Methfessel–Paxton scheme36 with a smearing parameter of 0.1 eV. The convergence of plane wave energy cutoff and that of k–points were achieved to a precision of 0.1 meV/atom. The value of ENCUT used was 900 eV which was 2.25 times the default value as per the POTCAR files of Ru and C. Both the lattice parameters and the atomic coordinates of all the structures were relaxed until energies converged to a precision of less than 10-10 eV/atom and Hellmann–Feynman forces to less than 10-5 eV/A0. Two semi-empirical macroscopic models based on elastic properties21-24 are employed in this work for the estimation of hardness of the Ruthenium Carbide systems. In our previous work20 the semi-empirical microscopic model based on bond strength 25-27 has been employed to estimate hardness

Table 1. Structural Data of Ruthenium Carbides

Stoichiometry	Structure (space group)	Lattice parameters (lengths in A°)	Formation energy/ formula unit (eV)
Ru_3C	Zinc blende ($F\bar{4}3m$/216)	a = 4.565 (4.566[a], 4.59[b]) (4.575[c], 4.608[d])	0.0127 (0.91[c])
Ru_7C_3	Rhombohedral ($R3m$/166)	a = 6.492, α = 21.75°	0.7239
Ru_2C	Hexagonal ($P\bar{6}m2$/187)	a = b = 2.783, c = 7.126	0.9466

[a]Ref. 15(GGA) [b]Ref. 12(LDA) [c]Ref. 17(GGA) [d]Ref. 18(GGA).

Thermodynamical stability has to be determined with respect to the formation energy. If it is negative, it means that the system can be spontaneously formed from its constituent elements. The formation energies of these Ruthenium Carbide systems are calculated with reference to crystalline Ruthenium and Graphite. All the structures have positive formation energies that show that they are not thermodynamically stable, i.e. they cannot be spontaneously formed under ambient conditions. In order to synthesize them, sufficient energy should be supplied and possibly high temperature and pressure. The synthesis of Ruthenium Carbide[12,13] under high pressure and high temperature testify to this result.

Elastic properties

As the elastic constants tensor is symmetric, there are at most 21 independent elements for the 6 x 6 matrix

Elastic moduli like the Bulk modulus, Rigidity modulus and Young's modulus can be calculated in terms of the elastic stiffness constants C_{ij}. In generalized form, the elastic stiffness constants C_{ijkl} and stress tensor σ_{ij} can be refined as $C_{ijkl} = \frac{1}{V_0}\frac{\partial^2 E}{\partial \varepsilon_{ij}\partial \varepsilon_{kl}}$ and $\sigma_{ij} = \frac{1}{V_0}\frac{\partial E}{\partial \varepsilon_{ij}}$ where V_0 is the volume of the unstrained crystal, ε_{ij} are components of the strain tensor and E is the energy of a deformed crystal. Using these expressions, the energy E_f can be expanded as a Taylor series[37],

$$E(V,\varepsilon) = E(V_0,0) + V_0\sum_{i,j=1}^{3}\sigma_{ij}\varepsilon_{ij} + \frac{V_0}{2}\sum_{i,j,k,l=1}^{3}C_{ijkl}\varepsilon_{ij}\varepsilon_{kl} + \cdots \quad (1)$$

where $E(V_0, 0)$ is the corresponding ground state energy. In Voigt notation scheme[38] the subscripts (i,k,l) of strain tensors are expressed as : $11 \rightarrow 1$, $22 \rightarrow 2$, $33 \rightarrow 3$, $23 \rightarrow 4$, $31 \rightarrow 5$ and $12 \rightarrow 6$. Then equation (1) becomes :

$$E(V,\varepsilon) = E(V_0,0) + V_0\sum_{i=1}^{6}\sigma_i\varepsilon_i + \frac{V_0}{2}\sum_{i,j=1}^{6}C_{ij}\varepsilon_i\varepsilon_j + \cdots \quad (2)$$

$C_{\alpha\beta}$, for the triclinic crystal. As the symmetry of the crystal increases, some of the matrix elements would be connected by symmetry relations and the number of independent matrix elements would be further reduced. Thus, rhombohedra has 6 independent elements, hexagonal has 5 and cubic has only 3. By applying small specific elastic strains ?_i(i = 1–6) to the equilibrium unit cell, a set of elastic constants Cij can be obtained from the corresponding change in energy. From the independent elastic constants of a system, bulk modulus (B) and shear modulus (G) are calculated using the standard formulae for the relevant crystal classes39-41 in Voigt42 and Reuss43 approximations.

Cubic [Independent elastic constants : C11, C12, C44]:

The elastic constants and the average values of B, G, Y and v (in GPa) are tabulated in Table 2[20].

$$B_V = B_R = (C_{11} + 2C_{12})/3 \quad (3)$$

$$G_V = (C_{11} - C_{12} + 3C_{44})/5 \quad (4)$$

$$G_R = \frac{5(C_{11}-C_{12})C_{44}}{4C_{44}+3(C_{11}-C_{12})} \quad (5)$$

Hexagonal [Independent elastic constants : $C_{11}, C_{12}, C_{13}, C_{33}, C_{44}$] :

$$B_V = [2(C_{11} + C_{12}) + 4C_{13} + C_{33}]/9 \quad (6)$$

$$G_V = [C_{11} + C_{12} + 2C_{33} - 4C_{13} + 12C_{44} + 12C_{66}]/30 \quad (7)$$

$$G_{66} = (C_{11} - C_{12})/2 \quad (8)$$

$$B_R = \frac{[(C_{11}+C_{12})C_{33} - 2C_{13}^2]}{C_{11}+C_{12}+2C_{33}-4C_{13}} \quad (9)$$

$$G_R = \frac{\frac{5}{2}[(C_{11}+C_{12})C_{33}-2C_{13}^2]C_{44}C_{66}}{3B_VC_{44}C_{66}+[(C_{11}+C_{12})C_{33}-2C_{13}^2](C_{44}+C_{66})} \quad (10)$$

Rhombohedral [Independent elastic constants : $C_{11}, C_{12}, C_{13}, C_{33}, C_{44}, C_{14}$] :

B_V, G_V and B_R are the same as those of Hexagonal symmetry

$$G_R = \frac{5[(C_{11}+C_{12})C_{33}-2C_{13}^2](C_{44}C_{66}-C_{14}^2)}{3B_V(C_{44}C_{66}-C_{14}^2)+[(C_{11}+C_{12})C_{33}-2C_{13}^2](C_{66}+C_{44})} \quad (11)$$

where, B_V is given by Eqn (A 4) and C_{66} by Eqn (A 6)

Voigt approximation corresponds to the upper bound and Reuss approximation corresponds to the lower bound of the elastic modulus. Hill approximation[44] gives the average of the two :

$$B_H = (B_V + B_R)/2 \text{ and } G_H = (G_V + G_R)/2 \quad (12)$$

From B and G values, Young's modulus Y and Poisson's ratio ν are calculated[45] .

$$Y = 9BG/(3B + G) \quad (13)$$

$$\nu = (3B - 2G)/[2(3B - G)] \quad (14)$$

Calculated values of Debye temperature from previous computational works have also been given for

Table 2. Elastic Properties of Ruthenium Carbide.

Elastic constants and elastic moduli	RuC- Zinc blende	RuC- Rhombohedral	RuC- Hexagonal
C_{11}	342.46	522.51	547.47
C_{12}	220.93	158.10	162.37
C_{13}		158.09	210.54
C_{14}		-38.09	
C_{33}		508.14	600.62
C_{44}	82.40	138.37	121.37
B	261.44	287.45	316.99
G	91.74	163.23	157.48
Y	171.70	411.75	405.37
ν	0.301	0.262	0.288
B/G	2.84	1.76	2.01

comparison. The values of Θ_D are consistent with the observed trends in bulk, shear and Young's moduli for the two systems of Ru_1C_1 stoichiometry. Together these values imply that rhombohedral system could be mechanically more stable.

The Madelung–Einstein formula for Debye temperature was modified by incorporating hardness by Abrahams and Hsu[21] and further improved for fitting with the data by Deus and Schneider[22] into the form:
The calculated values of B/G ratio for the given systems (Table 2) are larger than 1.75, the critical value to

$$\Theta_D = \frac{h}{k_B}\left(\frac{3n}{4\pi V_a}\right)^{1/3} v_m \quad (15)$$

where h is Planck's constant, k_B is Boltzmann constant, V_0 is the unit cell volume and N_0 is the number of atoms in the unit cell. The average wave velocity v_m in the polycrystalline material is given by[44].

$$v_m = \left[\frac{1}{3}\left(\frac{2}{v_t^3} + \frac{1}{v_l^3}\right)\right]^{-1/3} \quad (16)$$

where v_t and v_l are the mean transverse and longitudinal elastic wave velocities in the material, respectively. They can be deduced from the Navier's equations in terms of the Voigt-Reuss-Hill-averaged values of polycrystalline bulk and shear moduli as follows[46,47]:

$$v_t = (G/\rho)^{1/2} \quad (17)$$

$$v_l = [(3B + 4G)/3\rho]^{1/2} \quad (18)$$

The results of the calculations are tabulated in Table 3.

Table 3. Volumic density (in kg/m^3), transverse, longitudinal and average sound velocities (in m/s), and Debye temperature (in Kelvin)

Structure	ρ	v_t	v_l	v_m	Θ_D
RuC–Zinc blende	7896	2796	6598	3161	612.36 (427.02[a])
RuC Rhombohedral	8883	4787	7541	4769	644.46 (688[b])
RuC–Hexagonal	8248	5793	6938	4229	551.72

separate brittleness and ductility, according to Pugh's criterion[45]. This indicates that these systems are all ductile.

Hardness model based on Debye temperature

The Debye temperature (Θ_D) can be calculated from the average sound velocity v_m[46], which, in turn, is

$$\Theta_D = aH^{1/2}\rho^{-1/6}M^{-1/3} + b \quad (19)$$

obtained from the elastic constant data.

where Θ_D is Debye temperature in K, H is Vickers hardness in GPa, ρ is the density of the system in kg/m^3, M is the molar mass of the system in g and a and b are the fitting parameters. The parameter b should be of the order of Θ_D (Table 3). With the fitting parameters a=2500 and b=200 and data from table 3, the hardness values (H_D) obtained from Eqn.(19) are given in table 4. As the Debye temperature of RuC–Zinc blende system is significantly smaller than the values of other systems, any level of fitting based on this model will yield only a relatively small value of hardness for it.

Table 4. Hardness values of Ruthenium Carbides from models based on bond strength (Hb), Debye temperature (HD) and Pugh's ratio (HP)

Hardness (GPa)	RuC- Zinc blende	RuC- Rhombohedral	Ru_3C- Hexagonal
H_b	36.66 (36.91[a], 42.8[b])	21.15 (28[b])	12.42
H_D	3.36	15.45	20.24
H_P	3.30	17.82	14.93

Note: a Ref. 16 b Ref. 17 c Ref. 19

Ru3C-Hexagonal system has higher molar mass and higher density compared to the systems of Ru1C1 stoichiometry (Table 3). This causes an increase in hardness as given by the above formula for Ru3C–Hexagonal system. However, this trend is against the expectation that an increase in metallic component should result in a decrease in hardness, and such a variation is observed in the case of the hardness values obtained from the model based on bond strength (Table 4).

Hardness model based on Pugh's ratio

Using the Pugh's ratio (k = G/B) and the shear modulus (G), Chen et al.23 derived a semi-empirical formula of hardness, H= 〖2k^2 G〗^0.585-3. However, as this formula sometimes yields negative values of hardness, Tian et al.24 modified it with new fitting parameters :

$$H=0.92k^{1.137}G^{0.708} \quad (20)$$

Substituting G in GPa yields the hardness in GPa from this formula. Using this modified formula and the data from table 2, the hardness of the Ruthenium Carbide systems are estimated and the values (HP) are given in table 4. Except for the RuC–Zinc blende system, the hardness values obtained from the microscopic model based on bond strength and the macroscopic model based on Pugh's ratio are of the same order. As RuC–Zinc blende system is a semiconductor (Fig.8), and since the model based on bond strength by Šimunek et al. is better suited for covalent crystals, the value of hardness from that model could be a better estimate of hardness for this system, compared to the value from the model based on Pugh's ratio. It can also be noted that another microscopic model based on the valence electron density48 has yielded a value17 close to the one from the model based on bond strength (Table 4). The hardness values from the model based on Pugh's ratio reflect the expected trend that an increase in metallic component should result in a decrease in hardness, going from Ru1C1 to Ru3C1 stoichiometry. In table 4,

HP decreases from RuC–Rhombohedral to Ru3C–Hexagonal though not in the same order as the values given by the hardness model based on bond strength. As both Pugh's ratio and Debye temperature are derived from the elastic constants [Eqns.9–12], the hardness values obtained from these two models can be expected to correspond to each other. Their predictions match with each other except in the case of the increase in metallic component (Table 4).

Conclusions

Between the hardness model based on Debye temperature and that based on Pugh's ratio, the latter predicts the decrease in hardness as the metallic component increases. Both models fail to predict the high hardness of the strongly covalent system like RuC-Zinc blende. It is concluded that the semi–empirical microscopic model based on bond strength by Šimunek et al.25-27 gives better estimates of hardness for Ruthenium Carbide systems compared to the two macroscopic models derived from elastic constants.

Acknowledgements

This work is completed under the University Grants Commission (UGC) and Department of Atomic Energy (DAE) joint CRS project. Grant No. is CRS–NK/ CRS–44/ 2012–2013/ 734. The authors acknowledge the computational resources at UGC–node, Kalpakkam and IUAC, New Delhi.

References

1. PaKaner R B, Gilman J.J. and Tolbert S.H., 2005. Materials science – Designing Superhard Materials. Science 308, 1268-1269.
2. Gilman J.J., Cumberland R.W. and Kaner R.B., 2006. Design of Hard Crystals. Int. J. Refract. Met. Hard Mater. 24, 1-5.
3. Levine J.B., Tolbert S.H. and Kaner R.B., 2009. Advances in the Search for Superhard Ultra-Incompressible Metal Borides. Adv. Funct. Mater. 19, 3519-3533.
4. Toth L.E., 1971. Transition Metal Carbides and Nitrides, Academic, New York.
5. Guillermet A.F. and Grimvall G., 1989. Cohesive properties and vibrational entropy of 3d-transition-metal compounds: MX (NaCl) compounds (X=C, N, O, S), complex carbides, and nitrides. Phys. Rev. B 40, 10582-10593.
6. Haguland J., Grimvall G., Jalborg T. and Guillermet A.F., 1991. Band structure and cohesive properties of 3d-transition-metal carbides and nitrides with the NaCl-type structure. Phys. Rev. B 43, 14400-14408.
7. Haguland J., Guillermet A.F., Grimvall G. and Korling M., 1993. Theory of bonding in transition-metal carbides and nitrides. Phys. Rev. B 48, 11685-11691.
8. Grossman J.C., Mizel A., Cote M., Cohen M.L. and Louie S.G., 1999. Transition Metals and Their Carbides and Nitrides: Trends in Electronic and Structural Properties. Phys. Rev. B 60, 6343-6347.

9. Hugosson H.W., Eriksson O., Jansson U. and Johansson B., 2001. Phase stabilities and homogeneity ranges in 4d-transition-metal carbides: A theoretical study. Phys. Rev. B 63, 134108-134119.
10. Zheng J.C, 2005. Superhard hexagonal transition metal and its carbide and nitride: Os, OsC, and OsN. Phys. Rev. B 72, 052105-052109.
11. Guo X., Xu B., He J., Yu D., Liu Z. and Tian Y., 2008. Structure and mechanical properties of osmium carbide: First-principles calculations. Appl. Phys. Lett. 93, 041904-041907.
12. Kempter C.P. and Nadler M.R., 1960. Preparation and Crystal Structures of RuC and OsC. J. Chem. Phys. 33, 1580-1581.
13. Sanjay Kumar N.R., Chandra Shekar N.V., Sharat Chandra, Joysurya Basu, Divakar R. and Sahu P.Ch., 2012. Synthesis of novel Ru2C under high pressure–high temperature conditions. J. Phys.: Condens. Matter. 24, 362202-362208.
14. Fan C.Z., Zeng S.Y., Zhan Z.J., Liu R.P., Wang W.K., Zhang P. and Yao Y.G., 2006. Low compressible noble metal carbides with rocksalt structure: Ab initio total energy calculations of the elastic stability. Appl. Phys. Lett. 89, 071913-071916. 15. Zhao E., Wang J. and Wu Z., 2010. Structural Stability and Phase Transition in OsC and RuC. J. Comput. Chem. 31, 2883-2888.
16. Abidri B., Rabah M., Rached D., Baltache H., Rached H., Merzoug I. and Djili S., 2010. Full potential calculation of structural, elastic properties and high-pressure phase of binary noble metal carbide: ruthenium carbide. J. Phys. Chem. Solids 71, 1780-1784.
17. Zhao Z., Wang M., Cui L., He J., Yu D. and Tian Y., 2010. Semiconducting Superhard Ruthenium Monocarbide. J. Phys. Chem. C 114, 9961-9964.
18. Soni H.R., Gupta S.K. and Jha P.K., 2011. Ab initio total energy calculation of the dynamical stability of noble meta lcarbides. Physica B 406, 3556-3561.
19. Guang Z.M., Yan Y.H., Tai Z.G. and Hui W., 2012. The ground-state structure and physical properties of RuC: first-principles calculations. Chin. Phys. B 217, 076103-076109.
20. Harikrishnan G., Ajith K.M., Sharat Chandra and Valsakumar M.C., 2014. Evolutionary algorithm based structure search for hard Ruthenium Carbides. Modelling Simul. Mater. Sci. Eng. (in communication).
21. Abrahams S.C., and Hsu F.S.L., 1975. Debye temperatures and cohesive properties. J. Chem. Phys. 63, 1162-1165.
22. Deus P., and Schneider H.A., 1983. Estimation of the Debye temperature of diamond-like semiconducting compounds from bulk modul and microhardness. Cryst. Res. Technol. 18, 491-500.
23. Chen X.Q., Niu H.Y., Li D. and Li Y., 2011. Modeling hardness of polycrystalline materials and bulk metallic glasses. Intermetallics 19, 1275-1281.
24. Tian Y., Xu B. and Zhao Z., 2012. Microscopic theory of hardness and design of novel superhard crystals. Int. J. Refract. Met. Hard Mater. 33, 93-106.
25. Šimůnek A. and Vackář J., 2006. Hardness of Covalent and Ionic Crystals: First-Principle Calculations. Phys. Rev. Lett.

96, 085501-085505.

26. Šimůnek A., 2007. How to estimate hardness of crystals on a pocket calculator. Phys. Rev. B 75, 172108-172112.
27. Šimůnek A., 2009. Anisotropy of hardness from first principles: The cases of ReB2 and OsB2. Phys. Rev. B 80, 060103-060107.
28. Oganov A.R. and Glass C.W., 2006. Crystal structure prediction using ab initio evolutionary techniques: Principles and applications. J. Chem. Phys. 124, 244704-244719.
29. Glass C.W., Oganov A.R. and Hansen N., 2006. USPEX – evolutionary crystal structure prediction. Comput. Phys. Commun. 175, 713-720.
30. Kresse G. and Hafner J., 1993. Ab initio molecular dynamics for liquid metals. G. Phys. Rev. B 47, 558-561.
31. Kresse G. and Furthmüller J., 1996. Efficient iterative schemes for ab initio total-energy calculations using a plane-wave basis set. Phys. Rev. B 54, 11169-11186.
32. Blochl P.E., 1994. Projector augmented-wave method. Phys. Rev. B 50, 17953-17980.
33. Kresse G. and Joubert D., 1999 From ultrasoft pseudopotentials to the projector augmented-wave method. Phys. Rev. B 59,
    1758-1775.
34. Monkhorst H.J. and Pack J.D., 1976. Special points for Brillouin-zone integrations Phys. Rev. B 13, 5188-5192.
35. Perdew J.P., Burke K. and Ernzerhof M., 1997. Generalized gradient approximation made simple Phys. Rev. Lett. 77, 3865-
    3870.
36. Methfessel M. and Paxton A.T., 1989. High-precision sampling for Brillouin-zone integration in metals. Phys. Rev. B 40,
    3616-3621.
37. Wallace D.C., 1972. Thermodynamics of Crystals, Wiley, New York.
38. Nye J.F., 1985. Physical Properties of Crystals: Their Representation by Tensors and Matrices, Oxford University Press,
    Oxford.
39. Watt J.P. and Peselnick L., 1980. Clarification of the Hashin-Shtrikman bounds on hexagonal, trigonal, and tetragonal symmetries. J. Appl. Phys. 51, 1525-1530.
40. Dieter G.E., 1988. Mechanical Metallurgy, SI Metric ed. McGraw-Hill.
41. Mehl M.J., Kein B.M. and Papaconstantopoulos D.A., 1994. in : Westbrook J.H., and Fleischer R.L. (Eds.), Intermetallic Compounds : Principles and Practice, John Wiley and sons, London.
42. Voigt W., 1928. Lehrbook Der Kristallphysik, second ed. Teubner, Leipsig.
43. Reuss A. 1929. Berechnung der Fließgrenze von Mischkristallen auf Grund der Plastizittitsbedingung fiir Einkristalle

Math. Mech. 9, 49-58.

44. Hill R., 1952 The elastic behaviour of a crystalline aggregate. Proc. Phys. Soc., London 65, 349-354.
45. Pugh S.F., 1954. Relations between the elastic moduli and the plastic properties of polycrystalline pure metals. Philos. Mag.

    45, 823-843.
46. Anderson O.L., 1963. A simplified method for calculating the Debye temperature from elastic constants. J. Phys. Chem. Solids 24, 909-917.
47. Schreiber E., Anderson O.L. and Soga N., 1973. Elastic Constants and their Measurements, McGraw-Hill, New Tork.
48. Guo X.J., Li L., Liu Z.Y., Yu D.L., He J.L., Liu R.P., Xu B., Tian Y.J. and Wang H.T., 2008. Hardness of covalent compounds: Roles of metallic component and d-valence electrons. J. Appl. Phys. 104, 023503-023510.

Scientia
Vol.9, No. 1, Jan - Dec. 2013, pp87-96
Scientia Jan- Dec. 2013
ISSN : 0976 - 8289

Kavitha. S[1], Asha. N.V[2] and Lakshmi.M[3]

[1]Departmkent of Physics, Christ College, Calicut University, Irrinjalakkuda, Kerala, India

[2]Department of Physics, M.E.S Kalladi College, Calicut University, Mannarkkad, Kerala, India

[3]Department of Physics, Mercy College, Calicut University, Palakkad, Kerala, India

Abstract

Dye-sensitized solar cell (DSSC) is a promising device to convert solar energy to electrical energy, with relatively low production cost compared to those of conventional semiconductor solar cells. DSSC comprise of a dye-adsorbed nano crystalline TiO_2 layer fabricated on a transparent conducting oxide (TCO) as the working electrode, platinum (Pt) as the counter electrode and an electrolyte solution with iodide/ triiodide redox reagents. The TiO_2 coated films were characterized by UV-Visible, XRD and SEM studies. In this work focus is on DSSC based on natural electrolytes. The effect of combination of natural as well as organic electrolytes on the efficiency of the DSSC is studied. The combination of some natural electrolytes with Ethylene glycol is found to enhance the efficiency of DSSC. The results indicate that there is scope for highly efficient DSSCs which will work in harmony with nature.

Keywords: DSSC, Natural Electrolyte, Organic Electrolyte.

Introduction

The growth of global population along with industrial developments will pose an enormous challenge in meeting the rising energy demand in future. The global electricity generation is projected to grow by 2.2% per annum from 2008 to 2035[1]. Renewable energy resources such as solar, hydropower, wind, biomass, etc have the potential to meet the rising energy demand to a great extent. Human efforts to energize the world have much expectation on solar cells. Electricity production without the exhaust of greenhouse gases or nuclear waste as byproducts is the attractive feature of solar cells. Dye sensitized solar cell is a third generation solar cell invented by Michael Gratzel and Brian O'Regan in 1991. It promises a less inexpensive method for conversion of solar energy to electrical energy. Record conversion efficiencies of DSSCs up to 12% have been achieved in DSSC using Acetonitrile based electrolytes. Though Ruthenium based complex dyes are the most successful dyes they are very expensive and poisonous. In the present work we have replaced ruthenium dye with natural dye extracted from pomegranate. This study attempts to enhance the efficiency of DSSC by altering the electrolyte composition using natural electrolytes.

Materials and methods

Electrode preparation

*****Corresponding author, Email: honeysebi@yahoo.co.in*

1.5 g of TiO_2 nano powder (Degussa, size: 25nm) is blended with 9 ml glacial acetic acid and 3 drops of Triton X-100 (surfactant). The aggregated TiO_2 powder is dispersed by grinding in a mortar till the colloidal paste is formed. Surfactants are added to lower the surface tension of the colloid in order to facilitate easier spreading on to the conducting glass plate by doctor blade technique. After spreading the TiO_2 layer on FTO glass slide, it is annealed at 450^0C for one hour in order to remove the organic additives and enhance continuity of the film[2]. Pomegranate (Punica granatum) fruit is used as the source of dye and Anthocyanin is the major pigment in it. The TiO_2 film is immersed in pomegranate dye sensitizer solution for 24 hour to absorb the dye on the porous film. This treatment produce intense colouration of thin film and the photo anode is ready to be used. Commercially available Platinum coated FTO was used as the counter electrode.

Preparation of electrolytes

Acetonitrile based electrolyte is prepared by dissolving 2.075g (0.5M) potassium iodide (KI) to 25 ml acetonitrile. The mixture is stirred using a magnetic stirrer for 20 minutes. 1.3g of iodine (0.05M) is added to this solution and stirring is continued until a rich solution of I^-/I_3^- oxidation reduction pair is formed [3]. Ethylene glycol based electrolyte is prepared by dissolving 0.83g (0.5M) potassium iodide (KI) in 10 ml Ethylene glycol. After stirring for 15 minutes, 0.127g (0.05M) iodine is added and further stirred. Water based iodine electrolyte is prepared by adding 0.01N iodine solution to equal amount of 0.01M potassium iodide to form the final electrolyte.

Preparation of natural electrolytes-The rich solution extracted from turmeric, tamarind and ginger was centrifuged to obtain clear solution and then filtered. ORS (Oral Rehydrate Solution) solution, lemon extracts and coconut water are directly used as electrolytic solutions.

DSSC fabrication

The DSSC was assembled by filling the liquid electrolyte between the photo anode and platinum counter electrode which are clipped together. Electrical contacts were taken out from the TCO layer of both electrodes. The photovoltaic measurements were done under diffused natural sunlight. The intensity of light falling on the cell were measured using power meter. I-V characteristics were plotted by means of solar cell application software and Source Measuring Unit (Keithley). The open circuit voltage (Voc), short circuit current (Isc), fill factor (FF) and efficiency of the cell were analyzed.

Results and discussion

Optical characterisation

UV-VIS-NIR spectrophotometer (U-3410 model - Hitachi make) was used for optical studies in the range 200 nm to 900nm. Optical characterisation was done to understand the nature of (i) absorption of TiO_2 thin film (ii) absorption region of dye (iii) adhesion of dye on TiO_2. Fig 1 shows absorption spectrum of TiO_2 nanopowder. The band gap of TiO_2 was calculated to be 3.17eV. Fig 2 shows absorption spectrum of dye

and Fig 3 shows absorption spectrum of dye coated on TiO_2. The red shift observed in the absorption spectrum of dye when coated on TiO_2 suggests chemical bond formation between dye and TiO_2. Absorption edge of pure dye is found to be in the in visible region.

Fig1. Absorption spectrum of TiO_2 nanopowder

The absorption spectra of extract from pomegranate and its spectra when coated on TiO_2 shows two absorption edges, one in the violet region and other in the middle region of visible spectrum. When

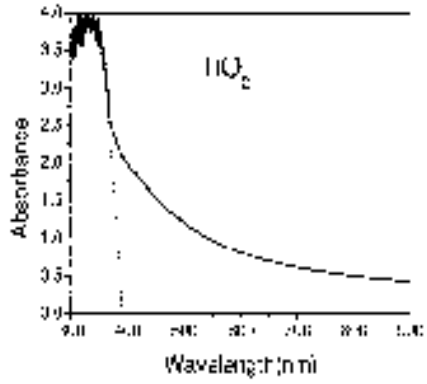

pomegranate is coated on TiO_2, the absorption edge of TiO_2 shows a red shift and this can make the

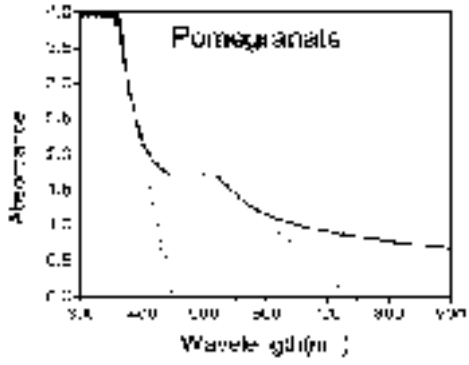

Fig 2. Absorption spectrum of pomegranate.

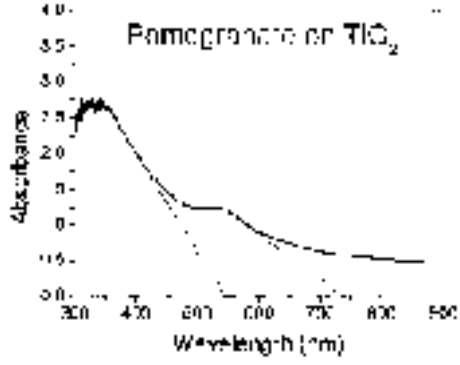

Fig3. Absorption spectrum of Pomegranate on TiO_2

Sample	Absorption edge (nm)	Energy gap (eV)
TiO_2	390	3.17 eV
Extract from Pomegranate	450, 735	2.75eV, 1.6eV
Extract from Pomegranate coated on TiO_2	540, 740	2.29eV, 1.67 eV

photo anode more active in the visible region of solar spectrum.

Structural characterization of TiO_2

X-ray diffraction is the most convenient tool for crystallographic structural analysis. This analysis was done using Rigaku (D.Max.C) X-ray diffractometer. The XRD analysis was used to confirm the crystalline nature and the actual phase of TiO_2. X-ray source used was 1.5A° Cu-Kα. The grain size was determined from the Scherr's formulae. It relates wavelength

Fig.4. XRD of (A) FWHM (β) and grain size as Grain size= (0.9* λ)/ (β cos(θ)

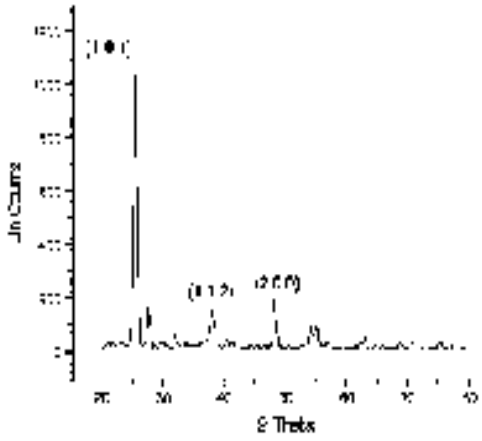

Table 2. Evaluation of grain size- TiO_2 film on a glass plate

Fig 4 shows XRD spectrum of TiO_2 film on a glass plate. It was found to be highly crystalline and the

Sl.No hkl	2theta (degree)	FWHM observed	d(A°)Experimentally	d(A°) as per JCPDS file 21-1272	
1	25.514	.386	3.488	3.520	101
2	38.022	.372	2.364	2.332	112
3	48.237	.445	1.885	1.892	200

grain size was calculated from the FWHM of the peaks. On comparison with standard JCPDS data (card no: 21-1272) the phase was identified as anatase.

Morphological characterization of TiO_2

Scanning electron microscope image of TiO_2 electrode was taken to confirm the uniformity. Fig.5 and Fig.6 shows the SEM of TiO_2 film before annealing and after annealing. The morphological characteristics of both samples are the same with good uniformity.

Electrical characterization of solar cell

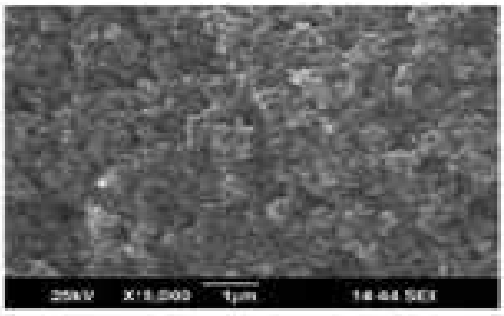

Fig 5 SEM of an unannealed TiO_2 sample

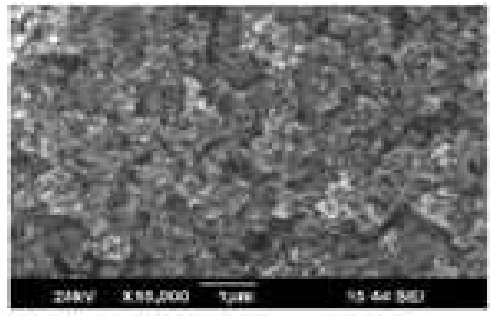

Fig 6 SEM of an annealed TiO_2 sample

The photo response of the cell was studied in natural sunlight as well as under halogen lamp using solar cell application software. In this work we have tried first to find out the best base for I^-/I^{3-} redox electrolyte used in DSSC. Among the four different bases tried viz. Acetonitrile, Ethylene glycol, water and Triethanol amine, the best performance was obtained for the cell with Ethylene glycol. Efficiency obtained was around 0.244%. As a second stage of trials we tried pure natural electrolytes without using redox couple. Among the various natural electrolytes used for the study, lemon extract resulted in best efficient cell with an efficiency of 0.0163%. Pure natural electrolytes are found to be less efficient than iodine redox electrolyte. As a third stage, iodine redox electrolyte in ethylene glycol was selected for the combination study with natural electrolytes. The electrolytic combination of lemon and ethylene glycol resulted in the best efficient cell with an efficiency of 0.336 % (Fig 7).

The combination of some natural electrolytes like lemon, turmeric and ORS with Ethylene glycol is found to enhance the efficiency of DSSC while electrolytes like tamarind, tomato, ginger and coconut water showed a negative effect on efficiency.

In order to know the photo response of the cell under halogen lamp (50 watt), all the above studies were repeated under this source. The cells studied under diffused light as well as in halogen lamp have shown similar performance.

Table 3. Different bases tried with iodine redox couple

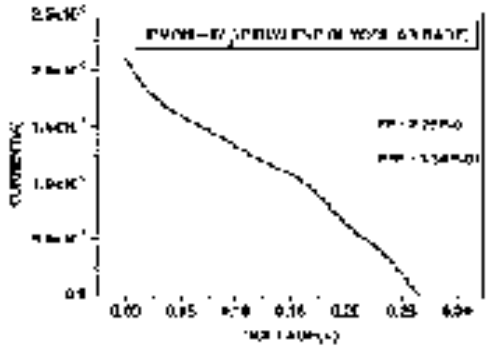

Fig 7 V-I characteristic of best cell

Table 4. Different natural extracts as electrolytes

Sl.No.	Electrolyte I^-/I_3^- in	Fill factor	Efficiency
1.	Ethylene Glycol (EG)	2.5E-01	2.44E-01
2.	Acetonitrile(ACN)	2.41E-01	1.63E-01
3.	water	2.5E-01	4.44E-02
4.	triethanolamine	4.2E-01	5.42E-03

But the limitation of the analysis with halogen lamp was that it was difficult to get constant irradiation for

Sl.No.	Electrolyte	Fill factor	Efficiency
1.	Lemon juice	2.03E-01	1.55E-02
2.	ORS	1.26E-01	3.64E-03
3.	Ginger extract (Zingiber officinale)	2.09E-01	9.76E-05
4	Coconut water	3.90E-01	5.17E-03
5.	Turmeric extract (Curcuma longa)	2.34E-01	3.05E-03
6.	Tomato juice	1.94E-01	7.14E-03
7.	Tamarind extract (Tamarindus indica)	2.75E-01	1.11E-03

the cell since the intensity changed considerably with slightest change in position of the cell relative to the lamp. This problem of radial source could be overcome with diffused sunlight, as the test cell and the power meter can be exposed to constant irradiation conveniently. For this reason, the results obtained from direct natural sunlight are considered more authentic. The data given below shows solar cell parameters of DSSC under diffused sunlight.

Table 5. Combination of natural extracts and iodine redox couple in Ethylene Glycol base

Conclusions

Sl.No.	Electrolyte I^-/I_3^- in	Fill factor	Efficiency
1.	Lemon juice	2.90E-01	3.35E-01
2.	Turmeric extract (Curcuma longa)	2.36E-01	3.74E-01
3.	ORS	2.47E-01	2.79E-01
4.	Tomato juice	2.30E-01	1.87E-01
5	Turmeric extract (Tamarindus indica)	2.42E-01	1.56E-01
6	Coconut water	2.07E-01	1.70E-01
7.	Ginger extract (Zingiber officinale)	2.28E-01	5.91E-02

TiO_2 nano films were prepared using doctor blade technique. The absorption spectrum of the TiO_2 nano film and dye was studied using U-V visible spectrophotometer and the absorption edge of samples was determined. The red shift observed in the absorption spectrum of TiO_2 and dye confirmed the formation of chemical bond between dye and TiO_2. The anatase phase of TiO_2 was confirmed and its grain size was calculated using XRD analysis. The surface morphological nature of annealed sample was verified using SEM.

The photo response of the DSSC cell was studied in diffused sunlight and in halogen lamp using Keithley source meter unit and 24xxx solar cell software. Ethylene glycol, Acetonitrile, Water and Triethanol amine were the various bases tried for I^-/I_3^- redox system. Results show that Ethylene Glycol is the best organic base to produce an efficient DSSC with Pomegranate extract. Among the various natural electrolytes tried lemon extract resulted in the most efficient cell in diffused light. The electrolytic combination of lemon and ethylene glycol is confirmed to be the best combination to produce most efficient cell with an efficiency of 0.336%. The studies conducted in halogen lamp have also given a similar performance as in diffused light. But the results were less dependable. The results show that there is scope to produce highly efficient DSSCs using a combination of natural electrolytes and I^-/I_3^- redox system leading to low cost solar cell.

Acknowledgement

The authors gratefully acknowledge BRNS, Department of Atomic Energy, Government of India for funding the project 2010/34/43/BRNS. Authors are also thankful to STIC, Cochin University of Science and Technology for extending SEM and XRD facility.

References

1. Ze Yu, 2012. Liquid Redox Electrolytes for Dye-Sensitized Solar Cells, *Doctoral Thesis*.

2. Huizhi Zhou Liqiong Wu, Yurong Gao and Tingli Ma, Dye-sensitied solar cells using 20 natural dyes as sensitizers, *Journal of Photochemistry and Photobiology A: Chemistry* 219, 188-194.

3. Eiji yamazaki Masaki Marayama, Naominihikawa, Masash Shoyama and Osamu Kurita, 2007. Utilization of natural carotenoids as photosensitizer for dye-sensitized solar cells, *Solar energy* 81,512-516.

Insecticidal activity of *Phyllanthus maderaspatensis* L. on the larvae and pupae of *Culex quinquefasciatus* (Lis.)

Mary Fabiola

Department of Zoology, Nirmala College for Women Coimbatore - 641018, Tamil Nadu, India

Abstract

A preliminary study was conducted to investigate the effects of *Phyllanthus madraspatensis* L. extract against the larval and pupal activity of *Culex quinquefasciatus* under various concentrations. The 50 ppm plant extract exhibited the larval mortality of about 65.43% in the 1st instar larvae and it was reduced to 55.60%, 35.76% and 27.61% in 2nd, 3rd and 4th instar larvae respectively. The pupal mortality in the case of *Culex quinquefasciatus* was ranging from 27.61% to 89.65% after treated with 50 to 300 ppm over the period of 24 h. The results suggest that the methanol extract of *Madras patensis* have the potential as larvicidal and pupicidal agent against *Culex quinquefasciatus*

Keywords: *Culex quinquefasciatus, Phyllanthus madraspatensis* L., methanol extract

Introduction

The mosquito is the principal vector of many of the vector borne diseases affecting human beings and other animals. *Culex quinquefasciatus,* a vector of lymphatic filariasis and its widely distributed tropical diseases with around 120 million people infected worldwide and 44 million people have common chronic manifestation[1]. Traditionally, plants and their derivates were used to kill mosquitoes and other household and agricultural pests. Now a day, chemical control methods using synthetic insecticides are in practice due to their speedy action and ease of application. Repeated use of synthetic insecticides for mosquito control has disrupted natural biological control systems and led to resurgences in mosquito populations. It has also resulted in the development of resistance[2], undesirable effects on non – target organisms, and fostered environmental and human health concern.

In the light of earlier literature, it is known that larvicidal agents play a vital role in controlling mosquitoes in their breeding sites, but still vectors bio control measures are in vogue, their effective control of larval mosquitoes has not been hither to highlighted, whereas possibilities of plant extract and isolation of active components have been fragmentally documented. Hence, an attempt has been made to evaluate the role of *Phyllanthus madraspatensis* L. leaf extracts against *Culex quinquefasciatus*.

Materials and Methods

Selection of plant species

The plant species *Phyllanthus madraspatensis* L. belongs to Euphorpiaceae family is widely found in the

Coimbatore District Tamil Nadu. It was collected from foot hills of Maruthamalai, Coimbatore District Tamil Nadu.

Laboratory rearing of mosquitoes

Culex quinquefasciatus eggs were obtained from National Institute of Communicable Diseases, Mettupalayam, Coimbatore, Tamil Nadu. To start the colony the larvae were reared in plastic and enamel trays containing tap water. Larvae were fed a diet of Brewer's yeast, dog biscuits and algae in the ratio of 3:1:1 respectively. Pupae were transferred from the trays to a cup containing tap water and were maintained in our insect cage (45x45x40 cm) where adult emerged.

Adults were maintained in glass cages and were continuously provided with 10% sucrose solution in a jar with a cotton wick. On day 5 the adults were given a blood meal from chicks placed in cages overnight for blood feeding by females. Glass Petri dishes with 50 ml of tap water lined with filter paper was kept inside the cage for oviposition.

Preparation of *Phyllanthus madraspatensis* L. leaf extract

Twenty gram of *Phyllanthus madraspatensis* L. leaf powder was placed in the pouch made by Whatmann No. 1 filter paper and placed in the sohxlet's apparatus, mixed with 250 ml of 80% methanol and soxlet's for 6h. It was poured in petriplates and made to get dry at room temperature. The dried material was weighed and dissolved by using the suitable emulsifying agent. The stock solution was prepared by dissolving 1.00 gm of dried material with 1ml of emulsifier (1000rpm). Different concentrations of plant extract were prepared from the stock solution by using distilled water. The concentration of 50, 100, 150, 200, 250 and 300 ppm were selected on the basis of killing range minimum to maximum larval mortality after 12h duration.

Bioassay

Larvicidal activity was evaluated by following WHO method with slight modifications. 30 numbers of 1^{st}, 2^{nd}, 3^{rd}, 4^{th}, instars of *P. madraspatensis* were placed in a separate 500ml petri disc with 249ml of dechlorinated water and 1.0ml of the desired plant extract concentrations. Five replicates were maintained for each concentration. Mortality rate was observed at 24h of the exposure time. The mortality was calculated by Abbots method[3] for computing effectiveness of an insecticide.

Pupal mortality was evaluated by following WHO method. Pupae of *P. madraspatensis* (30 numbers) were placed in 500 ml petri dish with 249 ml of dechlorinated water and 1.0 ml of the desired plant extract concentrations. Five replicates were maintained for each concentration. Mortality rate was observed at 24h of the exposure time. The mortality was calculated by Abbots method[3] for computing effectiveness of an insecticide.

Results and Discussion

The larval mortality of *Culex quinquefasciatus* larvae when treated with the extract of *P. madraspatensis* (Table 1) the 50 ppm plant extract exhibited the larval mortality 65.43% in the 1st instar larvae and it was reduced to 55.60%, 35.76% and 27.61% against 2nd, 3rd and 4th larval stages respectively. The pupal mortality in the case of *Culex quinquefasciatus* was ranging from 27.61% to 89.65% after treated with 50 to 300ppm over the period of 24h. Khanna and Kannabiran[4] reported the role of tannin compounds extracted from *Hemidemus indicus, Gymnema sylvstre* and *Eclipta prostrate* showing effective mortality in *Culex quinquefasciatus* larvae. Sivagnaname and Kalyanasundaram[5] showed the methanolic extract of *Atlandia monophylla* was effective against fourth instar larvae of *Culex quinquefasciatus.*

Table 1. Effect of methanol extract of *P. madraspatensis* on the larvae and pupae of *Culex quinquefasciatus* after 24h

Concentration of plant extract (ppm)	Number of insects used	Percentage mortality				
		Larvae				Pupae
		1st	2nd	3rd	4th	
50	30	65.43	55.60	35.76	27.61	27.61
100	30	66.70	57.17	48.29	48.29	58.63
150	30	77.80	57.85	58.62	58.62	68.97
200	30	79.05	56.70	57.17	58.97	78.58
250	30	78.47	77.80	67.68	79.31	80.29
300	30	88.47	68.97	78.58	89.65	89.65
LC50			19.91	40.02	91.67	

Note: values are the mean of 5 replications. Corrected by C. Ba /100 where, T = % damage in treatment C = % damage in Control

This investigation revealed that *P. madraspatensis* is very effective in the mortality rate of *Culex quinquefasciatus.* The results also revealed that there is a possibility of further investigation of efficacy on the larvicidal and insecticidal properties of natural product extracts. These results will be useful in promoting research aim at the development of new agent for mosquito control based on bioactive chemical compounds from indigenous plant source.

References

1. Bernhard L., Bernhard P., and Magnussen P., 2003. Management of patients with Lymphoedema caused by Filariasis in North – eastern Tanzania: alternative approaches. Physiotherapy, 89, 743 – 749.
2. Brown A.W.A., 1986. Insecticide resistance in mosquitoes: pragmatic mosquitoes: pragmatic review. J. An. Mosq. Control. Assoc., 2, 123 – 40.
3. Abbott W.S., 1925. A method for computing effectiveness of an insecticide. J. Econ. Entomol., 18, 265 – 267.
4. Khanna V.G., Kannabiran K., 2007. Larvicidal effect of Hemidesmus indicus, Gymnema sylvestre, and Eclipta prostrata against Culex qinquifaciatus mosquito larvae. Afr. J. Biotechnol., 3, 307-311.

Scientia
Vol.9, No. 1, Jan - Dec. 2013, pp97-106
ISSN : 0976 - 8289

their activity against third instar larvae of *Helicoverpa armigera*

Nithyasree G. and Sajani Jose

Department of Zoology, Nirmala College for Women Coimbatore - 641018, Tamil Nadu, India

Abstract

Indiscriminate use of synthetic insecticides has resulted in problems like pest resurgence, environmental pollution, destruction and toxicity to non-target organisms including, human beings. Some of these insecticides are still used for its control due to non-availability of alternative insect control agent. These problems have led to the search for more sustainable, cost-effective and eco-friendly alternatives like phytochemicals as potential insecticides particularly against phytophagous insects. *Helicoverpa armigera*, a polyphagous pest, plays an important role in reducing the crop yields. Hence, this study shows that the leaf extracts of *Adathoda vasica* Nees. and *Hibiscus rosa-sinensis* can be used as bio-insecticides control *Helicoverpa armigera.*

Keywords: *Helicoverpa armigera*, phytochemical analysis, medicinal plants

Introduction

Indiscriminate use of synthetic insecticides has resulted in problems like pest resurgence, environmental pollution, destruction and toxicity to non-target organisms including human beings[1]. This resulted in greater attention on bioactivity of pytochemicals as potential insects particularly against pytophagous insects. *Helicoverpa armigera* is a polyphagous pest that plays an important role in reducing the crop yield. The hot and humid climate is conducive to the proliferation of insect pests, especially the American bollworm; *H. armigera* that causes considerable losses[2]. In recent years, *H. armigera* became the major cause of cotton yield reduction. Tomato is the one of the most important vegetable crops, especially in the Indian sub continent where the diet only predominantly vegetarian in nature. Tomato is extensively damaged by the lepidopteron insect *Helicoverpa armigera*, also called as tomato fruit borer[3]. In the present study, the response of *H. armigera* to different phytochemicals was studied.

Plants produce a range of chemical compounds to protect themselves from various insect pests. These include alkaloids, terpenoids, flavonoids and acetogenins, such as azadirachtin, isolated from the foliages of some medicinal plants. Secondary metabolites from microbes are also known to kill various insects including *H. armigera. Hence, an attempt was made* to determine the efficacy of certain medicinal plant products against resistant to 3rd instar larvae of the American bollworm, *H. armigera.*

Materials and Methods

The present study were undertaken to assess the feeding preference and damage potential of this pest to some promising genotypes and a hybrid in the laboratory as well as under field conditions so that a better

Corresponding author, Email:jeejatharakan@gmail.com

assessment of losses in relation to the severity of this pest could be made.

Test insect and source

Third instar larvae of *Helicoverpa armigera* of the Order, Lepidoptera was collected from Tamil Nadu Agricultural University Farm, Coimbatore.

Collection of medicinal plants

The fresh medicinal leaves of selected medicinal plants such as *Adathoda vasica* Nees. (extract of the plant possess significant insecticidal, nematicidal, anti-feedent, anti-fungal, anti-plasmodial, anti-ulcerogenic, anti-inflammatory and analgesic activities) and *Hibiscus* leaf (known for several potential therapeutic activity) were collected from in and around Coimbatore District. The leaves were authenticated, washed and were allowed to shade dry for about 9 hours every day for 3-4 days until they became crispy while retaining the greenish colouration. The dry leaves were powdered separately. About 30gms were taken for phytochemical analysis and the rest were amended with vermicompost for plant growth in pot culture.

Preparation of medicated tomato foliage

Earthern pots of uniform size (3 Nos.) were selected for pot culture study with Tomato. Two different pot set up were arranged. Two pots were amended with soil, compost and medicinal plant powder in the ratio 3:2:1 and one pot as control with soil and compost. The seeds of tomato, obtained from Tamil Nadu Agricultural University Coimbatore were sowed in each pot with proper spacing. From the day of sowing the pots were watered regularly. The germination and growth of the seedlings were observed every day after one week of sowing. The larvae of *H. armigera* feed mainly on flower buds, flowers, developing seed, and fruits, and also on foliage. Hence, the leaves of tomato were given as feed for the larvae.

Test for foliage protection

For this test, 3 sterile petri dishes were obtained and 4 leaves from each treatment pot were placed in each petri dish separately and five test larvae were transferred. Moistened filter papers were spread onto the plate to avoid desiccation of leaves. Control was maintained with 4 untreated leaves. Each treatment was replicated 3 times along with an untreated control under complete randomized design. Activity of worm was assessed after 24 hrs, few worms showed less response to stimulation by touch. Few were not so active by stimulation of touch. Consumption rate of leaves by the larvae were recorded by percentage.

Result

The result is based on phytochemical analysis of certain medicinal plant product and the feed utilization (Table 1) by the third instar larvae of *H. armigera*.

***Adathoda vasica* Nees.**

In tomato at 24 hrs, third instar larvae of *H. armigera* has utilized only 1/4th of the leaves given from tomato plant grown in *Adathoda* leaf extract mixed with soil and vermicompost. From the weight loss of *H. armigera* it was examined that it has only consumed 30% of total leaves.

Hibiscus rosa-sinensis

All most every leaves were utilized by third instar larvae of *H. armigera* from the tomato leaves from tomato plant grown in *Hibiscus* leaf extract mixed with soil and vermicompost. The maximum 75% of leaves were consumed by *H. armigera* this was inferred by its weight gain.

Control

The third instar larvae utilized all the leaves given from tomato plant grown Control mixed with soil and vermicompost. At 24 hrs of observation third instar larvae of *H. armigera* showed the maximum (90%) of leaf consumption showing highest weight gain from other experimental treatment. The other treatment groups expect control showed significance on feeding rate.

Table 1. Utilization of tomato leaves by third instar *H. armigera* larvae against different treatments

Phytochemical analysis of medicinal plants

Plant extract	No. of leaves	No. of larvae	Utilization of leaves (%)
Adathoda vasica Nees.	4	4	30
Hibiscus rosa sinensis	4	5	75

The Phytochemical investigation of *Adathoda* leaf showed the presence of methanol solvent contains alkaloids, amino acids, antroquinones, flavonoids, saponins, steroids and tannins extraction. The Phytochemical screening of *Hibiscus* showed the presence of carotin, chlorophyll, flavonoids, phenols, sugar and tannins in the methanolic extraction.

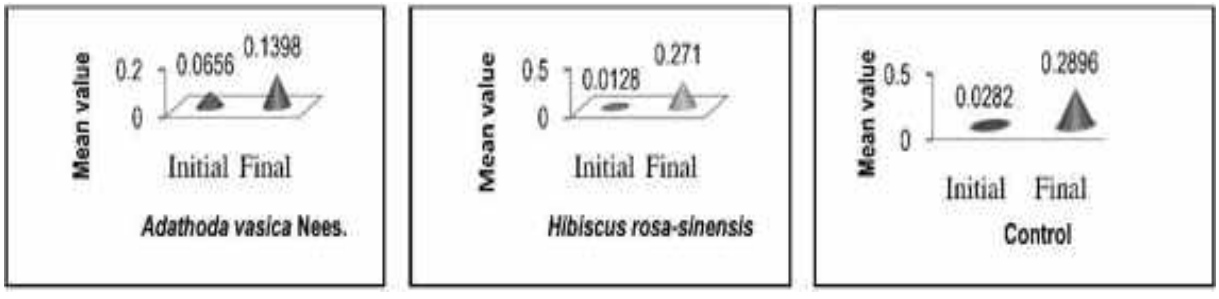

Fig. 1. Weight changes (gm) of *H. armigera* larva after feeding medicated tomato leaves

Discussion

The chemical composition of host plants significantly affects survival, growth, and reproduction of pytophagous insects. Food consumption and utilization link plant attributes with insect performance. For polyphagous insects, the availability of different host plants plays an important role in triggering population outbreaks[4]. Growth, development, and reproduction of insects are strongly dependent on the quality and quantity of food consumed.

The extracts contain alkaloids, amino acids, antroquinones, flavonoids, saponins, steroids and tannins in high concentration. But, carotin, chlorophyll and sugar are lacking. So the rate of consumption of the feed by the larvae is reduced 30% may be due to the antimicrobial activity found in *Adathoda vasica* Nees. which has been reported by Simpson *et al.* and Wagh *et al.*[5, 6]. Feed utilization by 75% was observed in treated larvae against *Hibiscus*. This may be due to positive responses of plant based natural products reacts with certain cells of the larvae and which act as toxins[7].Compared to the treatments the feed utilization in the control seems to be higher 90%. 90% of the feed (tomato leaf) is utilization by the third instar larvae of *H. armigera*. All the treatments showed a positive result in controlling the pest by using certain medicinal plant product extract.

Conclusion

Plant derived extracts and phytochemical have been intensively investigated for the past 30 years in an effort to develop alternatives to conventional insecticides but with reduced health and environmental impacts. Synthetic insecticides can leave potentially toxic residues in food products and can be deleterious to non-target organisms in the environment. Several workers have explored the utility of plant products as one of the potential source of managing agricultural pests in search for effective, ecofriendly and economically viable options. This work explains the rational for the use of the plant in control the pest. The plant could be a veritable and cheaper substitute for conventional drugs since the plant is easily obtainable and the extract can easily be made via a simple process of maceration or infusion. It is essential that research should continue to isolate and purify the active components of this natural herb and use in controlling certain pest.

References

1. Ahmad M. Arif Mc., Ahmad Z., 2002.Resistance to carbonate insecticides in Helicoverpa armigera (Lepidoptera: Noctuidae) in Pakistan. Crop Port, 20, 427-432.
2. Lohar M.K., 1994. Insect pests of cotton, in: Applied Entomology, pp.106.
3. Atwal A.S., 1986. Agricultural Pests of India South East Asia. Kalyani publishers, New Delhi.
4. Shen J. and Wu Y., 1995. Resistance of Helicoverpa armigera insecticides and its management. China Agricultural

Press, 58-88.

5. Simpson S.J. and Raubenheimer D., 1996. A multi–level analysis of feeding behavior, in, The geometry of nutritional decisions. Philosophical Transactions of the Royal Society of London Series B: Biological Sciences 342(1302), 381-402.
6. Wang D., Qiu X., Ren X., Zhang W., Wang K., 2007. Effects of spinodad on H. armigera from China: tolerance status, synergism and enzymatic responses. Pest Manage. Sci. 65, 1040-1046.
7. Sharma B. and Kumar P., 2009**.** Extraction and pharmacological evaluation of some extracts of *Tridax procumbens* and *Capparis decidua*. Int. J. Applied Res. Nat. Prod., 1, 5-12.

Coimbatore District of Tamilnadu

PawlinVasanthi Joseph[1*]and Balasubramanian S[2]

[1]Department of Zoology, Nirmala College for Women (Autonomous), Coimbatore

2 Director of Research, JSS Medical University, Mysore, Karnataka 570 015

Abstract

Water quality is recognised as the foundation for any health improvement strategy, accompanied by programmes for increased water quality and sanitation. However, in the absence of changes in personal behaviour and hygiene practices, the incidence of water related diseases especially diarrhoeal illness is likely to remain high in contaminated environments. The present study deals with the descriptive statistics of water quality parameters in Coimbatore district, Tamilnadu for the period 2000 to 2009. The water quality variables namely turbidity, electrical conductivity, total alkalinity, total dissolved salts, pH, Ferrous, manganese, ammonia, nitrite, nitrate, chloride, fluorine, sulphate, phosphate, faecal coli and residual chlorine were obtained from the Tamilnadu Water supply and Drainage Board, Government of Tamilnadu for a period of ten years from 2000 to 2009.Descriptive statistics was analyzed using SPSS 12.0 (Statistical package of socialsciences). Most of the variables show significant magnitude of percentage of co-efficient of variation. Coimbatore South showed high values for Electrical conductivity, total dissolved solids, total alkalinity, total hardness, fluorine and sulphate. Tiruppur showed high concentrations of nitrite, nitrate, phosphate and alkaline pH. Ammonia, chlorides, faecal coli and Residual chlorine was high in Mettupalayam while Coimbatore North showed high values for ferrous and manganese. Turbidity was high in Avinashi. There are considerations to be taken into account when evaluating the relationship between health outcomes and exposure to changes in rainfall, water availability and quality.

Keywords: water quality, descriptive statistics, co-efficient of variation, variables, health outcomes.

Introduction

Water quality is recognised as the foundation for any health improvement strategy, accompanied by programmes for increased water quality and sanitation. However, in the absence of changes in personal behaviour and hygiene practices, the incidence of water related diseases especially diarrhoeal illness is likely to remain high in contaminated environments. Poor water quality continues to pose a major threat to human health. Diarrhoeal disease alone amounts to an estimated 4.1 % of the total daily global burden of disease and is responsible for the deaths of 1.8 million people every year[1]. It was estimated that 88% of that burden is attributable to unsafe water supply, sanitation and hygiene and is mostly concentrated on children in developing countries.

A retrospective study of drinking water related outbreaks of acute gastroenteritis illness in the United States[2] revealed that 20% and 40% of ground water and surface water outbreaks

respectively between 1971 and 1994 were statistically associated with extreme percipitation. El Niño–southern oscillation connection to rates of enteric illness in South America has been demonstrated[3, 4] and the levels of entire microorganisms in Coastal areas of South Florida, United States[5] and Cholera in Bangladesh[6]. In Bangladesh, post flood increases in rotavirus diarrhoea have been reported[7, 8]. Floods adversely affect water sources and supply systems as well as sewage and waste disposal systems. Sewage which is known to contain large number of infectious rotavirus particles may be disposed of in raw forms and infectious rotavirus can be recovered from sewage polluted surface waters[9]. Since water used for bathing and for washing utensils was suspected of being involved in virus spread in the outbreak of rotavirus gastroenteritis in Brazil[10]. Faecal contaminated water supply was the primary vehicle in an outbreak of rotavirus gastroenteritis with 1200 cases in China[11].The present study deals with the descriptive statistics of water quality parameters in Coimbatore district, Tamilnadu for the period 2000 to 2009.

Materials and Methods

The water quality variables namely turbidity, electrical conductivity, total alkalinity, total dissolved salts, pH, Ferrous, manganese, ammonia, nitrite, nitrate, chloride, fluorine, sulphate, phosphate, faecal coli and residual chlorine were obtained from the Tamilnadu Watersupply and Drainage Board, Government of Tamilnadu for a period of ten years from 2000 to 2009.

The collection of data forms the fundamental basis for all statistical analysis. It is necessary to verify and check whether the data collected are reliable and useful for the purpose inquiry. The data are collected to draw a conclusion after the analysis using descriptive statistics such as mean (x), standard deviation (SD) and the variance (σ). The mean, median and mode measure the central tendency. The SD and variance are the dispersion parameters of the mean. The measure of the slope of the distribution is the skewness and kurtosis.

In probability theory and statistics, the coefficient of variation (CV) is a measure of dispersion of a probability distribution. It is defined as the ratio of the standard deviation σ to the mean μ;

$$CV = \sigma / \mu$$

The co-efficient of variation is a dimensionless number. For the distribution of positive valued variables, it allows comparison of the variation of populations that have significantly different mean values. It is often reported as a percentage (%) by multiplying the above calculation by 100. When the mean value is near zero, the co-efficient of variation is sensitive to change in the

standard deviation, limiting its usefulness. The co-efficient of variation is also common in applied probability fields. The standard deviation of an exponential distribution is equal to its mean, so it's co-efficient of variation is equal to 1. Distributions with CV<1 (Ehrlang distribution) are considered as low variance, while those with CV >1 (Hyper-exponential distributions) are considered as high variance.

The percentage co-efficient of variation using the standard deviation and mean values of nine taluks are calculated and presented in the tables. The descriptive statistics are analyzed using the SPSS 12.0 (Statistical package of socialsciences). Most of the variables show significant magnitude of percentage of co-efficient of variation. The co-efficient of variation is used to compare the relative variability in different distributions. It is otherwise called as signal-to-noise ratio.

Results and Discussion

Turbidity

Maximum mean turbidity is 5.88 in Avinashi and minimum of 3.72 in Pollachi. The range is from 1.58 to 5.38 (Fig.1). The values are negatively skewed for Avinashi and Coimbatore North and leptokurtic for Palladamtaluk. The % CV ranges from 11.01 to 36.57. The temporal analysis shows maximum turbidity of 5.98 in 2006 and a minimum of 4.09 in 2008.

Fig. 1. Turbidity in Coimbatore district of Tamilnadu (2000 to 2009)

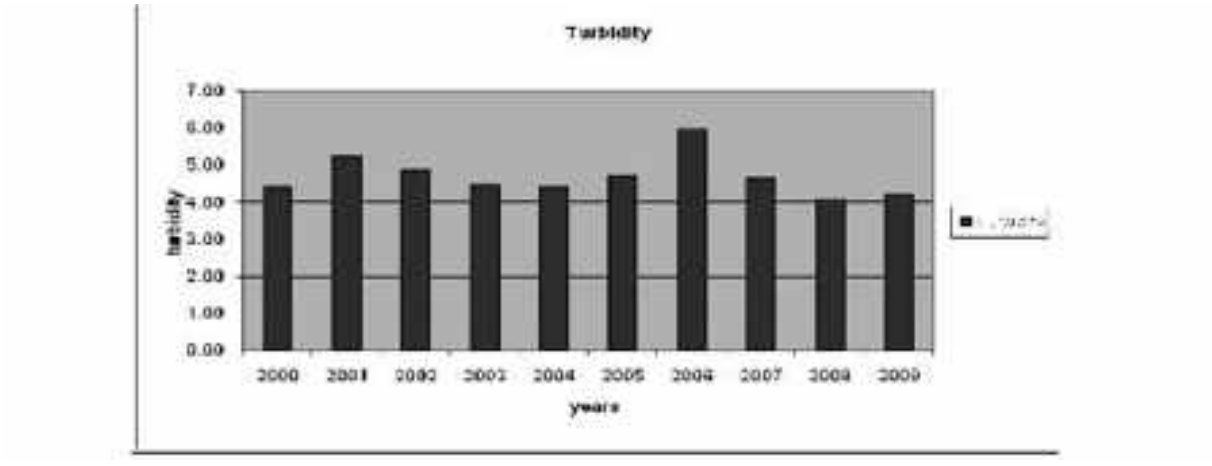

Electrical Conductivity

Maximum electrical conductivity of 199.08 was observed in Coimbatore South and minimum of 42.19 in Valparai. The range is from 6.08 to 57.44 (Fig.2). The values are negatively skewed in Avinashi, Mettupalayam, Palladam and Tiruppur. All the taluks are platykurtic. The %CV ranges from 3.16 to 11.73. The temporal analysis shows maximum electrical conductivity in 2006

(106.61) and minimum in 2002 (98.37).

Fig. 3. Total Dissolved Solids in Coimbatore district of Tamilnadu (2000 to 2009)

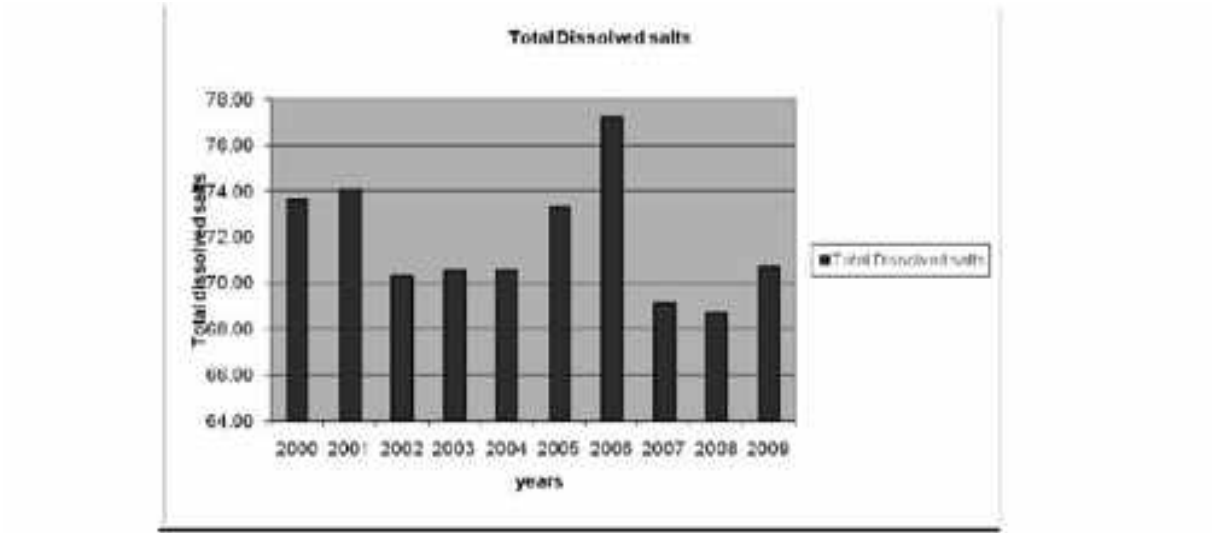

pH

The mean pH varies from 7.64 in Tiruppur to 7.44 in Pollachi. The range extends from 0.10 to 1.34. Positive skewness is seen in Palladam, Udumalpet and Valparai while the other taluks are negatively skewed. Kurtosis value is leptokurtic for Coimbatore South and platykurtic for the other taluks (Fig.4). The %CV ranges from 0.42 to 5.27. The temporal trend shows maximum pH of 7.62 in 2000 to a minimum of 7.42 in 2004.

Fig. 4. pH in Coimbatore district of Tamilnadu (2000 to 2009)

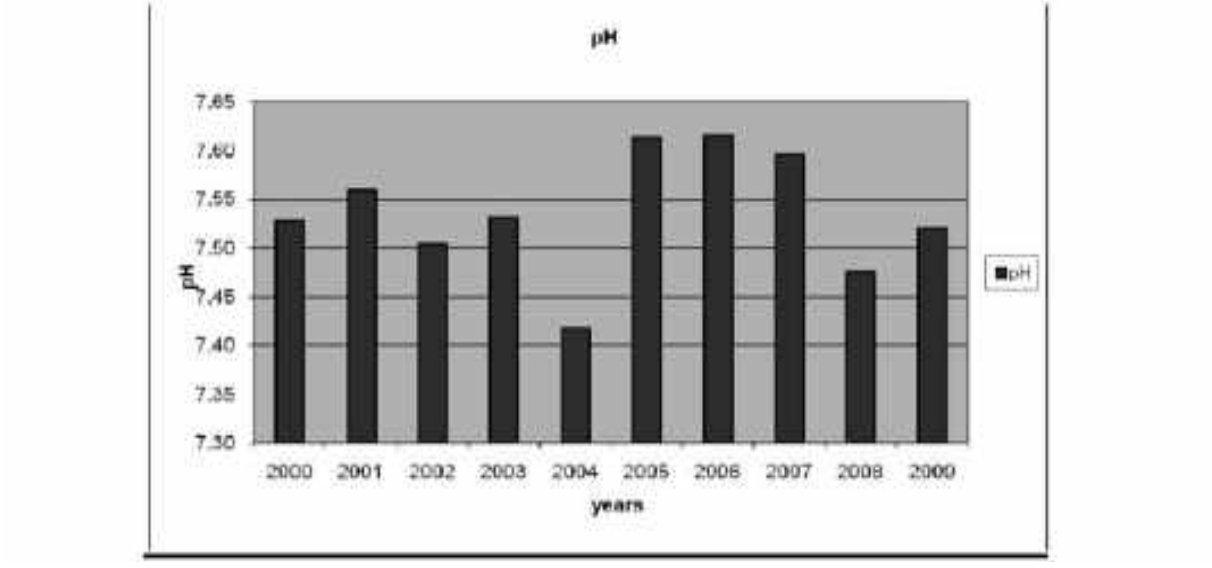

Total Alkalinity

The mean total alkalinity ranges from a maximum of 64.91 in Coimbatore South to a minimum of 12.08 in Avinashi. The range is from 2.17 to 28.29. The values are negatively skewed for Coimbatore North and Udumalpet and platykurtic for all the other taluks (Fig.5.). The % CV is from 4.07 to 15.44. The temporal trend shows maximum total alkalinity in 2006 (4.71) and minimum in 2008 (27.30).

Total Hardness

The maximum mean total hardness occurs in Coimbatore South (72.12) and minimum at Valparai (13.67). The range varies from 1.62 to 26.38(Fig.6). The skewness is negative for Coimbatore North, Palladam and Valparai and positive for the rest of the taluks. Coimbatore South is leptokurtic while the other taluks are platykurtic. The %CV ranges from 3.54 to 14.38. The temporal analysis shows maximum total hardness in the year 2006 (39.27) and minimum in 2008.

Fig. 6. Total Hardness in Coimbatore district of Tamilnadu (2000 to 2009)

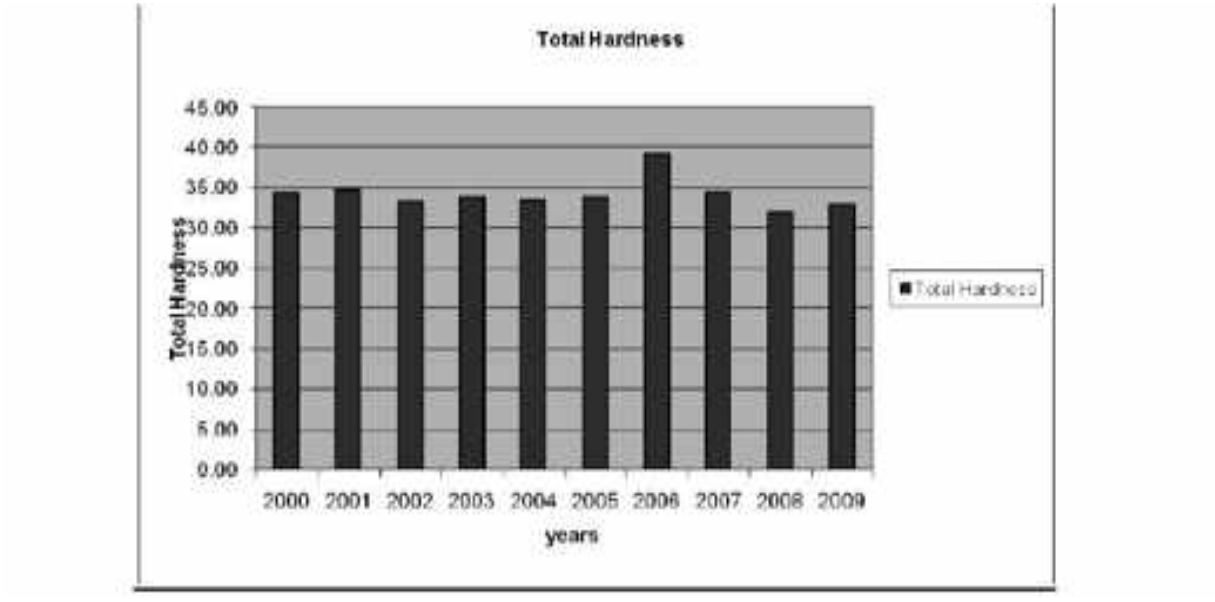

Ferrous

The maximum mean concentration of ferrous is observed in Coimbatore North (0.37) and the minimum in Pollachitaluk (0.19). The range is from 0.20 to 1.50 (Fig.7). The values are negatively skewed for Avinashi and Coimbatore North and positively skewed in the other taluks. The value for Coimbatore South is leptokurtic while the other taluks are platykurtic. The %CV ranges from 24.47 to 122.88. The temporal trend shows maximum concentration of ferrous in 2006 (34.44) and minimum in 2008 (33.92).

Fig. 7. Ferrous in Coimbatore district of Tamilnadu (2000 to 2009)

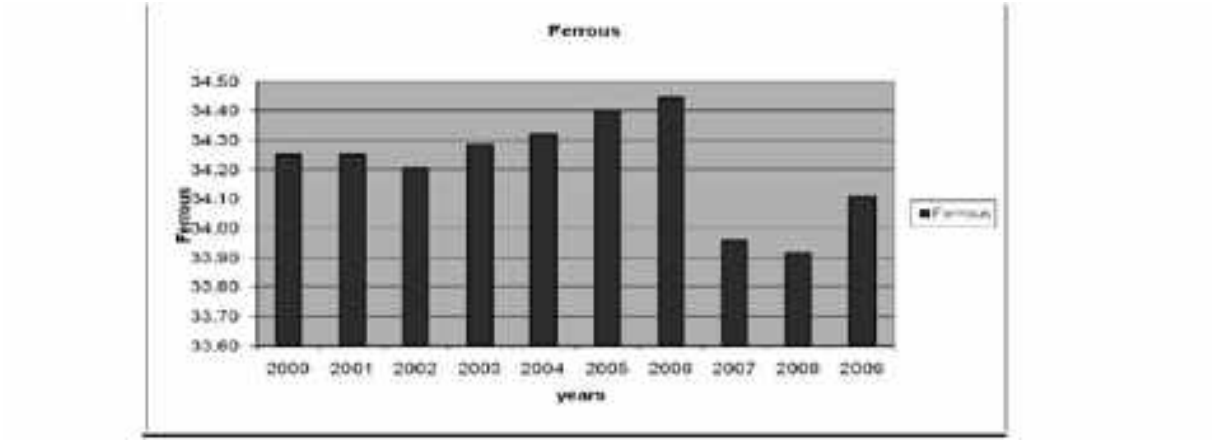

Manganese

The maximum mean concentration of manganese is found in Coimbatore North (0.006) and no traces observed in Coimbatore South and Udumalpet. It is negatively skewed in Avinashi and Valparai and the values are platykurtic for all the taluks (Fig.8). The %CV ranges from 0 to 210.0. The temporal trend shows 0.003mg/lit of manganese in2001, 2005 and 2007 and no traces in 2000, 2008 and 2009.

Ammonia

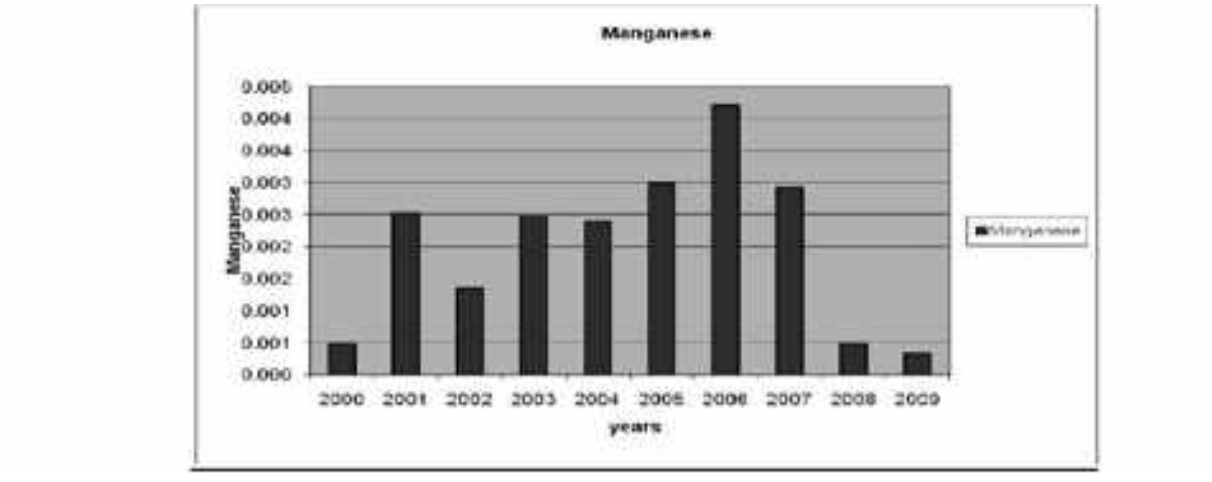

No traces have been observed in Coimbatore South and Udumalpet while the maximum mean concentration of ammonia (0.012) was observed in Mettupalayam. The range is from 0 to 0.12 (Fig.9.). The values are positively skewed in all the taluks and kurtosis shows peak value for Mettupalayam. The temporal trend shows maximum value of ammonia 0.018 in 2006 and no traces in 2000, 2008 and 2009.

Fig. 9. Ammonia in Coimbatore district of Tamilnadu (2000 to 2009)

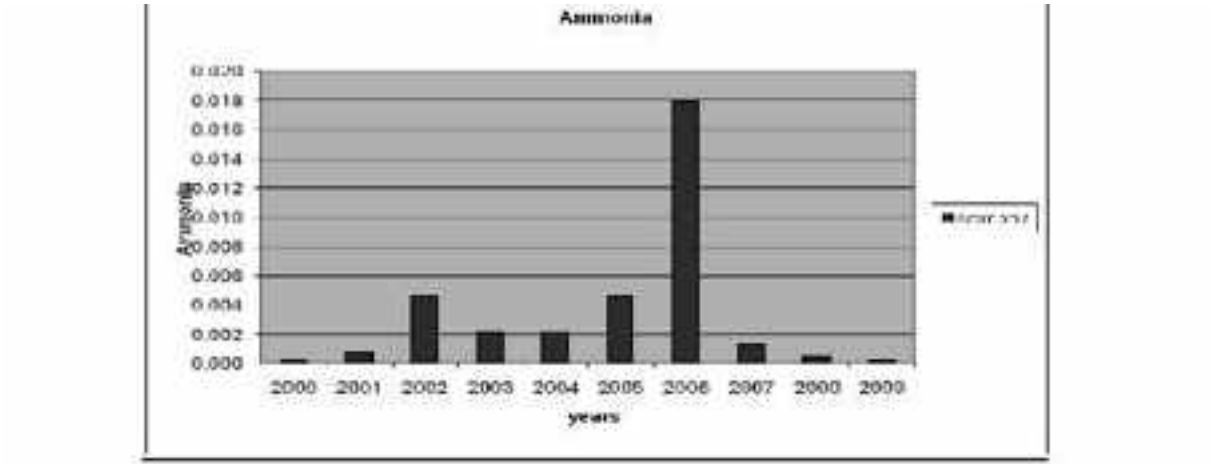

Nitrite

The maximum mean concentration of nitrite was found in Tiruppur (0.061) and minimum concentration at Avinashi and Coimbatore North (0.002). The range varies from 0.001 to 0.192.(Fig.10.) The values are positively skewed in all the taluks. The value is leptokurtic in Mettupalayam and platykurtic in all the other taluks. The %CV ranges from 13.05 to 153.99. The temporal analysis shows maximum nitrite concentration in 2006 (0.055) and minimum in 2000 (0.004).

Nitrate

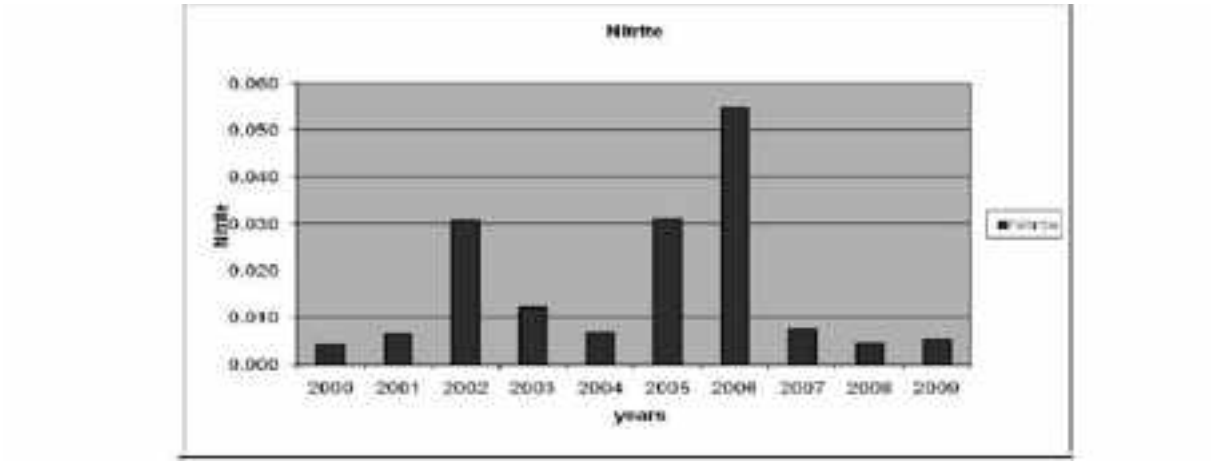

Tiruppur taluk showed the maximum concentration of nitrate (6.501) and the minimum was found in Avinashi (1.219). The range varies from 0.390 to 34.780 (Fig.11.). The values are negatively skewed for Avinashi, Combatore North and Mettupalayam and positively skewed for other taluks. Tiruppurtaluk shows peaked value for kurtosis. The % CV is from 10.59 to 167.66. The temporal trend shows a high value in 2005 (6.23) and a low value in 2009 (2.26).

Fig. 11. Nitrate in Coimbatore district of Tamilnadu (2000 to 2009)

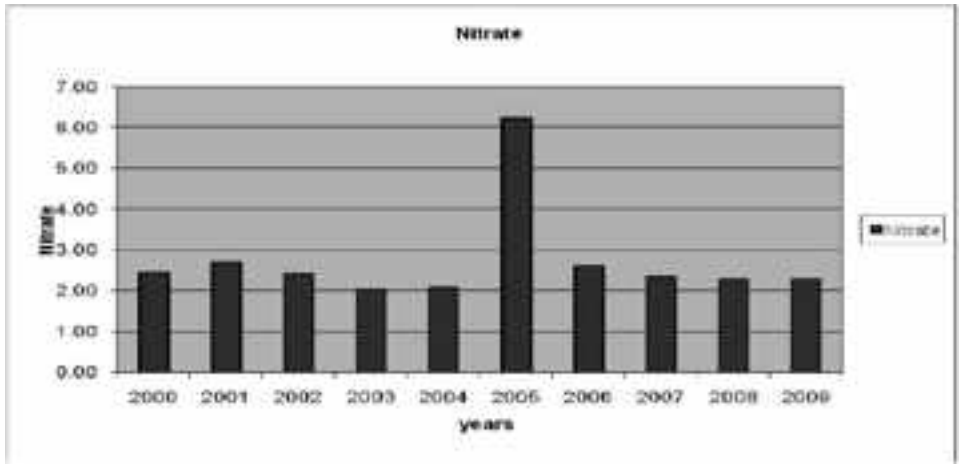

Chloride

The maximum mean concentration of chlorides was found in Mettupalayamtaluk (14.37) and minimum at Valparai (5.83). The range is from 0.610 to 5.150. The values are negatively skewed for Avinashi, Coimbatore North, Tiruppur and Udumalpet (Fig. 12). All the taluks show platykurtic values. The %CV ranges from 2.85 to 14.50. The temporal analysis shows maximum concentration of chloride in 2004 (9.64) and minimum concentration in 2006 (8.72).

Fig.12. Chloride in Coimbatore district of Tamilnadu (2000 to 2009)

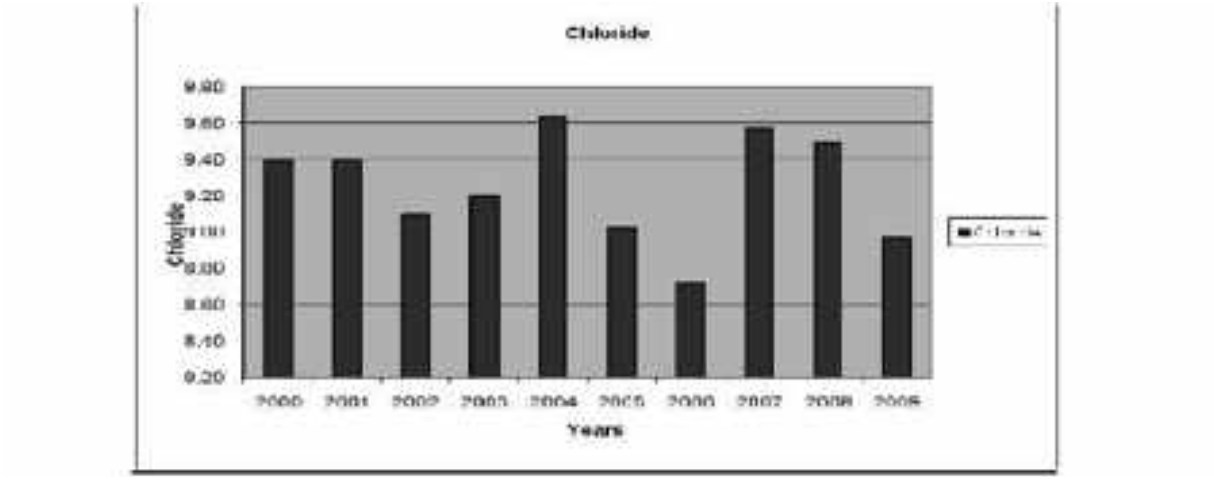

Fluorine

Coimbatore South was observed to have the maximum concentration of fluorine (0.22) and the minimum was found in Valparai (0.002). The range varies from 0.001 to 0.720. The values are negatively skewed for Coimbatore north and South, Mettupalayam, Palladam and Valparai (Fig.13.). The

kurtosis is peaked in Udumalpet and Valparai and platykurtic in other taluks. The %CV is from 2.24 to 125.67. The temporal trend shows maximum concentration in 2001 (0.129) and minimum in 2008 (0.109).

Fig. 13. Fluorine in Coimbatore district of Tamilnadu (2000 to 2009)

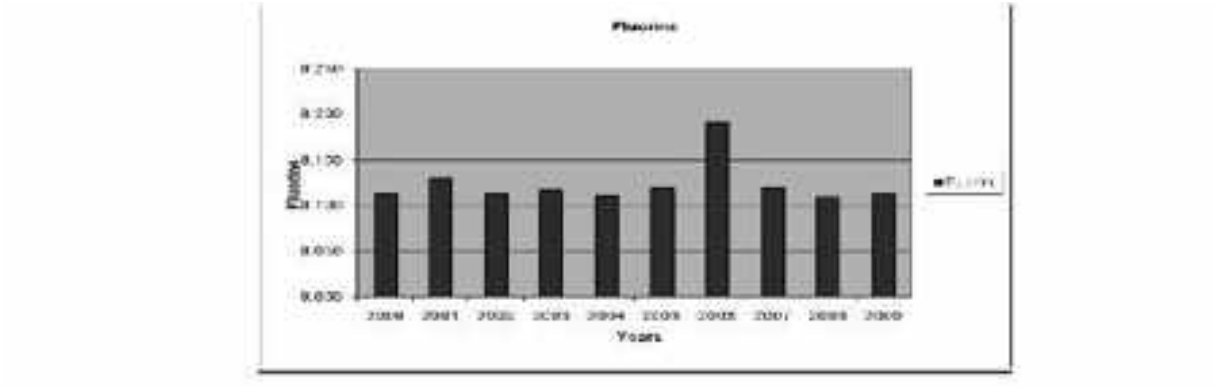

Sulphate

The maximum concentration of sulphate was observed in Coimbatore South (19.01) and minimum in Avinashi (2.029). The range varies from 0.75 to 93.71. (Fig.14.) The values are negatively skewed for Coimbatore North, Mettupalayam, Palladam and Tiruppur. Kurtosis values are peaked for Coimbatore South. The %CV ranges from 9.11 to 152.51.The temporal trend shows maximum concentration in 2009 (15.58) and minimum in the year 2008 (4.57).

Fig. 14. Sulphate in Coimbatore district of Tamilnadu (2000 to 2009)

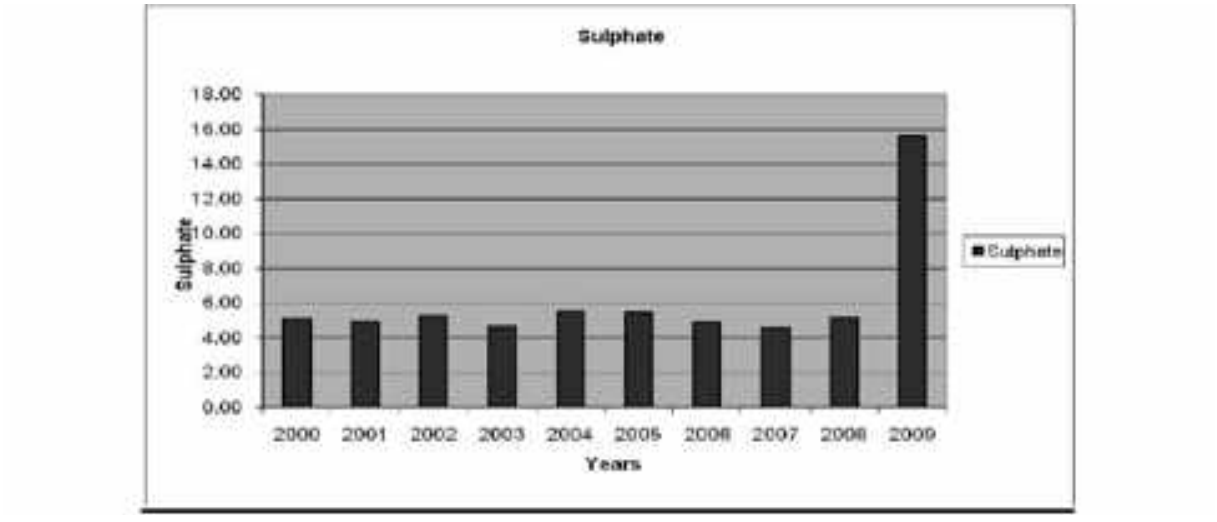

Phosphate

Tiruppur taluk shows the maximum concentration of phosphates (0.07) and no trace is seen in Coimbatore South. The range varies from 0 to 0.23. Negative skewness is seen in Avinashi, Coimbatore

North and Valparai. Kurtosis is peaked in Valparai. The %CV ranges from 0 to 210.81. The temporal trend shows the maximum value of 0.054 in 2002 and 2005 and minimum value of 0.001 in 2000 and 2009.

Fig. 15. Phosphate in Coimbatore district of Tamilnadu (2000 to 2009)

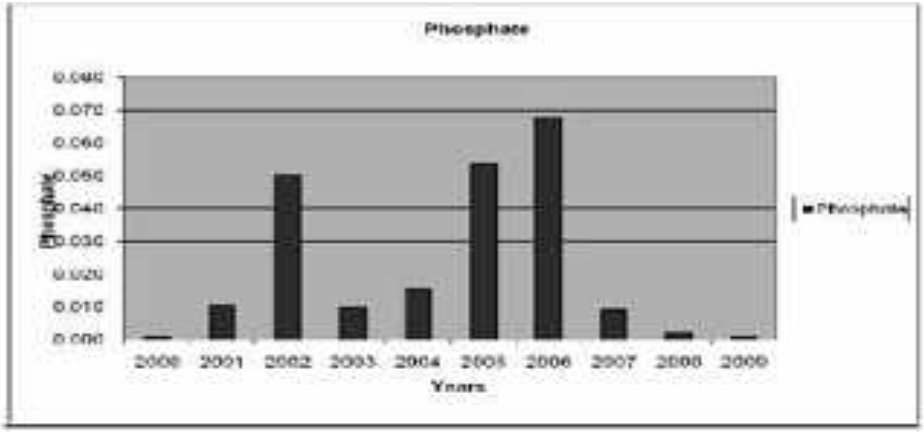

Faecal coli

The maximum faecal coli was found in Mettupalayam (534.92) and minimum in Valparai (115.90). The range varies from 89.76 to 692.91. The values are negatively skewed in Coimbatore North and South, Mettupalayam, Palladam and Tiruppur (Fig.16) . The values are peaked in Coimbatore South and Valparai. The % CV ranges from 15.13 to 70.43.The temporal trend shows maximum concentration of faecal coli in 2003 (387.82) and minimum in 2009 (147.21).

Fig. 16. Faecal coli in Coimbatore district of Tamilnadu (2000 to 2009)

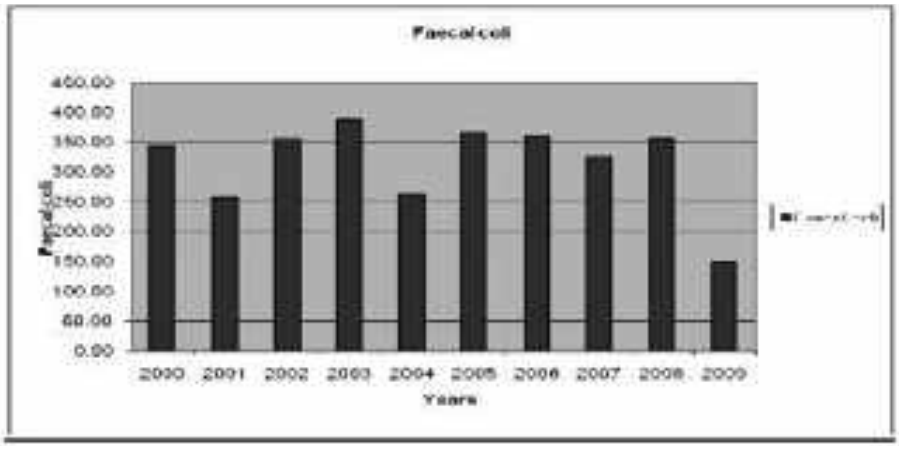

Residual Chlorine

The maximum mean residual chlorine was found in Mettupalayam (1.86) and minimum in Valparai (0.34). The range varies from 0.06 to 6.72. All the taluks are positively skewed and platykurtic. The %CV ranges from 5.92 to 149.61. The temporal trend shows maximum concentration in 2009 (1.266) and

minimum in 2006 (0.417) (Fig.17.).

Fig . 17. Residual Chlorine in Coimbatore district of Tamilnadu (2000 to 2009)

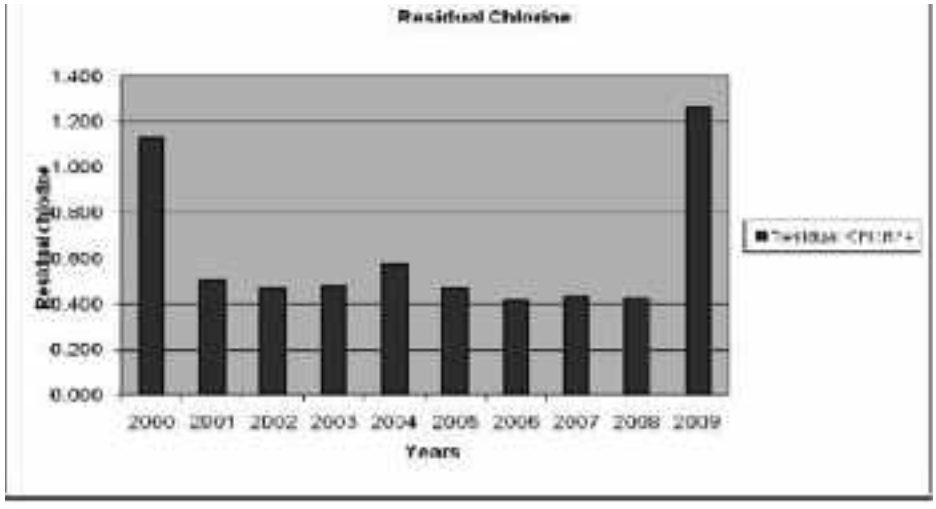

Water is an elixir of life. It is an important component to human survival. Water should be purified for a better life style. It is the basic duty of every individual to conserve water resources. The pH value of drinking water is an important index of acidity or alkalinity. A number of minerals and organic matter interact with one another to give the resultant pH value of the sample. In the present study, pH ranges from 6.6-7.9, which lies in the range prescribed by WHO.[14]The EC values for most samples range between 1020-2910(µ mho/cm). The EC value is directly proportional to the Total dissolved matter. All the samples show higher EC values than the permissible limit. When EC value exists at 3000 µ mho/cm, the generation of almost all the crops would be affected and it may result in much reduced yield.[15] Alkalinity of water is defined as the ionic concentration, which can neutralize the hydrogen ions. The phenolphthalein alkalinity value is zero indicating absence of any carbonate and hydroxyl ions. The bicarbonate alkalinity is expressed as a total alkalinity, which ranges between 218-460mg/L. The alkalinity value of all the samples are within the permissible limit of 600ppm. However, little abnormal value of alkalinity is not harmful to human beings[16] . The maximum tolerance range for sulphate is 200-400 mg/L. The excess amount of sulphate causes diarrhoea. All samples are free from sulphate problems. Sulphate produces an objectionable taste at 300-400 mg/L and bitter taste at 500 mg/L[17]. chloride is normally the most dominant anion in water. According to ICMR the maximum permissible limit for chloride in drinking water is 250- mg/L[18].

The four main considerations to take into account when evaluating the relationship between health outcomes and exposure to changes in rainfall, water availability and quality (IPCC, 2007)

is : To be aware of linkages between water availability, household access to improved water, and the health burden due to diarrhoeal diseases. To know the role of extreme rainfall (intense rainfall or drought) in facilitating water-borne outbreaks of diseases through piped water supplies or surface water. Knowledge of coastal, recreational and surface waters.

Acknowledgement

The author is grateful to the Tamilnadu Water supply and Drainage Department, Government of Tamilnadu for providing the necessary data for the work.

References

1. WHO. 2004. Guidelines for drinking water quality.Vol 1, 3rd edition.
2. Rose J.B., Daeschner S., Easterling D.R.,Curriero F.C., Lele S.,Patz J.A.,2000. Climate and waterborne disease outbreaks. J.Am water works Asso. 92,77-87.
3. Checkley W.I., Epstain L.D., Gilman R.H., Figueroa R.I., Cama J.A., Patz J.A., Black R.E. 2000. Effect of El nino and ambient temperature on hospital admissions and diarrhoeal diseases in Bolivian children. Lancet.355, 422 – 450.
4. Gueri M., Gonzalez C., Morin V., 1986. The effect of the floods caused by El nino on health. Disaster.10, 48 -124.
5. Lipp EK, Schmidt N, Luther E and Rose JB (2001).“Determining the effects of El Nino southern orcillation events on coastal water quality”. Estuaries 24 : 491 – 497
6. Colwell R.R., 1996. Global climate and infectious disease: the cholera paradigm. Science.274 (5295), 2025 – 2031.
7. Ahmed M.U., Urasawa S., Tenijulin K., Urasawa T., Kobayashi N., Wakasagi F., Islam A.M.,Sahikh H.A., 1991. Analysis of human rotavirus strains prevailing in Bangladesh in relation to nationwide floods brought by the 1988 monsoon. Journal of Clinical Micro. 29, 1359.
8. Fun B.N., Unicomb L., Rahim Z., Banu N., Podder G., Clemens J., Van Loon F.P., Rao M.R., Marek A.,Tzipori S., 1991. Rotavirus associated diarrhoea in rural Bangladesh: two year study of incidence and serotype distribution. Journal of Clinical Microbiology. 29, 1359-1363 [PMC free article] [Pub Med].
9. Smith E.M.,Gerba C.P., 1982. Development of a method for detection of human rotavirus in water and sewage..Applied and Environmental Biology. 43, 1440 – 1450.
10. Linhares A.C., Pinheiro F.P., Freitas R.B., Gabbay Y.B., Shirley J.A., Beards G.M., 1981. An outbreak of rotavirus diarrhoea among a non-immune, isolated south American Indian community. American Journal of Epidemiology. 113, 703-710. [Pub Med].
11. Hung T., Cheng G.M,, Wang C.G., Yao H.L., Fang Z.Y., Chao T.X., Ye W., Chang X.Z., Den S.S., 1984. Water borne outbreak of rotavirus diarrhoea in adults in China caused by a novel Rotavirus. Lancet.1139-1142 [Pub Med].
12. SPSS for Windows 12.0 SPSS Inc.

13. IPCC Fourth Assessment Report: Climate change 2007. Working Group II: Impacts, Adaptation and Vulnerability. Contents 88.28.2.5.Water and Disease.
14. APHA. Standard methods for examination of water and wastewater, 19th edn., American Public Health Association, Washington, D. C. (1995)
15. Srinivas. C. H., Ravi Shankar Piska, C. Venkatesan, M. S. Sathya Narayana Rao, and R. Ravinder Reddy., 2000. Pollution Research, 19 (2), 285).
16. Singh T. B., Indhu Bala, and D. Singh. 1999. Pollution Research, 18 (1), 111.
17. Gitanjali G., and A. Kumaresan., 2006. Pollution Research, 25(3), 583.
18. Jothivenkatachalam. K., and K. Suresh., 2008. NEPT Journal, 7(2), 283 (2008).

Praveena V* and Karpagam B

Department of Zoology, Nirmala College for Women (Autonomous), Coimbatore- 641018.

Abstract

An investigation was carried out to evaluate the effect of selected plants (*Coleus aromaticus* and ***Solanum verbasifolium*)** supplemented feed on the growth parameters such as weight, specific growth rate and feed utilization on total feed consumed, feed efficiency ratio, protein efficiency ratio and survival rate of *Oreochromis mossambicus*. The fishes were fed with these supplemented feed for 45 days and the results were obtained. The data were subjected to one way analysis of variance and the means were separated using least significant differences. The fishes fed with supplemented feed showed maximum increase in weight gain, specific growth rate, feed consumed, feed efficiency ratio, protein efficiency ratio and survival rate than the control fishes. This study indicated that inclusion of plant ingredients in fish feed resulted in superior growth performance and the formulation of plant based diet for fish will provide new opportunities.

Keywords: tilapia, plant supplemented feed, growth.

Introduction

Fish is a vital source of high-quality protein, providing approximately16% of the animal protein consumed by the world's population[1]. It is particularly an important protein source in the regions where livestock is relatively scarce. Fish supplies less than 10% of animal protein consumed in North America and Europe, but 17% in Africa, 26% in Asia and 22% in China [2]. The FAO estimates that about one billion people world-wide rely on fish as their primary source of animal protein[2] .

According to the UNO food and agricultural organization, aquaculture is growing more rapidly than all other animal food production sectors [3]. Indian agricultural has demonstrated six and half fold growth over the last two decades where fresh water aquaculture contributing over 95% of total aquaculture production. Variety of fishes were farmed and it includes carps (Catla, Rohu, Mirgal), Tilapia, Salmon, Channa etc.

Among these fishes, tilapia is one of the main economical fresh water fish that constitutes the 3rd largest group of farmed fin fish, right after carp and salmonids, with annual growth rate around 11.5%, much of the rapid increase in aquaculture production has come from the increasing of existing systems [4]. Tilapia is a unique fish in the inland fish production. There are possibilities to enhance tilapia culture further through other systems of aquaculture practices. However the feed cost is the highest operating cost in the aquaculture practices and an economically efficient feed would play major role in stimulating feed based aquaculture of tilapia.

In fish culture, nutrition plays an important role in the maintenance of a healthy and marketable product. Therefore, uses of functional feed are novel to the aquaculture industry. There are large numbers of feed additives available to increase fish growth performance. Some of the additives used in feed meal are chemical products especially hormones and antibiotics which may cause unfavorable side effects. To keep a sustainable growth pattern and health management, strategies must go beyond antibiotics and chemotherapeutics which create resistant bacteria and immune supplement in host [5]. Herbs have been used as a medicine and as an immune booster for humans for thousands of years. Throughout the world, as many of them are rich sources of volatile oil, saphonins, phenolics, tanins, alkaloids, polysaccharides and polypeptides which are responsible for various activities like anti stress, tonic, antimicrobial and immunostimulant [6,7]. Some plants are found to have natural affects for example, tonics, antiparasitic, antibacterial, stimulant, carminative, antifungal, antimicrobial and antiseptic [8]. Recently in aquaculture numerous medicinal plant extract have been tested in good results for the growth of fishes. Therefore, in the present study an attempt was made to evaluate the supplementation of selected plant leaves as growth promoter.

Materials and Methods

An investigation was carried out in our laboratory to evaluate the effect of formulated feed on the growth of Tilapia fish (*Oreochromis mossambicus)*. The materials and methods used for the present study are described under the following headings.

Collection and Acclimatation of Experimental Animal

The experimental animal selected for present study was tilapia fish (*Oreochromis mossambicus).*The fish was collected from Aliyar dam near Pollachi were acclimatized to fresh water condition for 2-3 weeks in laboratory. Care was taken to avoid contamination.

Collection of plants

Fresh leaves of ***Coleus aromaticus*** and ***Solanum verbasifolium*** were collected.

Preparation of plant powder

Fresh leaves of selected plants were collected, washed, shed dried and ground into fine powders and used for preparation of feed.

Preparation of fish feed

Fish feed were prepared by adding equal proportions of soya bean powder, wheat flour and coconut oil cake in the ratio of 1:1:1 and corn flour as a binder. These substances were mixed thoroughly with hot water and it was boiled for 25-30 minutes and then cooled at room temperature for 30 minutes and

the multi vitamin and mineral tablets were added and pellets were prepared by using domestic appliances with 0.5mm diameter. It was dried as a small pellet by keeping in the sun. Five experimental diets were prepared by adding 5 grams of plant powders were added separately and the feed without plant powder was kept as control (Table.1).

Experimental Set Up

The laboratory experiment was laid in completely randomized design (CRD). Three replications

Ingredients	Moisture (gm)	Crude protein (gm)	Ether extract (lipid) (gm)	Carbohydrates (gm)	Crude fibre (gm)	Energy (k cal)
Wheat flour	12.3	13.1	1.7	69.4	1.9	341
Coconut oil cake	8.7	23.8	2.4	47.9	9.8	312
Soyabean	8.1	43.2	19.5	20.9	3.7	432
Corn flour	11.9	10.4	1.9	72.6	1.6	349

from each concentration and control were maintained simultaneously. The experiment was conducted using 15 liter plastic troughs. The troughs were stocked with 5 fishes with mean initial body weight of 5grams in uniform size. The fishes were starved for a night prior to the experiment. The experiment was conducted for 45 days and the fishes were fed with experimental diets. The medium was changed daily in order to remove the faecal and unconsumed wastes.

Growth Parameters

After 45 days feeding trail the following observations were recorded for each treatment and control every 15 days once.

1. Weight Growth Rate (gm/day) = Final weight of the fish – Initial weight of the fish/No. of days
2. Specific growth rate (%/day) = (Final weight of the fish – Initial weight of the fish/ No. of. Days) x100
3. Total feed consumed (gm/day) = (Weight of the dry feed given – Dry weight of the unconsumed feed) x100
4. Feed efficiency ratio (gm/day) = (Average total weight gain/ Total dry feed weight) x 100
5. Protein efficiency ratio (gm/day) = W weight Gain (gm)/ protein intake) x No. of fish
6. Survival rate (%/day) = final no. of fish – initial no. of fish/100

Statistical Analysis

The data on growth parameters were transformed into arc sine values before subjecting into

ANOVA. To find out the significance of comparative efficacy of different leaf extract on weight, specific growth rate, total feed consumed, feed efficiency ratio, protein efficiency ratio and survival rate. One way analysis of variance was used. Mean differences of each variable were further analyzed using least significant differences.

Results and Discussion

The growth parameters using plant powder feed on weight, specific growth rate, feed efficiency ratio, total feed consumed, protein efficiency ratio and survival rate of *Oreochromis mossambicus* were described below. The statistical analysis of the data revealed highly significant between the control and different treatments. After 45th day of observation, supplemented feed showed maximum increase in all the parameters (Table 2.).

This study indicated that the appetite of hybrid Tilapia is influenced by the concentration of feed attractants. The inclusion of leaf extract in the experimental diet resulted in improvement in body weight gain, length gain and specific growth rate. This result suggests that hybrid Tilapia was chemo reaction as well as olfaction to detect and select its feed. This pattern is similar to that observed by several researchers reported that appetite is a good criterion for testing effectiveness of feed attractants 9,10,11. Coleus aromaticus belongs to family Lamiaceae is known as a must have plant in medicinal herb garden. The plant is well known for its antimicrobial and pharmacological activities. It is also reported to possess antioxidants and food additive property.

Table 2. Effect of supplemented feed on growth parameters after 45 DaysIt is a good source of nutritious compounds and can be used as food supplement. It consists of methanolic extract

Parameters	Control	*Coleus aromaticus*	*Solanum verbasifolium*
Initial weight	5±0.01	5±0.01	5±0.01
Final weight	6.09	6.54	6.66
Difference	0.9	1.54	1.66
Weight gain	1.34%(6.64)c	1.52%(7.08)a	1.39%(6.78)b

Specific growth rate	2.58%(0.24)c	3.40%(0.52)a	3.02%(0.00)b
Total feed consumed	29.74%(33.04)c	34.67%(36.07)a	31.59%(33.82)b
Feed efficiency ratio	44.33%(41.74)c	51.56%(45.89)a	46.43%(42.95)b
Protein efficiency ratio	5.61%(13.60)c	6.43%(14.49)a	5.77%(13.90)c
Survival rate	99.99%(89.90)a	99.99%(89.90)a	99.99%(89.90)a

which act mainly as an antibacterial form of activity. It is considered to be immunostimulant and a growth promoter.

Conclusion

The results of present study indicate that inclusion of plant ingredients in the fish feed results in superior growth performance compared to control feed. The formulation of plant based diets for fishes will provide new opportunities for regionally available plant materials in fish feed use.

References

1. **FAO,** 1997. Food and Agriculture Organization of the United Nations. Review of the State of World Aquaculture. *FAO Fisheries Circular* No. 886, Rev. 1. Rome, Italy.
2. **FAO,** 2000. Food and Agriculture Organization of the United Nations. The State of World Fisheries and Aquaculture. FAO, Rome, Italy.
3. **FAO, 2006**. Food and Agriculture Organization of the United Nations. The State of World Fisheries and Aquaculture. Rome, *FAO Fisheries Technical Paper,* 500, 145pp.
4. Bittencourt .N.L.D., L.M. Molinari, Scoaris D.de o., R.B. Pedroso, C.V. Nakamura, T.Veda-Nakamura, B.A.de A.Filho, and B.P.D.Filho.,2003. Haematological and Biochemical Values for Nile Tilapia *Oreochromis niloticus* cultured in Semi- intensive System , *Actas cintarium. Biological Sci. Maringa*.25,385-389.
5. Panigrahi A., and Azad I.S., 2007.Microbial intervention for better fish health in aquaculture: The Indian Scenario. *Fish Physiol. Biochem*. 33, 429-40.
6. Citarasu T., VenkatRamalingam. K., Raja JeyaSekar., MichealBabu M., Marian M.P., 2003. Influence of the antibacterial herbs, *Solanum trichobatum*, *Anorographs Paniculata* and *Psoranea corynyfona* on the survival, growth and bactericidal load of *Penaeus monodon* post larvae. *Aqua .Int.* 11, 581-595.
7. Citarasu T., Babu M.M., Sekar R.J.R., Marian P.M., 2002. Developing Artemia enriched herbal diet for producing

quality larvae in *Penaeus monodon, Fabricius*. *Asian Fish Sci*. 15, 21-32.

8. Soliman A.Z., Abd El-Malak,N.Y., and Abbas A.M., 1995. Effect of using some commercial feed additives as promoters on the performance of growing and adult rabbits. *Egypt.J.App.Sci*. 10, 501-15.
9. Takei M., 1967. Studies on fish favorite foods: I. Feeding test of carp, yellow tail and rainbow trout. *Bull Takei Regional Fish Res Lab*. 49,119-129.
10. Harada. K.., 1990. Attraction activities of spices for oriental weather fish (*Misgurnus anguilicaudatus)* and yellow tail (*Seriolaquin quaradiata)*. *Bull Jap Soc Sci Fish* (Japan. 56(12), 2029-2033.
11. ElDakar A.Y, Hassanien G.D.I., Seham S., Gad and Sakr S.E., 2004. Use of medicinal and aromatic plants in fish diets:Effect of dried marjoram leaves on Performance of hybrid Tilapia *Oreochromis niloticus* X *Oreochromis aureus*, Fingerlings. *J Egypt Acad Soc Environ Devpt* 5(1), 67-83.

Scientia
Vol.9, No. 1, Jan - Dec. 2013, pp134-139
Scientia Jan- Dec. 2013
ISSN : 0976 - 8289

Olfactory discrimination and transitive inference in mice

Preeji K P*, Sowmya Raj and John K Thomas

Animal Behaviour and Wetland Research Laboratory, Department of Zoology,

Christ College, Irinjalakuda, Kerala, India 680125

Abstract

Female mice are able to discriminate the social status of males based on the pheromone content of the urine. We tested whether this ability of female mice is innate or whether it develops through learning during contact with the male urine. Further we tested the ability for transitive inference of the mice by pairing the male urine with odorous edible oil. The results showed that without prior contact with male urine, virgin females were able to discriminate urine of dominant male from that of the subordinate male and thus, it is an innate ability of female mice. It was found that virgin females exhibit significant preference to the odour of oil paired with the dominant male urine as compared with that of the odour of the oil paired with the subordinate male urine. The preference shown by virgin females to the oil associated with dominant male urine was not significantly different from response shown to the urine of dominant male urine. The present study shows that the virgin female mice are able to transfer the value of dominant male urine to odour of the edible oil through associative memory. It was found that this associative memory lasts for two oestrous cycles and then fades off.

Keywords: Keywords: Dominant male urine, subordinate male urine, pheromone, olfactory discrimination, transitive inference

Introduction

Olfactory information is essential for a wide range of mouse behaviors, including navigating, foraging, avoiding predators, kin recognition, bond formation, mate selection, sexual and parental behaviors[1,2,3,4,5,6]. The onset of estrus and successful fetal implantation in female mice are both modulated by male odors [7]. Mice have the ability to discriminate conspecifics that differ in MHC odor type [8] and can determine whether others of their species are infected by viruses or parasites, presumably a skill useful in selecting a healthy mate [9,10]. Females of several species of mammals exhibit preference for dominant male and olfactory signals have been shown to be involved in this type of identification in hamsters, lemmings, mice and European rabbits[11]. In common with many species, male house mice advertise their location, successful territory ownership and dominance through scent marks continually deposited around their defended territory[12]. Such social odors are typically produced in urine or secreted from scent glands distributed over the body. Both volatile and nonvolatile cues are known to be produced[13,14,15,16]. Olfactory memory refers to the recollection of odors. Studies have found various characteristics of common odor memory including persistence and high resistance to interference. Recently several tests have been

**Corresponding author,Email: ashasebastian13@gmail.com*

adapted to assess olfactory memory in mice[17,18,19,20]. Among different laboratory tasks used to investigate recognition memory in rats and mice, the social recognition/social discrimination task has several advantages. For instance, this task does not require the application of additional stimuli in order to provoke the behavioral response used as an index for the memory performance[21,22]. More specifically, the task takes advantage of the innate drive of an adult animal to investigate nonfamiliar over familiar conspecifics. Both rats and mice are macrosmates for which store and recall of information acquired by olfaction and this is a prerequisite for a successful interaction with the living and nonliving world[23,24]. Performance on the social recognition/social discrimination task requires olfactory information and male mice are able to store the "olfactory signature" of a given conspecific for at least 7 days[25].

It has been demonstrated that female mice are able to identify its stud male based on olfactory cues and the presence of the stud male or its urine protects the female from alien male induced implantation failure (The Bruce effect)[26]. Further it has been shown that when implantation blocked females are re-exposed to the stud males the majority of the females exhibited pseudo pregnancy, indicating that the activation of the olfactory memory by pheromones of the stud male releases the hormones essential for the maintenance of pregnancy in this species[27].

Transitive inference (TI) is a form of deductive reasoning that allows one to derive a relation between items that have not been explicitly compared before. In a general form, TI is the ability to deduce that if Item B is related to Item C and Item C is related to Item D, then Item B must be related to Item D.TI assumes that the animal assigns each stimulus with a value. The stimulus gets its own value, independent of the other stimuli. According to the theory of value transfer, in any simultaneous discrimination task, some of the value associated with the S+ is transferred to the accompanying S- The value transfer theory, predicts that the animal solves the TI task by assessing the value of the items being presented[28]. These values are acquired through training. The positive value of an item is transferred to the other item with which it is being presented[29]. Previous studies on mice have reported mixed results on whether this species is capable of associative inference[30],[31] and one study has reported that mice show transitive inference in the hierarchical series variant of the task[32].

The present study is designed to evaluate the ability of the oestrous female to discriminate the social status (dominant/ subordinate) of the male through pheromones present in the urine and whether the female is

able to transfer the value of information they gained to any other substances through associative memory and transitive inference.

Materials and Methods

All studies were conducted in Balb/c mice purchased from Veterinary College, Mannuthy, Trissur, Kerala. Animals were housed under standard laboratory conditions of constant temperature of 23^{o}C; 12:12 reverse light/dark cycle (lights on at 5 p.m.) and food and water were provided *ad lib*. Estrous cycle of female mice was assessed using standard vaginal smear method. Selected females were grouped into four, GP I, GP II, GP III and GP IV. Discrimination test was done in the first three sets. Associative memory test was conducted in the remaining GP IV. There were 3 mice in each group except the IVth group which had 8 mice. All tests were done during the estrous day (cornified+leucocyte cells in the smear) of females.

Study of the estrous cycle by examination of the vaginal smear

Stages of oestrous cycle of the mice are reflected in the changes in appearance and composition vaginal cells. The oestrous cycle of the animal can very easily be determined by examining the vaginal cells under a microscope. Vaginal smears are obtained by gentle scraping of the dorsal wall of the vagina with a steel spatula with smooth edges. The female is held in head down position and the tip of the spatula moistened with water is introduced into the vagina and the vaginal wall is gently scraped to obtain the smear. The technique will not cause any injury to the vagina or cervix. A small sample of the cells from the vaginal epithelium was spread on a clean glass slide, dried and examined without staining under a microscope. The approximate proportion of each cell type in the smear was recorded.

Y-maze Tests for olfactory discrimination

Dominant and subordinate status of the male mice is determined through a dyadic encounter across a Plexiglas partition. Male showing higher aggressive behaviour indicated by higher frequency of aggressive postures and tail rattling is assumed to be the dominant male.

The maze consisted of a Plexiglas box (120 x 90 x30cm) plus two goal boxes and one start box (45 x30 x 30cm). A Plexiglas triangle at one end of the box divided it into a Y-shaped maze. The top edges of the Y-maze were covered with Plexiglas panels. Stimuli were placed in goal boxes, separated from the rest of the maze by perforated, opaque doors. The maze and start box were washed with a dilute soap solution and 70% ethanol between subjects.

Prior to the experiment, subjects were placed in the empty Y-maze for five min to familiarize them with the apparatus. Each testing session began by placing the subject in the start box for 30 seconds and then raising the door, allowing the animal to approach a goal box (free trial). A choice was recorded when the subject touches one of the goal box doors with her nose or front paw and the time spent near the goal box and latency to approach the goal box was recorded. If the subject failed to make a choice within 120s, it was

returned to the start box and the trial was repeated.

After completion of a free trial, the subject was placed back into the start box, the arm of the Y-maze leading to the previously chosen goal box was blocked off using a wooden block and the start box door was raised, forcing the animal to approach the goal box not chosen on the previous trial (guided trial). In this way subjects were reminded of which stimulus lay behind each goal box door. Each day's testing session consisted of eight free trials alternating with seven guided trials. The locations of the stimuli were alternated on each test. The tests were done as follows;

Discrimination test

GP I – Urine of dominant male/ Urine of subordinate male (D/S)

GP II – Urine of dominant male + Groundnut oil/ Urine of subordinate male + Gingili oil (D+GN/S+GG)

GP II a – Groundnut oil/ Gingili oil (GN/GG)

GP III – Urine of dominant male+ Gingili oil/ Urine of subordinate male+ Groundnut oil (D+GG/S+GN)

GP III a - Gingili oil/ Groundnut oil (GG/GN)

GP IV - Urine of Dominant male+ Groundnut oil/ Urine of Subordinate male + Gingili oil (D+GN/S+GG

GP IV a- Groundnut oil/ Gingili oil (GN/ GG)

GP IV b- GN/GG

GP IV c- GN/ GG

GP IV d- GN/GG

Virgin female mice of 30-32g body weight were tested for their preference to approach Y-maze goal boxes containing the stimulus (Fig.1). In GPI the preference of the subjects to urine of dominant/subordinate male urine is tested. In GII one drop of the urine of dominant male was paired with ground nut oil and urine of the subordinate male was paired with gingili oil and tested their preference. One drop of male urine (Dominant/subordinate male) is placed on one end of a glass slide and one drop of oil was placed on the other side to avoid mixing up. In order to test the associative memory and value transfer ability of the females GP II were exposed to one drop of ground nut oil/gingili oil and tested their preference (GPII a). It is assumed that if the animal is able to associate the smell of the oil with that of the male urine paired with it, the subjects will exhibit preference to the respective oil in the absence of the urine of the male. To rule out the possibility of any natural preference of the animals to the oil, in GP III, urine of dominant male is paired with gingili oil and the urine of the subordinate male is paired with ground nut oil (D+GG/S+GN) and tested the preference of the subjects. In GP IIIa the same subjects were exposed to oil alone and their

preference is tested. Frequency of visits to the stimuli, latency to approach the stimuli and the time spent near the stimuli were recorded. Proportion of equality test was used to assess statistical significance of the preference of the female mice.

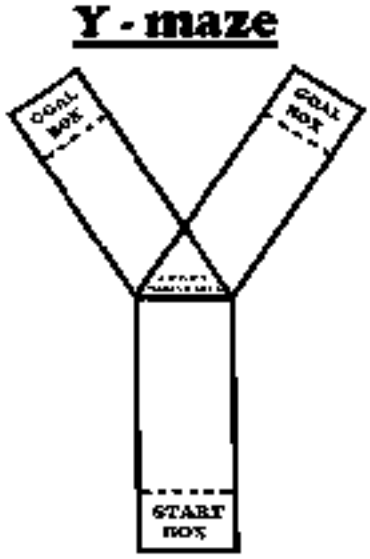

Fig.1. Test for duration of associative memory

The eight mice in the GP IV were initially exposed to the urine of Dominant male+ Groundnut oil/ urine of Subordinate male+ Gingili oil and tested their preference. All tests were conducted during the oestrous day of the female mice in a Y maze, as explained earlier. They were then divided into four sub groups (GP IV a, GP IV b, GP IV c and GP IV d) consisting of two mice in each group. In order to test the duration of associative memory of the four subgroups, olfactory preference of the subjects were tested by presenting only oil, in the absence of male urine. Test was done 6 days after first exposure in the case of GP IV a. In GP IV b, the experiment was done on the 12^{th} day, leaving one oestrous day in between. In GP IV c, test was done on the 18^{th} day after leaving two consecutive oestrous days without experiment. In GP IV d, the test was done after leaving three consecutive oestrous days without test ie., on 24^{th} day after the first exposure. Here also the frequency of visits, latency to reach the stimuli, and the time spent by the subjects near the stimuli during the free trials were noted. Proportion of equality test was done to analyse the statistical significance.

Result and Discussion

The results demonstrate that given a choice between urine of dominant and subordinate male, virgin female mice preferred the urine of dominant male. This is indicated by the fact that the frequency of visit of the female and time spent near the stimulus containing the urine of dominant male was significantly higher

than that of the stimulus containing urine of subordinate male (Fig.2and 4) and the latency to reach the preferred stimuli was lower in all cases (Fig. 3). It is evident that virgin female is able to discriminate dominant male urine from that of the subordinate male and exhibited preference to it. Individual recognition is very crucial among social species in which each member depends on the identity of the other. It is suggested that one of the important functions of vertebrate pheromones is to designate the identity of the emitter[33]. These urinary scents provide a broad range of individual-specific information on a male's genetic compatibility and quality that is used by female mice in mate selection, influencing the relative attractiveness of individual males and their scents[34,35]. Female mice range over several male territories under natural conditions, strongly preferring to mate with dominant territory owners, and approach selected males when ready to mate[36,37,38]. In Syrian hamsters given a choice between dominant and subordinate males the females always preferred the dominant male[39]. In the house mouse (*Mus musculus*), where females were allowed free movement between confined dominant and subordinate males, they accepted more intromissions and ejaculations from the dominant than from the subordinate males[40]. In mice it has been shown that difference in the H-2 major histocompatibility locus and Tla regions of chromosome 17 is the basis for the individual odour difference[41]. Laboratory evidences suggest that female house mice choose males based on variation in traits such as the major histocompatibility locus and t alleles[42,43,44,45].

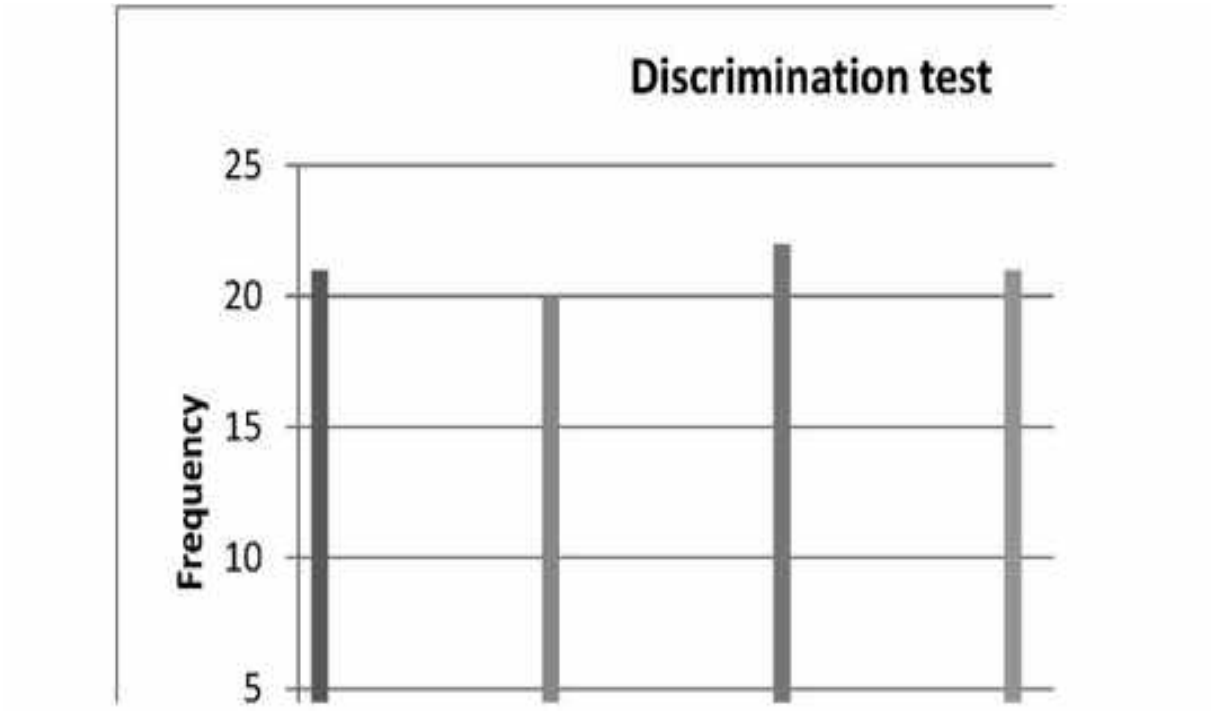

Fig. 2. Showing the frequency of visits by the female mice towards the stimuli during free trials.Fig.

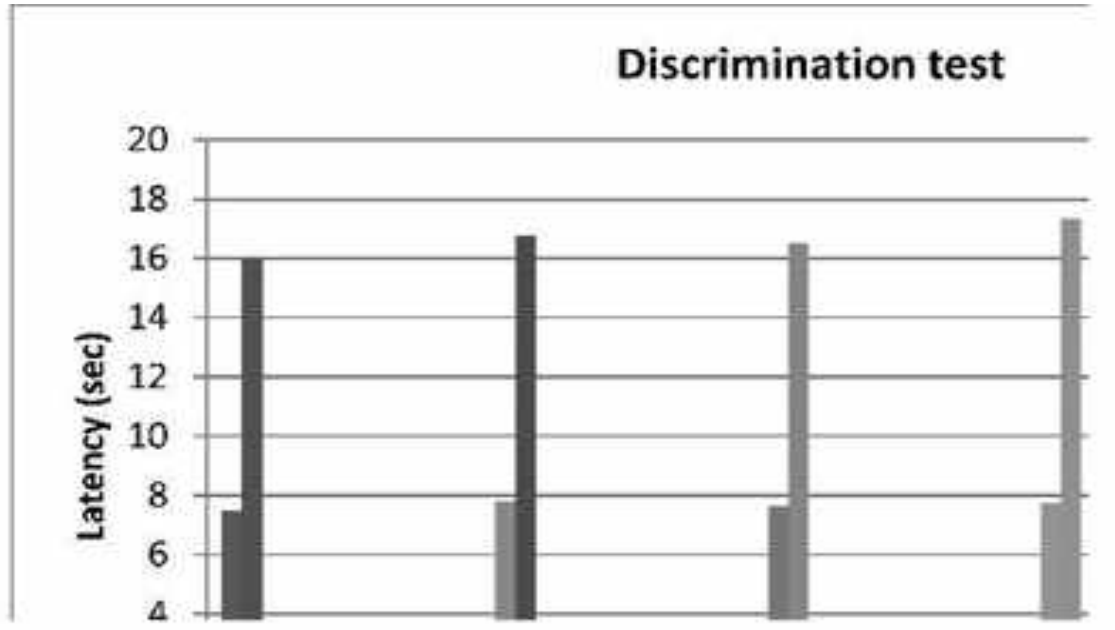

Fig. 3. Showing the time taken by the female mice to reach the stimuli during free trials.

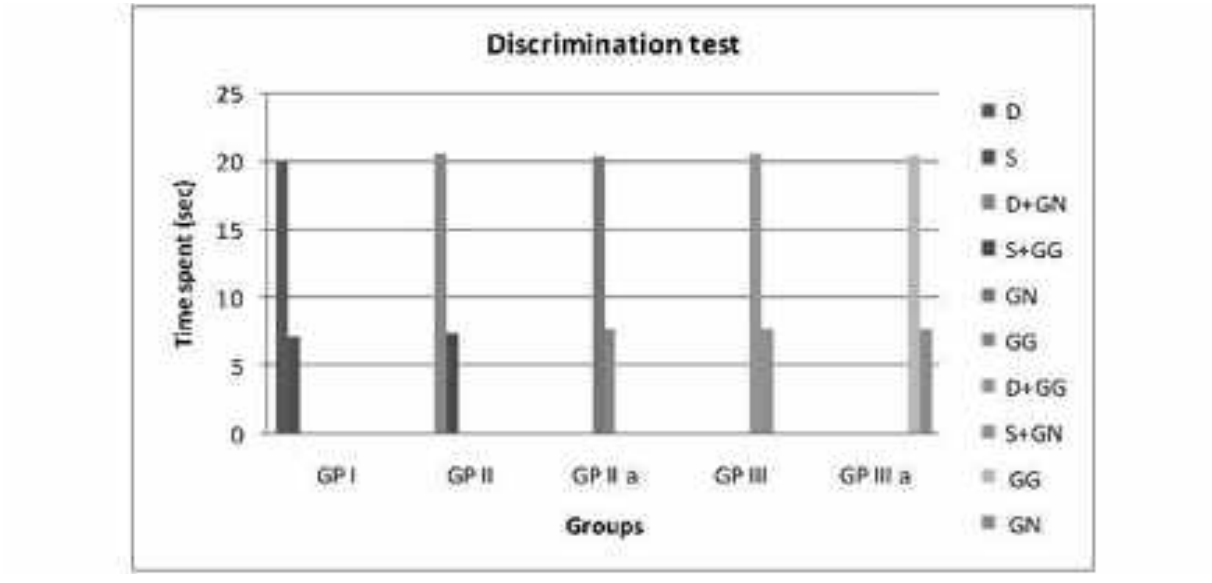

Fig. 4. Showing the time spent by the female mice near the stimuli during free trials

(The table value for proportion of equality test is 1.645 and if we get values greater than table value means that the proportions are not equal and has significant variation. If the calculated values are lower or equal to table value means that the proportions are equal or has no significant variation. Calculated values for fig.2, GP I=5.55, GP II=4.38, GP II a=7.385, GP III=5.55 and GP III a=7.385, for fig.3, GP I=1.88, GP II=1.94, GP II a=1.94, GP III=2.08 and GP III a=2.04 and for fig.4, GP I=2.86, GP II=2.88, GP II a=2.72,

GP III=2.73 and GP III a=2.76. The result shows that all values are greater than the table value means that proportions are not equal and have significant variation).

The present study shows that naive oestrous females always preferred dominant male urine and its associated stimuli, edible oil to that of the subordinate male and also take lesser time to reach the preferred stimuli. Likewise, time spent near the goal post presented with the urine of dominant male or oil associated the urine of dominant male indicates that the female associates the smell of the edible oil with olfactory signals emanating from the dominant male urine. The discrimination tests revealed that, preference towards groundnut oil or gingili oil is based on their association with the urine of dominant male and not depended on the quality of the oil (Fig. 2, 3 and 4).

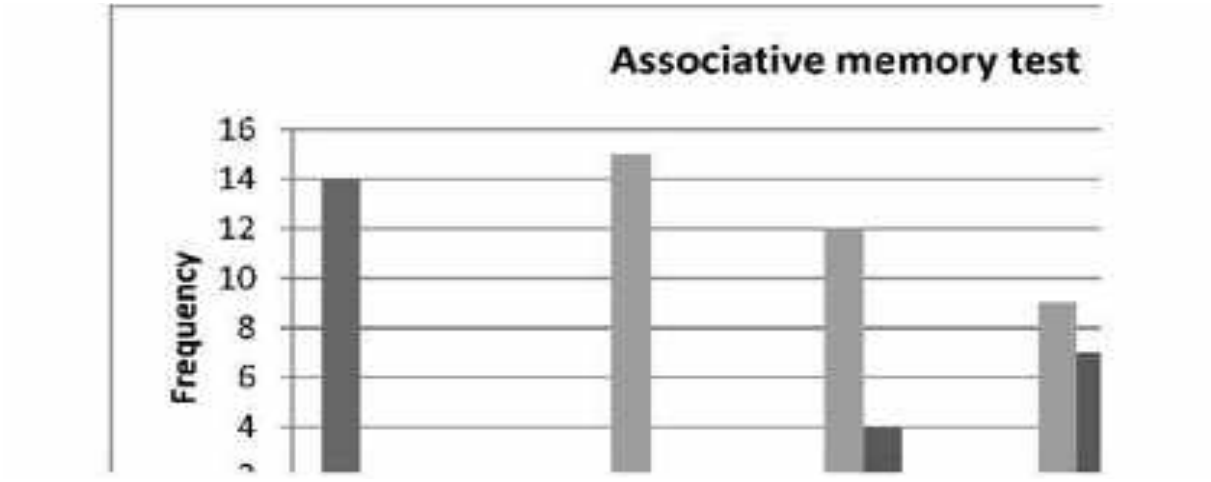

Fig. 5. Showing the frequency of visits by the female mice towards the stimuli during free trials.

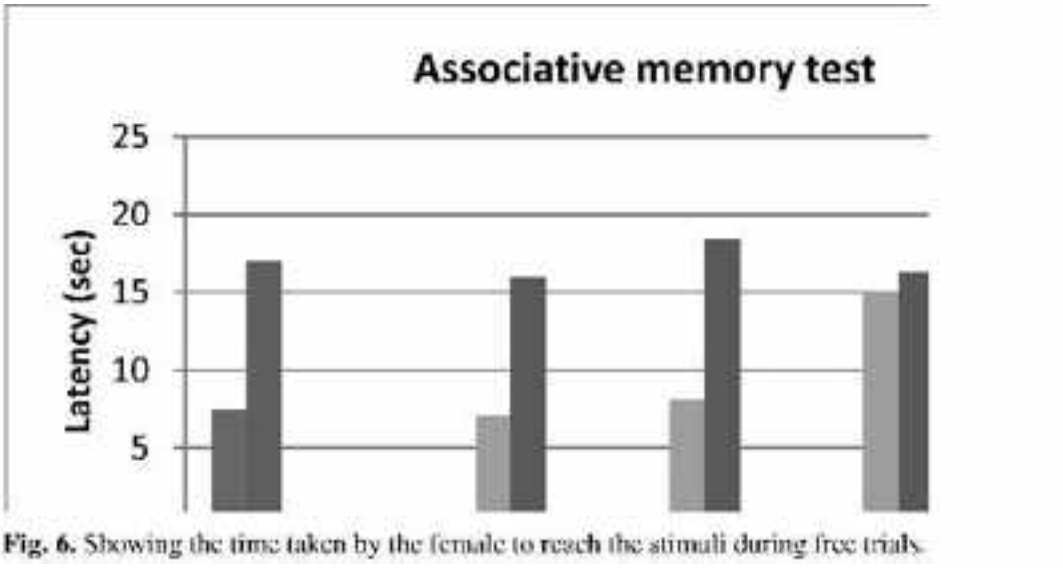

Fig. 6. Showing the time taken by the female to reach the stimuli during free trials.

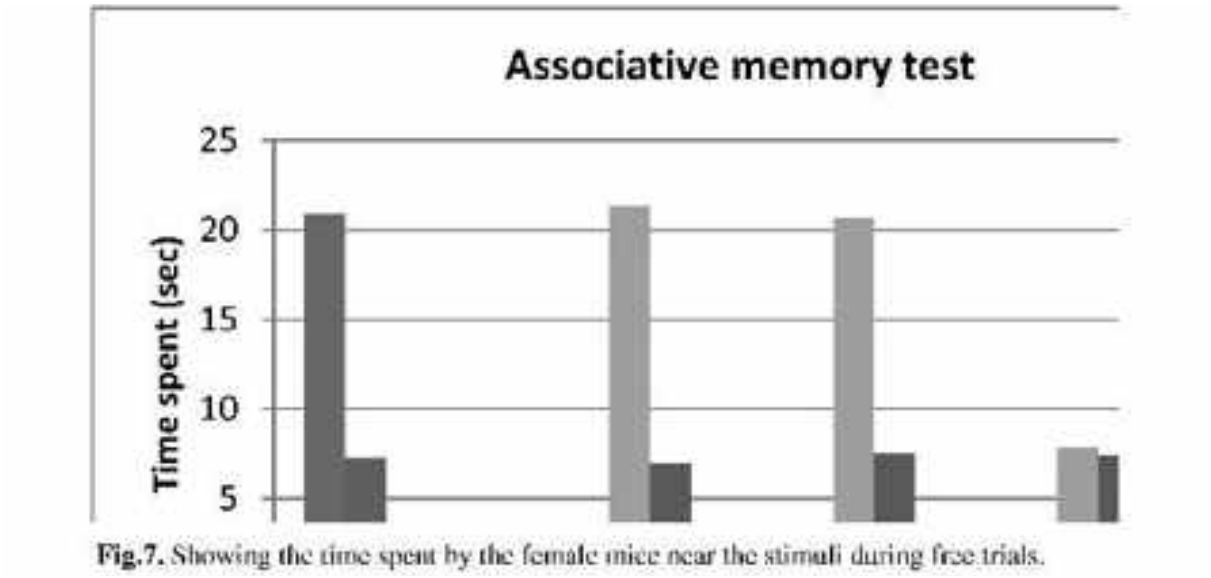

Fig.7. Showing the time spent by the female mice near the stimuli during free trials.

(Table value is 1.645. Calculated values for fig.5, GP IV=4.53, GP IV a=7.2295, GP IV b=2.31, GP IV c=0.5039 and GP IV d=.0.5039. Result shows that there is significant variation in the proportions of GP IV, GP IV a and GP IV b but variation in the proportions are not significant in the case of GP IV c and GP IV d. For fig.6, GP IV=2.07, GP IV a=1.99, GP IV b=2.17, GP IV c=0.21 and GP IV d=0.18 indicates that GP IV c and GP IV d shows insignificant variation in their proportions but others shows significant variation in their proportions. For fig.7, GP IV=2.93, GP IV a=3.13, GP IV b=2.81, GP IV c=0.12 and GP IV d=0.09 shows that variation in the proportions are not significant in GP IV c and GP IV d but significant in the remaining groups).

The test for the duration of retention of associative olfactory memory shows that the female preferred the smell of the edible oil associated with the dominant male urine till the end of second oestorus cycle (about 12-18 days). The sub groups of GP IV (Fig. 5,6 and 7) showed that, from the third oestrous day onwards, there is no significant difference in the frequency of visits, and duration of time spent near the associated oil of urine of both males. Moreover, there is no significant difference in the latency to reach the stimuli from the third oestrous day onwards, indicating that the olfactory memory of the female mice is higher during the early days of exposure and decrease significantly as the time passes on. The results indicate that female mice retains the memory of the urine of dominant male and the associated oil, only up to the third oestrous day.

Selecting dominant male as the mate provides several advantages to the female. In wild baboons (*Papio*

ursinus) the age structure of MHC-*DRB* heterozygosity suggested higher longevity for heterozygotes, which should favour preferences for MHC dissimilarity[46]. It has been shown that female house mice accrue viability benefits for their offspring when they mate with males they prefer versus with males they do not prefer[47]. In another study in deer mice, *Peromyscus maniculatus*,[48] has shown that through four generations, the sons of dominant males generally were dominant to the sons of subordinate males.

It is interesting to note that the female mice have the ability to form associative memory of olfactory signals of the edible oil paired with the male urine and exhibit differential response to the oil paired with male urine even in the absence of male urine. It has been shown that neonatal mice, as young as 3 days old exhibit associative learning ability and learned preference for the conditioned odorant over a novel control odorant after removal of the dam from the home cage for 2 h, pre-`weanling CD-1 mice of ages 3, 5, and 10 days postnatal[49]. One of the interesting findings of the present study is that odour of edible oils can be conditioned by pairing with biologically important olfactory signal of urinary pheromone from a male and through this learned association; same odour can elicit situation specific and appropriate behavioural responses. Further studies are needed to elucidate the role of associative memory in individual recognition and mate choice in mammals.

References

1. 1. Doty R. L., 1986. Odor-guided behavior in mammals. *Experientia*. 42, 257–271.
2. Schellinck H. M., Smyth C., Brown R. and Wilkinson M., 1993. Odor-induced sexual maturation and expression of c-fos in the olfactory system of juvenile female mice. *Brain Res Dev Brain Res*. 74, 138– 141.
3. Brennan P.A. and Keverne E. B., 2004. Something in the air? New insights into mammalian pheromones. *Curr Biol*. 14, R81–89.
4. Keverne E. B., 2004. Importance of olfactory and vomeronasal systems for male sexual function. *Physiology & behavior*. 83, 177–187.
5. Restrepo D., Arellano J., Oliva A. M., Schaefer M. L. and Lin W., 2004. Emerging views on the distinct but related roles of the main and accessory olfactory systems in responsiveness to chemosensory signals in mice. *Hormones and behavior*. 46, 247–256.
6. Kavaliers M., Choleris E., Agmo A., Braun W. J., Colwell D. D., Muglia L. J., Ogawa S. and Pfaff D.W., 2006. Inadvertent social information and the avoidance of parasitized male mice: a role for oxytocin, in: Proc. Natl. Acad. Sci. USA, 103, 4293–4298.
7. Gangrade B. K. and Dominic C. J., 1984. Studies of the male-originating pheromones involved in the Whitten effect and Bruce effect in mice. *Biol. Reprod*. 31, 89–96.

8. Yamaguchi M., Yamazaki K., Beauchamp G. K., Bar J., Thomas, L. and Boyse E. A., 1981. Distinctive urinary odors governed by the major histocompatibility locus of the mouse, in: Proc. Natl. Acad. Sci. USA 78, 5817–5820.
9. Beauchamp G. K., and Yamazaki K., 2005. Individual differences and the chemical senses. *Chem. Senses*. 30 (Suppl 1), 16–19.
10. Kavaliers M., Choleris E., Agmo A. and Pfaff D.W., 2004. Olfactory-mediated parasite recognition and avoidance: linking genes to behavior. *Horm. Behav*. 46, 272–283.
11. Johnston R. B., 1983. Chemical signals and reproductive behavior. In: J. G. Vendenbergh (Ed), Pheromones and Reproduction in Mammals. Academic press., New York, pp. 3-37.
12. Hurst J. L. and Beynon R. J., 2004. Scent wars: the chemobiology of competitive signalling in mice**.** *BioEssays.* 26, 1288-1298.
13. Leinders-Zufall T., Brennan P., Widmayer P., S P. C., Maul-Pavicic A., Jager M., Li X. H., Breer H., Zufall F. and Boehm T., 2004. MHC class I peptides as chemosensory signals in the vomeronasal organ. *Science*. 306, 1033-1037.
14. Rasmussen L. E., Lee T. D., Roelofs W. L., Zhang A. and Daves G. D. Jr., 1996. Insect pheromone in elephants. *Nature*. 379, 684.
15. Schaal B., Coureaud G., Langlois D., Ginies C., Semon E. and Perrier G., 2003. Chemical and behavioural characterization of the rabbit mammary pheromone. *Nature*. 424, 68-72.
16. Novotny M. V., Jemiolo B., Wiesler D., Ma W., Harvey S., Xu F., Xie T. M. and Carmack M., 1999. A unique urinary constituent, 6-hydroxy-6-methyl-3- heptanone, is a pheromone that accelerates puberty in female mice. *Chem. Biol*. 6, 377–383.
17. Berger-Sweeney J., Libbey M., Arters J., Junagadhwalla M. and Hohmann C. E., 1998. Neonatal monoam- inergic depletion in mice (Mus musculus) improves performance of a novel odor discrimination task. *Be- havioral Neuroscience*. 112, 1318–1326.
18. Bodyak N. and Slotnick B. 1999. Performance of mice in an automated olfactometer: odor detection, discrimination and odor memory. *Chemical Senses*. 24, 637-645.
19. Zagreda L., Goodman J., Druin D. P., McDonald D. and Diamond A., 1999. Cognitive deficits in a genetic mouse model of the most common biochemical cause of human mental retardation. *Journal of Neuroscience*. 19, 6175-6182.
20. Mihalick S. M., Langlois J. C., Kreienke J. D. and Dube W. V., 2000a. An olfactory discrimination procedure for mice. *J. Exp. Anal. Behav*. 73, 305-318.
21. Dantzer R., Bluthe R. M., Koob G. F. and Le Moal M., 1987. Modulation of social memory in male rats by neurohypophyseal peptides. *Psychopharmacology* (Berl). 91, 363–368.
22. Engelmann M., Wotjak C. T. and Landgraf R., 1995. Social discrimination procedure: An alternative method to investigate juvenile recognition abilities in rats. *Physiol. Behav*. 58, 315–321.
23. Eibl-Eibesfeldt I., 1950. Beiträge zur Biologie der Haus- und Ährenmaus nebst einigen Beobachtungen an anderen

Nagern. *Z. Tierpsychol*. 7, 558–587.

24. Eibl-Eibesfeldt I., 1952. Ethologische Unterschiede zwischen Hausratte und Wanderratte. *Verh. Deutsch. Zool. Ges. Freiburg*. 169–180.
25. Kogan J. H., Frankland P. W. and Silva A. J., 2000. Long-term memory underlying hippocampus- dependent social recognition in mice. *Hippocampus*. 10, 47–56.
26. Thomas K. J. and Dominic C. J., 1987a. Evaluation of the Role of the Stud Male in Preventing Male - induced Implantation Failure (the Bruce effect) in Laboratory Mice. *Animal Behaviour*. 35(4), 1257- 1260.
27. Thomas K. J. and Dominic C. J., 1987b. Induction of Pseudopregnancy in Pregnancy-Blocked Mice by Re-Exposure to Stud Males. *Physiology & Behaviour*. 41, 515-517.
28. Von Fersen L., Wynne,C. D. L., Delius J. D. and Staddon J. E. R., 1991. Transitive inference formation in pigeons. *Journal of Experimental Psychology*. 17, 334-341.
29. Cohen J. S., Drummond C. and Terrelonge N., 2001. Value transfer in simultaneous object discriminations by rats. *Animal Learning & Behavior*. 2 9, 326-335.
30. Ohta A., Akiguchi I., Seriu N., Ohnishi N., Yagi H., Higuchi K. and Hosokawa M., 2002. Deterioration in learning and memory of inferential tasks for evaluation of transitivity and symmetry in aged SAMP8 mice. *Hippocampus*. 12, 803–810.
31. Van Dijck A., Vloeberghs E., Van Dam D., Staufenbiel M. and De Deyn P. P., 2008. Evaluation of the APP23-model for Alzheimer's disease in the odour paired-associate test for hippocampus-dependent memory. *Behavioral Brain Research*. 190(1), 147–51.
32. DeVito L. M., Konigsberg R., Lykken C., Sauvage M., Young W. S. 3rd. and Eichenbaum H., 2009. Vasopressin 1b receptor knockout impairs memory for temporal order. *The Journal of Neuroscience*. 29, 2676-83.
33. Wilson E. O., 1970. Chemical communication within animal species, in: E. Sondheimer and J. B. Simeone (Eds), *Chemical Ecology*. Academic Press, New York, pp. 133-155.
34. Hurst J. L., 2009. Female recognition and assessment of males through scent. *Behav. Brain Res*. 2009, 295-303.
35. Zala S. M., Potts W. K. and Penn D. J., 2004. Scent-marking displays provide honest signals of health and infection. *Behav. Ecol*. 15, 338-344**.**
36. Hurst J. L., 1986. Mating in free-living wild house mice (*Mus domesticus*)**.** *J. Zool. (Lond)*. 210, 623-628.
37. Hurst J. L., 1987. Behavioral variation in wild house mice *Mus domesticus* Rutty-a quantitative assessment of female social organization**.** *Anim. Behav*. 35, 1846-1857.
38. Potts W. K., Manning C. J. and Wakeland E. K.**,** 1991. Mating patterns in seminatural populations of mice influenced by MHC genotype. *Nature*, 352, 619–621.
39. Brown P. S., Humm R. D. and Fischer R. B., 1988. The influence of a male's dominance status on female choice in Syrian hamsters. *Hormones and behaviors*. 22, 143-149.

40. Rolland C., Macdonald D. W., De Frainpont M. and Berdoy M., 2003. Free Female Choice in House Mice: Leaving Best for Last. *Behaviour.* 140, 1371-1388.
41. Yamazaski K., Beauchamp G. K., Wysocki C. J., Bard J., Thomas L. and Boyse E. A., 1983. Recognition of H-2 types in relation to the blocking of pregnancy in mice. *Science*. 221, 186-188.
42. Lenington S**.,** 1983. Social preferences for partners carrying 'good genes' in wild house mice. *Animal Behaviour*. 31, 325–333.
43. Egid K. and Brown J. L**.,** 1989. The major histocompatibility complex and female mating preferences in mice. *Animal Behaviour*. 38**,** 548–550.
44. Potts W. K., Manning C. J. and Wakeland E. K., 1991. Mating patterns in seminatural populations of mice influenced by MHC genotype. *Nature*, 352**,** 619–621.
45. Potts W. K., Manning C. J. and Wakeland E. K., 1994. The role of infectious disease, inbreeding and mating preferences in maintaining the MHC genetic diversity: an experimental test. *Philosophical Transactions of the Royal Society of London, Series B*. 346, 369–378.
46. Huchard E. L., Knapp A., Wang J., Raymond M. and Cowlishaw G., 2003. MHC, mate choice and heterozygote advantage in a wild social primate. *Nature Genetics*. 35, 103–106.
47. Drickamer L. C., Gowaty P. A. and Holmes C. M., 2000. Free female mate choice in house mice affect reproductive success and offspring viability and performance. *Animal Behaviour*. 59, 371–378.
48. Dewsbury D. A., 1990. Fathers and sons: genetic factors and social dominance in deer mice, *Peromyscus maniculatus. Animal Behaviour.* 39 (2), 284-289..
49. Armstrong C. M., DeVito L. M. and Cleland T. A., 2006. One-Trial Associative Odor Learning in Neonatal Mice. *Chem. Senses*. 31, 343–349.

Scientia
Vol.9, No. 1, Jan - Dec. 2013, pp134-139
ISSN : 0976 - 8289

Phytochemical analysis and antibacterial activity of *Aristolochia indica* L.

Savitha Rabeque C., Sandhya V. Kumar, Jelly Louis, Thulasi Jayaprakash

Department of Botany, Mercy College, Palakkad – 678006, Kerala, India..

Abstract

The success of chemotherapy lies in the continuous search for new drugs to counter the challenge posed by resistant strains. *Aristolochia indica* L. is an important medicinal plant belonging to the family Aristolochiaceae. In this experiment hexane, petroleum ether, chloroform, acetone and methanol extracts of *Aristolochia indica* L. were investigated for *in vitro* antimicrobial activity against pathogens namely, *Pseudomonas aeruginosa* ,*Escherichia coli* and *Serratia marcessens* by disc diffusion method. The extracts showed antimicrobial activity against these bacteria. Secondary metabolites are responsible for different medicinal activity in plants. Hence in the present study phytochemical screening of hexane, petroleum ether, chloroform, acetone and methanol extracts of *Aristolochia indica* leaves were carried out. Qualitative phytochemical analysis revealed the presence or absence of various phytochemicals such as alkaloids, flavonoids, aminoacids, glycosides, terpenoids, anthroquinones, steroids, and saponins from various solvent extracts. The phytochemical analysis is very important commercially as well as it has great interest in pharmaceutical companies for the production of the new drugs for curing of various diseases. It is expected that the important phytochemical properties recognized by our study in *Aristolochia indica* will be very useful in curing of various diseases.

Key words: *Aristolochia indica* L., antibacterial activity, phytochemical analysis, secondary metabolites.

Introduction

Aristolochia indica is a creeper plant belonging to the family Aristolochiaceae. The plant is traditionally acknowledged as a divine herb which can fight against any poisonous bite. *It* reaches a height of several meters on trees and covers the branches with thick foliage. It flowers once a year to produce seeds. It can also be propagated by roots. The plant has a number of historical medicinal uses. Various *Aristolochia* species have been used traditionally for the treatment of snakebite[1], leprosy, cough, diarrhea, fever, festering wounds, tumors and they remain in use particularly in Chinese herbal medicine[2]. A significant amount of research have been reported involving different species of *Aristolochia* viz. *A. bracteolata*[3], *A.cymbifera*[4], *A. chamissonis*[5], *A.cucurbitifolia*[6]. *A. elegans*[6], *A. fimbriata*[7], *A. indica*[8] etc. *Aristolochia indica* was used by the tribes like Siddis and Gowlis for the treatment of skin diseases[9].

This plant contains aristolochic acid which is reported to possess various biological activities such as antibacterial, anti-inflammatory, anti-tumor and antiviral activities[10]. The present study aims to analyze the antibacterial efficacy of this plant. Identification of antibacterial property in plants gives additional

*****Corresponding author, Email: shaniali@gmail.com*

source for antibacterial compounds. Confirmation of antibacterial property in plants leads to isolation and purification of the bioactive principles present in the plant. Antibacterial activity is due to the presence of various secondary metabolites in the plants. Secondary metabolites are chemical compound (flavanoids, alkaloids, terpenoids, quinines, saponins etc.) synthesized by plants. The phytochemical screening of *A.bracteata* revealed the presence of alkaloids, triterpenoids, steroids and sterols, flavonoids, saponin, phytosterols, carbohydrates, proteins, phenolic compounds and cardio glycosides[11].

In the present work was aimed to carry out the antibacterial activity of *Aristolochia indica* against pathogenic bacteria using disc diffusion method and to identify the secondary metabolites present in the leaf extracts.

Materials and Methods

Collection of the plant sample & preparation of extracts

Freshly collected samples of *Aristolochia indica* **leaves** from the Mercy College campus were washed 2-3 times with water followed by distilled water and shade dried. The dried leaves were pulverized by mechanical grinder to get the powder through 100-mesh sieve and then stored in a refrigerator. The shade dried powdered plant material (250g) was extracted first with hexane, petroleum ether, acetone, methanol using a soxhlet apparatus. Then the extract was evaporated to remove the excess solvent.

Bacterial strains tested

The test organisms were collected from the culture collection of the Institute of Microbial Technology (IMTECH), Chandigarh, India. *Pseudomonas aeruginosa, Escherichia coli, Serratia marcessens* was the bacterial strains tested. The bacteria were sub cultured on nutrient agar slants[12], incubated at 37 ^{0}C for 24 h. and stored at 4 ^{0}C in the refrigerator for further experiments. The cultures were maintained by periodic subculture in nutrient agar slants. The nutrient broth cultures of the bacterial strains, grown at 37 ^{0}C incubation conditions for approximately 3 to 4 hours were used as the inocula.

In vitro antibacterial assay

Antibacterial activity of the extracts of *Aristolochia indica* was evaluated using the disc diffusion method and determination of Minimum Inhibitory Concentration. The procedure adopted is that of Barry and Thornsberry[9]. Muller Hinton agar medium was used for the disc diffusion method. Dehydrated medium supplied by Hi Media Laboratories Ltd. Bombay was used for these tests.

To initiate bacterial culture for antibacterial screening, the bacteria (1 ml bacterial broth of 10^5 cells) were swabbed with sterile cotton swab on the sterile medium in the petridish, already prepared and kept, under the aseptic conditions of the inoculation chamber. Blank sterile discs (Hi- media Laboratory Pvt. Ltd. Bombay) of 6 mm diameter were used in the study. Each disc was impregnated with 25 µl of the extract

solution containing about 100-500µg (0.1-0.5 mg) of plant extract. For each set of experiments, controls were maintained where pure solvents were used instead of the extracts.

Streptomycin discs (25µg/disc)) were used as negative control so as to compare the degree of inhibition exhibited by the extracts. The dried discs were carefully placed over the spread cultures. The cultures were incubated overnight at 37^0C. On completion of the required period of incubation, the plates were examined for the presence of zone of inhibition. The result was obtained by measuring the zone diameter. The experiment was done three times.

Qualitative phytochemical analysis of leaf extracts

The condensed extracts of different solvents were used for preliminary phytochemical screening using standard procedures to test the presence of bioactive compounds[13, 14].

Test for alkaloids

2 ml of HCl was added to 5ml of the extract. To this acidic medium, 1 ml of Dragendroff's reagent was added. An orange or red precipitate produced immediately indicates the presence of alkaloids.

Test for flavonoids

To 1 ml of the extract, a few drops of dilute sodium hydroxide was added. An intense yellow colour was produced in the plant extract, which become colourless on addition of a few drops of dilute acid indicates the presence of flavonoids.

Test for amino acids

1ml of the extract was treated with few drops of Ninhydrin reagent. Appearance of purple colour shows the presence of amino acids.

Test for glycosides

The extract was hydrolysed with HCl for few hours on a water bath. To the hydrolysate,1ml of pyridine was added and a few drops of sodium nitro prusside solution was added and then it was made alkaline with sodium hydroxide solution. Appearance of pink to red colour shows the presence of glycosides.

Test for terpenoids

An amount of 0.8 g of the sample was taken in a test tube, then 10 ml of methanol was added to it, shaken well and filtered to take 5 ml extract of plant sample. Then 2 ml of chloroform were mixed with the extracts and 3 ml of sulphuric acid was added. Formation of reddish brown color indicates the presence of terpenoids.

Test for anthraquinones

5ml of the extract solution was hydrolysed with diluted conc. H_2SO_4 extracted with benzene. 1 ml of dilute ammonia was added to it. Rose pink coloration suggested the positive response for anthraquinones.

Test for steroids

1 ml of the extracts were dissolved in 10 ml of chloroform and equal volume of conc. H_2SO_4 was added by sides of the test tube. The upper layer turns red and H_2SO_4 layer showed yellow with green fluorescence. This indicated the presence of steroids.

Test for saponins

The extract was diluted with 20 ml of distilled water and it was agitated in a graduated cylinder for15 minutes. The formation of 1cm layer of foam showed the presence of saponins.

Results and Discussion

When the different extracts of *Aristolochia indica namely hexane, chloroform, acetone and methanol* where tested against the pathogenic bacterial strains of *Pseudomonas aeuroginosa, E. coli and Serratia marcessens,* it indicated the presence of antibacterial activity. The activity of the extracts were compared with that of the standard antibiotic streptomycin and the results were found to be rather comparable with the activity of antibiotic disc as it was used as negative control. The results showed that maximum zone of inhibition was noted in the hexane and chloroform extracts against *E.coli* bacterial strain followed by hexane and chloroform extracts against *Pseudomonas aeuroginosa* bacterial strain. The next maximum zone of inhibition was shown by acetone and methanol extracts against *E.coli* bacterial strain (Table1).

Table1. Antibacterial activity of leaf extracts of *Aristolocha indica*

Target Bacterial Strains	Extracts tested				Control
	Hexane	Chloroform	Acetone	Methanol	(Streptomycin)
Pseudomonas aeuroginosa	10	8	6	7	16
Serratia marcessens	0	0	7	8	14
Escherichia coli	12	10	6	6	16

Further the preliminary phytochemical analysis of hexane, petroleum ether, chloroform, acetone and methanol extracts of *Aristolochia indica* leaves have revealed the presence of various bioactive compounds such as alkaloids, glycosides, terpenoids, anthroquinones, steroids, and saponins. At the same

Table2. Phytochemical analysis of leaf extracts of *Aristolochia indica*

Phytoconstituents	Solvents used			
	Hexane	Chloroform	Acetone	Methanol
Alkaloids	-	-	+	+
Flavonoids	+	+	+	+
Amino Acids	-	-	-	-

Glycosides	–	–	+	+
Terpenoids	–	-	-	+
Anthraquinones	-	-	+	+
Steroids	–	-	+	+
Saponins	-	-	+	+

time it also revealed the absence of flavonoids and aminoacids in all the extracts. Glycosides were present in all the extracts whereas terpenoids were found to be absent in chloroform and acetone extracts. Alkaloids were present in the petroleum ether, acetone and methanol extracts. Anthraquinones were absent in hexane and chloroform extracts. Steroids were present in all extracts except chloroform. Saponins were found to be present in only acetone and methanol extracts (Table 2).

The results in our study showed that hexane and chloroform leaf extract of *Aristolochia indica* exhibited bioactive potentiality against the bacteria *Escherichia coli*. In the present study the observations highlighting the medicinal importance of this plant as a rich source of antibacterial compounds. The results obtained in this study also suggest that the identified phytochemical compounds may be the bioactive constituents responsible for the efficacy of the leaves of the plant studied. Hence it could be inferred that the plant extracts could be a source for the industrial manufacture of drugs useful in the chemotherapy of some microbial infection.

References1. Meenatchi Sundaram S. G., Prajish Parameshwari T., Subbraj and Michael., 2009. A study on anti venom activity of *Andrographis paniculata* and *Aristolochia indica* plant extracts against *Echis cainatus* venom. *J. toxicology*. 6(1):1559-3916.

2. Balachandran P., Wei F., Lin R., Khan I., and Pasco D., 2005.Structure activity relationships of Aristolochic acid analogues: Toxicity in cultured renal epithelial cells. *J. kidney international*.67: 1797-805.
3. Razzak M.A., Ali T., Ali S.I., 1992. The pollination biology of *Aristolochia bracteolate* Lamk. (Aristolochiaceae). *Pakistan J. Bot*. 24(1): 79-87.
4. Lopes L.M.X. and Bolzani V.S., 1988. Lignans and diterpenes of three *Aristolochia* species. *Phytochem*. 27: 2265-2268.
5. Bomm M.D., Zukeran-Schpector J. and Lopes L.M.X., 1999. Rearranged (4→ 2)- abeoclerodane and clerodane diterpenes from *Aristolochia chamissonis. Phytochem*., 50: 455-461.
6. Wu T.S., Tsai Y.L., Wu P.L., Leu Y.L., Lin F.W. and Lin J.K., 2000. Constituents from the leaves of *Aristolochia elegans*. *J. Nat. Prod*. 63:692-693.
7. Bliss B.J., Landherr L., dePamphilis C.W., Ma H., Hu Y. and Maximova S.N., 2009. Regeneration and plantlet

development from somatic tissues of *Aristolochia fimbriata*. *Plant Cell Tiss. Organ Cult*. 98:105–114.

8. Dey A. and De J.N., 2011. *Aristolochia indica* L: A Review. *Asian Journal of Plant Sciences*; Published online.
9. Barry, A.L. and Thornsberry, C., 1991. Susceptibility tests: Diffusion test procedures.
10. Achari, B., S.Chakrabarty and Pakrashi S C., 1981. Studies on Indian medicinal plants: An N-glycoside and steroids from *Aristolochia indica*. *Phytochem.* 20:1444-1445.
11. Periyasamy Ashokkumar, Rajkumar and Mahalingam Kanimozhi., 2010. Phytochemical screening and antimicrobial activity from five Indian medicinal plants against human pathogens. *Middle East India journal of scientific research*. 5(3):157-162.
12. Monica Cheesbrough, 1985. *Medical Laboratory Manual for Tropical Countries*. English Language Book Society London. *2*, 58-204.
13. Harborne J.B., 1998. Phytochemical Methods: A Guide to Modern Techniques of Plant Analysis (Chapman and Hall International Edition, New York) 3rd Edition.
14. Kokate C.K., 2001. Pharmacognosy, 16th edition (Nirali Prakasham Mumbai India).

Scientia
Vol.9, No. 1, Jan - Dec. 2013, pp140-154
ISSN : 0976 - 8289

Shijith P P[1*], S Nandakumar[2] and Jain J Therattil[3]
[1]Dept of Botany, Govt .College Kasargod, Vidyanagar, Kasargod - 671123
[2]Professor (Rtd), Department of Botany, University of Calicut, Tenjippalam.
[3]Dept. of Zoology, St.Aloysis College, Elthuruth, Thrissur.

Abstract

Anacardium occidentale L. belongs to Anacardiaceae is popularly known as the cashew tree. Invertase, the enzyme involved in the breakdown of sucrose to glucose and fructose. Invertase was purified from mature resting cotyledons of *Anacardium occidentale* using ammonium sulphate precipitation and Sephadex G-200 column chromatography. The fractions were stored in refrigerator and assayed on 1st, 10th ,20th ,25th ,35th and 40th days. Stability and retention of enzyme activity of invertase from *A. occidentale*.L is good under storage conditions up to 35 days of storage.

Key words: *Anacardium occidentale* L., invertase, stability, enzyme purification.

Introduction

Anacardium occidentale L. (Anacardiaceae) commonly called as the cashew tree is one of the popular crop trees found in Kerala. Invertase is an enzyme that catalyses the hydrolysis of sucrose to glucose and fructose. The nature and properties of invertase has been described. [1,2,3] Invertases could be distinguished into the following classes: those with pH optima in the range of 3.5-5.1are called acid invertases, those with pH optima in the range of 7.0-7.8 are called alkaline invertases and neutral invertases with pH optima around 6.0- 7.0. Study on invertase has been carried out in different plants such as Sugarbeet[4], Sugarcane[5], Potato[6] ,Maize[7], Tomato[8], and Coconut[9]. Invertase is important during seed germination as it mobilizes stored sucrose to glucose and fructose required by the germinating tissue. The seed is derived from the fertilized ovule. It has testa, perisperm and embryo. The embryo consists of embryo axis and cotyledons. In cotyledons of non-endospermic seeds are bulkier and count over 90% of seed mass[10]. Invertases show a maximum storage life of 20 days[11]. The aim of the present study is to purify invertase from mature resting cotyledons in *A. occidentale* L. and find out the stability under storage conditions.

Materials and Methods

Mature resting seeds were collected from a single tree during March-April season of the year to ensure uniformity. To ensure uniformity of maturity, the seeds were collected when cashew apple was fully ripe and either dropped off from the tree or were manually plucked. After removing the pseudo fruit, seeds were washed thoroughly under tap water and completely wiped free of water and sun-dried for three days. Dried seeds were kept in closed containers, with silica gel packets to prevent humidity during storage. Seeds of nearly uniform size and weight were used for the present study; abnormal sand deformed seeds were discarded.

*****Corresponding author, Email: rksheeba@gmail.com*

The whole seed was weighed before each analysis using Shimadzu ELB300 electronic balance. The seeds were cut open longitudinally and the cotyledons were scooped out of the shell using stainless scalpel blade. The adhering seed coats as well as the embryonic axis were carefully separated from the cotyledons. After blotting between the folds of filter paper to remove adhering water, the cotyledonary tissue was cut into small pieces and randomized. The weighed samples were kept frozen and used on the same day for the experiment.

Homogenate (10% w/v) was prepared by grinding the cotyledons using chilled mortar and pestle. During grinding the mortar was kept surrounded with crushed ice. Glass powder was used as abrasive. The homogenizing medium employed 20mM citrate phosphate buffer with pH 7.2, 5mM each of 2-Mercaptoethanol and EDTA. The homogenate (10% w/v) was centrifuged in Plastocrafts Rota 4R-V/FM at 11,200 x g for 20 minutes at 4^{O}C and the supernatant was used for purification. Ammonium sulphate concentration was first brought to 25%. The suspension was kept in ice for 30 minutes for flocculation. Centrifugation of flocculated homogenate was carried at 13200x g for 30 minutes.The precipitate (Fraction I) was suspended in a cold medium containing Citrate-phoshpate buffer pH 7.6, 2mM EDTA, 2mM 2- Mercaptoethanol and stored in ice. The supernatant was brought to 55% ammonium sulphate concentration for precipitation to obtain Fraction II. Fraction III was obtained by 100% saturation of ammonium sulphate. All three fractions were assayed for enzyme activity as per methods standardized earlier[12]. The active fraction was kept for overnight dialysis followed by Sephadex G-200 column chromatography in a cold-room at 4^{o} C. The first 18 ml of effluent was discarded as 'void volume". Following this 15 fractions of 4ml each were collected in tubes and tested for enzyme activity. The assay system consisted 0.6ml 200mM McIlvaine's buffer (pH 7.6), 0.2ml 500mM Sucrose, and 0.2ml enzyme. At the end of 30 minutes incubation, the reaction was stopped and colour was developed according to the method of Somogyi(1952)[13]. The assays were repeated on 10th, 20^{th}, 25^{th} and 35^{th} days after purification to study the stability of the enzyme under storage.

After the enzyme assay protein estimation was followed. The protein estimation was carried out according to Lowry et al (1951) as modified by Khanna et al (1969). Proteins were precipitated using trichloroacetic acid (TCA) at a final concentration of 5% (w/v) The tubes were kept in ice for a period of 30 minutes, to flocculate the protein precipitate and centrifuged for 5 minutes, at room temperature. The supernatant was discarded and the residue was washed twice with 2% TCA. After centrifugation, the residue was washed with diethyl ether to remove lipids, as the seed had rich lipid content, followed by washing once with anhydrous acetone the final washing was done with 80% acetone. The residue obtained was suspended 0.1N NaOH and the tubes were heated in a bath of boiling water for 5 to 10 minutes. After cooling under tap water, the tubes were centrifuged and the aliquots from the supernatant were taken for colorimetry,

using Folin-Ciocalteu phenol reagent. Bovine serum albumin (BSA, 100µg/ml) was used as standard.

Results and Discussion

Ammonium sulphate Fraction II showed highest enzyme activity (Table.1). In Sephadex G -200 purification process, fractions II, III and IV had enzyme activity of which Fraction III had highest enzyme

Table 1: Ammonium sulphate fractionation of invertase from the mature resting seeds of *A. occidentale L.*

Fraction	Enzyme activity, U/g	Protein mg/g tissue	Specific activity	Recovery
Supernatant	8.34±0.19	54.63±2.0	0.147	100%
0-25%	1.27±0.10	5.55±0.5	0.228	15%
25-55%	6.41±0.12	9.28±0.24	0.689	79%
55-100%	Nil	Not determined	Not calculated	Nil

Fig.1. Stability of invertase under storage

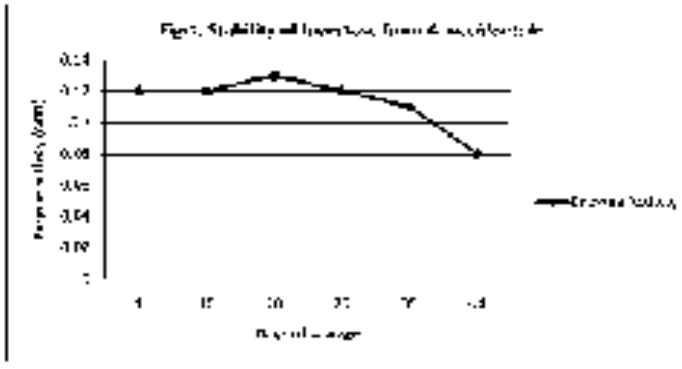

Activity (Table. 2). The stability of invertase under storage at 4° was found good till 35 days. The enzyme activity declined only after 35 days of storage as shown in the figure (Fig.1).

Table 2: Sephadex G-200 column chromatography of invertase from the cotyledons of *A. occidentale*

Enzymes are widely used in industrial processes. Invertase is used as a biocatalyst in sugar industry to

Fraction No.	Enzyme activity, units	Protein mg/g tissue	Specific activity
1	0	0	0
2	31.94±1.35	1.24±0.12	25.67
3	6.72±1.38	1.58±0.25	4.23
4	15.02±1.70	3.76±0.50	3.95

4	13.92±1.30	11.76±0.30	1.35
5	0	4.50±0.15	0
6	0	2.68±0.31	0
7	0	1.80±0.32	0
8	0	1.90±0.22	0
9	0	2.10±0.13	0
10	0	0	0
11	0	0	0
12	0	0	0
13	0	0	0
14	0	0	0
15	0	0	0

breakdown glycosidic bond in sucrose. The resulting mixture of glucose and fructose is sweeter than sucrose, hence important in confectionary processing[14]. In the present study, the stability of the purified invertase is found to be exceeding more than a month in storage. This may be explained from the fact that the enzyme was isolated from resting cotyledons of *A. occidentale.* L. The seeds of plants have the ability to survive various conditions of adversities [15]. The seeds of *Anacardium* germinate after a few months of seed dispersal. It is quite evident that the enzyme isolated from the seed cotyledons of this plant shows higher stability under storage conditions and thereby making this enzyme gather special attention for industrial applications.

References

1. Patel Piyush A, Patel Sangeeta P, Shah Jigesh V, Oza Haren V,2012.*Frequency and distribution of blood groups in blood donors in Western Ahmedabad – A hospital based study* NATIONAL JOURNAL OF MEDICAL RESEARCH Volume 2 Issue 2 Apr – June print ISSN: 2249 4995 eISSN: 2277 8810 Page 202-205.
1. Rees ap T 1974. Pathways of carbohydrate breakdown in higher plants. In: Northcote DH (ed) Int. Rev. Biochem. Vol. XI. Butterworth, London, pp 89-127.
2. Avigad G. 1982. Sucrose and other disaccharides. *Encycl Plant Physiology.*13A, 217-347.
3. Duffus C M and Duffus J H. 1984. In: Carbohydrate metabolism in plants. Longman, London and New York.
4. Bacon J S D, Mac Donald I R and Knight A H. 1965. The development of invertase activity in slices of the root of *Beta vulgaris* L.washed under aseptic conditions. *Biochem. J.* 94: 175-182.
5. Hatch M D, Sacher J A and Glasziou K T . 1963. Sugar accumulation cycle in sugarcane 1. Studies on enzymes of the cycle. *Plant physiol.* 38, 338-343.

6. Murata T . 1973. Invertase development in root slices of sweet potato. Nippon Nogei Kagaku Kaishi. 47: 557-562.
7. Jaynes T A and Nelson D E . 1971. An invertase inactivation in maize endosperm and factors affecting inactivation. *Plant physiol.* 47, 629-634.
8. Khanna, S K, Viswanathan PN, Tewari, CP, Krishnan PS, and Sanwel GG .1969. Colorimetric estimation of protein and orthophosphate in plant tissues rich in phenolics. *Indian J. Biochem.*,5:21-25.
9. Lowry OH, Rosebrough NJ, Farr AL, and Randall RJ. 1951. Protein measurement with the Folin phenol reagent. 193(1): 265-275.
10. Nakagava H, Kawasaki Y, Ogura N and Takehana H. 1972. Purification and properties of two types of β-fructofuranosidases molecules in senescent tomato fruit. *Phytochemistry.* 19:195-197.
11. Balasubramanian K and Alles N H. 1989. A preliminary study of the invertase activity in coconut. *Ann. Bot.* 64:253-255.
12. Bewly J D and Black M. 1983. Physiology and biochemistry of seeds in relation to germination. Vol 1. Springer- Verlag Berlin Heidelberg, New York.
13. Sanjay G and Sugunan S. .2005. Enhanced pH and thermal stabilities of invertase immobilized on montmorillonite K-10. Food Chemistry 94 (2006) 573–579
14. Shijith PP, Nandakumar S and Jain J Therattil. 2013. Determination of pH optimum and substrate saturation curve for Invertase enzyme in the mature resting cotyledons of *Anacardium occidentale* L. *Scientia.* Vol.9 (1). 156-159.
15. Somogyi M. 1952. Colorimetric estimation of glucose. *J.biol. chem.*195.
16. Tananchai P and Chisti Y. 2010. Stabilization of Invertase by Molecular Engineering . *Biotechnol. Prog.*, Vol. 26 (1). 111-117.
17. Roberts EH. 1972. Storage environment and the control of viability. in Viability of seeds (Roberts EH,ed.). London, UK: Chapman and Hall. Pages 14–58.

Spider assemblages of Marthoma college campus, Thiruvalla, Pathanamthitta Dt., Kerala.

Surabhi M.[1] and Joyce Jose[2]

[1]Department of Zoology, Mar Thoma College, College Road, Thiruvalla, Kerala – 689103, India

[2]Department of Zoology, St. Thomas College, Thrissur. Kerala – 680001, India

Abstract

Conservation actions require a measure of biodiversity, the assessment of which is difficult even for small areas and therefore the search for indicators of biodiversity has emerged as an active research topic. Spiders represent easily measured indicators of environmental changes and community level diversity. In this article, we provide qualitative and quantitative data on the spider assemblages in Mar Thoma College Campus which includes a preliminary checklist, alpha diversity, beta diversity across three microhabitats, response of spider assemblages to selected ecological parameters and guild information. Sampling, collection and preservation of specimens and data analysis was done during the period of March to June 2009 following standard protocols. Thirty seven species of spiders were recorded of which, three were unidentified. This is about 9% of Kerala's spider diversity. Eleven families (Araneidae, Clubionidae, Hersilidae, Lycosidae, Oxyopidae, Psecheridae, Salticidae, Sparassidae, Tetragnathidae Theridiidae and Pholcidae) were present in the study area which is 18.64% of documented spider families from India. Araneidae and Salticidae were most dominant and diverse. Guild structure analysis revealed seven feeding guilds. The three habitats (walls, arboreal and litter) showed minimum species turnover. Maximum species richness was found in the arboreal habitat followed by walls whereas maximum individuals were found in the walls followed by arboreal habitat. Both species diversity (S) and abundance (N) was higher in mornings than evenings. As rains increased both diversity and abundance decreased. This study highlights the promising potential in studying the ecological aspects of spider communities in a human inhabited environment offering complex and derived niches.

Key words: Spider, diversity, conservation, urban habitats, indicator species.

IntroductionThe conservation of biodiversity has gained prominence in ecological research for the last decades. Conservation actions require a measure of biodiversity such as species richness, but its assessment is very difficult even for small areas and therefore the search for surrogates (i.e. indicators) of biodiversity have emerged as an active research topic[1].

Spiders represent easily measured indicators of environmental changes and community level diversity, being exclusively predatory[2] and can be located with minimum effort as they are an abundant and widespread group of polyphagous predators in ephemeral and disturbed habitats, including cultivated land[3]. Studies have shown that spiders can categorize environmental conditions in habitats such as distinct

plant architecture, litter depth and complexity2,4,5,6. Thus spiders can be considered as a reliable environmental indicator7,8.

While there are many recent studies on Arachnids from Kerala and Western Ghats9,10,11,12,13 most of these studies have focused on specialized ecosystems and neglected the varied microhabitats available in and around human habitations. Since in-depth studies on spiders and their ecology have not been conducted it is almost impossible to formulate scientific management and conservation plans for spiders in urbanized environments or even utilize spiders as ecological indicators.

In this paper, we provide qualitative and quantitative data on the spider assemblages in Mar Thoma College Campus which includes a preliminary checklist, alpha diversity, comparison of diversity across three microhabitats (beta diversity), response of spider assemblages to selected ecological parameters and guild information.

Materials and Methods

Study area

The study area was the 15 acre Marthoma College Campus, Thiruvalla and included the nearby. Principal's quarters, Old Hostel, Canteen and Store sections. New hostel, Arts Block and Sports' Stadium were not included (Fig. 1). Marthoma College is situated in Thiruvalla taluk, Pathanamthitta District, Kerala State, India. Temperatures range between 34.4°C and 18.5°C. Rainfall averages 304 cm. Though clear divisions between seasons are absent, March to May can be classified as pre-monsoon dry spell, June to October as South West monsoon, November to February comprises of the post monsoon dry spell though a few showers attributed to the North West monsoons are present.\

Fig. 1. Study Area (not to scale) 09.23.828 °N to 09.23.961 °N and 76.35.821°E to 76.35.187°E

(1- Principal's Quarter's, 2- Old Hostel (Enclosed Courtyard), 3- Old Hostel Gate,4- Canteen and Store, 5- College Main Gate, 6- College Main Block,7- Behind Zoology Block, 8- Behind Waiting Room, 9 and 10- Stadium Ground and Arts Block (Not in Study Area)

Water bodies in the study area are manmade wells and tanks. The Kuttapuzha Canal, which is the continuation of Kaviyoor Punja (paddy field), flows near the College campus. Many plants, both introduced and native are found in the study area. They have not been listed in this study but since the relationship between plants and spiders are not being examined here.

Spider sampling

Sampling was done during the period of March to June 2009. The study area was visited every day during early morning and late evening. Time taken per visit was half an hour. There was no habitat wise restriction for sampling time. Spiders were collected by leading them into jars or bottles or by covering them with bottles. The specimens were transferred in clear polypet jars, photographed and preserved in 70% alcohol and labeled. Voucher specimens are at present in the Department of Zoology, Mar Thoma College, Thiruvalla. Spiders were identified by taking expert opinion and perusal of literature15,16,17,18 Quantitative data was collected by time constrained visual encounter survey (VES) along randomly selected zigzag linear paths19.The number of each species sighted per visit was recorded along with all relevant details19. Temperature, presence or absence of rainfall was recorded using standard methods. Sunset and sun rise time was compiled from newspapers. Spider guilds (functional groups) were identified by perusal of literature 20, 21.

Data analysis

Appropriate statistical methods 22, 23 were adapted to analyze the various aspects of diversity. The Data collected was tabulated in Excel. Species richness (S) was calculated with respect to families and months. The number of species and genus per family was computed. To study the differences in the morning and evening population patterns, data from morning and evening sampling was compared using paired samples student t test. To test the completeness of sampling collector’s curve (cumulative number of species against cumulative number of individuals) was plotted.

Alpha diversity measures (Dominance index D= ?(n_(i/n)^2),where, ni is number of individuals of taxon i;Shannon index H= ?(n_(i/n) ln? (n_i/n)),where, ni is number of individuals of taxon i;Margalef's richness index R=((S-1))/ln? (n) , where, S is the number of taxa, and n is the number of individuals and Eveneness (Buzas and Gibson's evenness) E2=e^(H/S),where, S is the number of taxa and H is the Shanon Index) were calculated.

Sorenson index [C_S= 2j/((a+b)), where, j is the number of species recorded in both sites, a is the number of species recorded in Site A and b is the number of species recorded in Site B] was calculated to

understand the similarities between the spider communities sampled in different sites. Data collected from the study area was used for analyzing relationships between species abundances and selected environmental variables using two tailed Spearman's correlation test. Data analysis was done using MS Excel 2007, PAST and SPSS 10.

Results and Discussion

Thirty seven species of spiders were recorded from the study area of which, three were unidentified. Of the identified 34 species, five were identified till family level, five till genus level and 24 till species level (Table 1). Of about 1442 species reported from India24, 37 species have been recorded from the study area which is about 2.57% of the documented spider diversity in India and about 9% percentage of spider diversity in Kerala.

Out of the 59 families24 reported from India, 11 families were present in the study area which is 18.64% of documented spider families from India. These are Araneidae, Clubionidae, Hersilidae, Lycosidae, Oxyopidae, Psecheridae, Salticidae, Sparassidae, Tetragnathidae Theridiidae and Pholcidae. The family Araneidae had nine species; Salticidae had eight species; Tetragnathidae had four species and Pholcidae had 3 species each.. Theridiidae, Lycosidae and Clubonidae had two species each. All the other families were represented by one species each (Fig. 2).

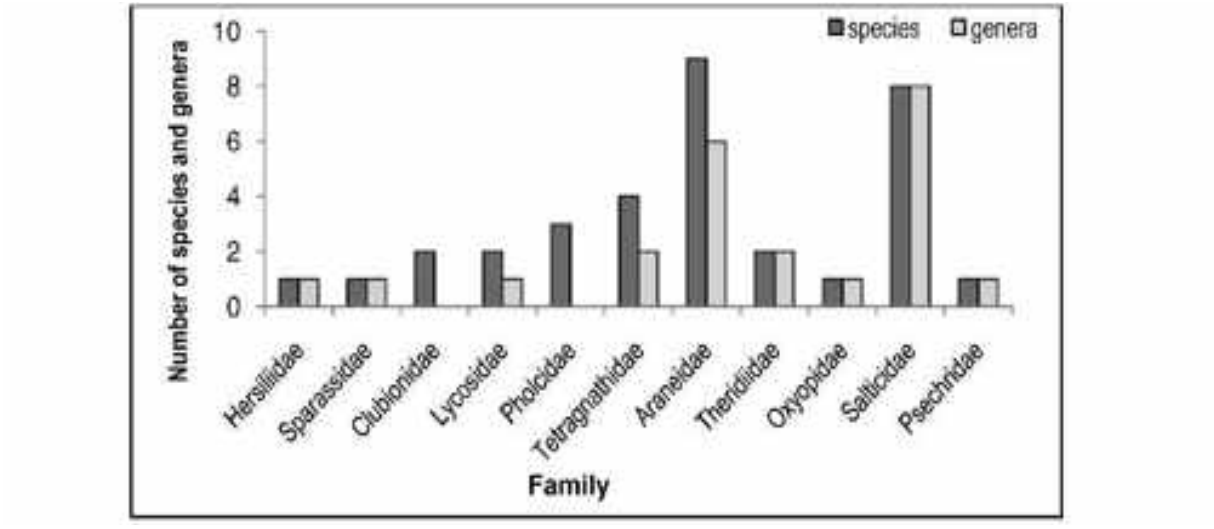

Fig. 2. Diversity within spider families

Many previous workers[25,26] have suggested that this concentration of biodiversity is not because of any superior habitat quality present in the study area, but because of intensive studies in unprotected forests/human habitations etc. Biodiversity in man- made habitats may be richer than in undisturbed natural habitats because disturbance can lead to the creation of new microhabitats which about may sustain more species.

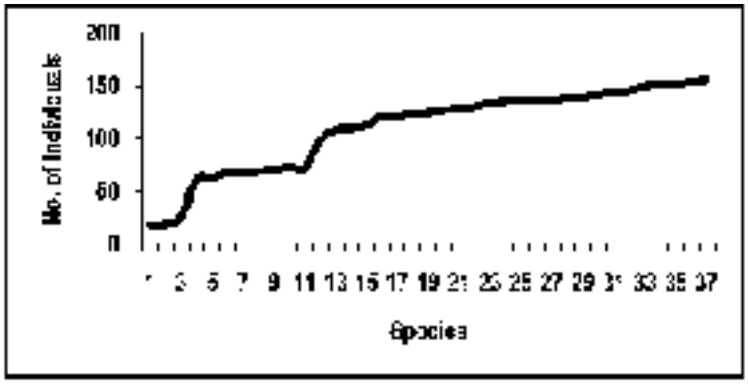

Fig. 3. Species accumulation curve

The most dominant species were Species Carhottus vidus, Pardosa birmanica and Hersilia savignyi with 35, 26, 17 individuals respectively. All species were found in maximum numbers during the month of March except for species Heteropoda venatoria and Oxyopes javanus. These were the only two species which were absent in March. Oxyopes javanus was found only in the month of June.

The collector's curve was plotted with number of species against their respective abundances (Fig. 3). The species accumulation curve has not yet formed an asymptote with the x axis indicating that there are many more species to be sampled in the area. . Even though a plateau has not been reached the upward trend of the curve seems to slow down and stabilize which indicates that most of the species may have been sampled. It has been universally accepted by ecologists that collector's curves for invertebrates never reach a plateau. This is basically because of the lack of taxonomic data, inadequate sampling methods, human errors and fixed time intervals allotted to studies. Even if all these factors were removed it would be a mammoth task to locate, identify and record the enormous number of invertebrates.

Guild structure analysis of the 34 species identified till family level revealed seven feeding guilds 20, 21. These were orb web weavers, stalkers, ground runners, foliage hunters, irregular web builders, scattered line weavers and tube web spiders. Orb Web Weavers (38.24%) followed by Stalkers (26.48%) and Foliage Hunters (11.76%) were the dominant guilds (Fig.4).

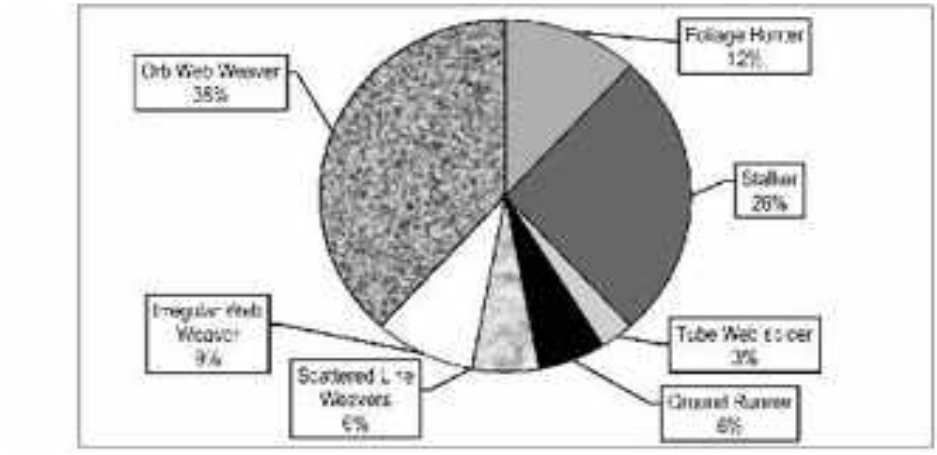

Fig. 4. Guild structure of identified spiders in the study area

In the three habitats studied namely, walls, arboreal (including trees till 2m height, shrubs, and associated places) and litter , maximum number of species were found in the arboreal habitat (19) followed by walls (12). The least richness was found in litter (5). In the case of abundance it was observed that maximum individuals were found in the walls (79) while minimum individuals were found in the arboreal habitat (41). Similarity between different habitats were very less when measured on a scale of 1. Maximum similarity was shown between walls and litter followed by walls and arboreal habitat. Arboreal habitat and litter habitat showed least similarity (Table 2). Species turnover between two habitats can be generally explained as the amount of species being exchanged between habitats. Greater the species turnover between habitats lesser the uniqueness of species composition in the each habitat. Also turnover is a biological indicator of environmental parameters in a habitat. As species will have unique abiotic requirements, turnover between two species will only be sustained if two habitats have similar environmental characters. The three habitats in the study area gave very low similarity indice values. This indicates minimum overlap between the three habitats and presence of different environmental conditions in these habitats.

Table 2. Similarities between different habitats

Habitat	Sorenson's Index
Walls and arboreal	0.1176=7
Arboreal and litter	0.0740741
Walls and litter	0.1904762

Both the species diversity and number of individuals showed a steady decline from the month of March (when the sampling started) towards the month of June (when sampling ended). Maximum number of species and abundance was observed in March (S-36, N- 85) and the least values were observed in June (s= 8, N- 17) (Figs.5 and 6).

The study shows that while diversity (S) was maximum in arboreal habitat and minimum in litter, abundance (N) was maximum in wall habitat but minimum in the arboreal habitat. The increase in diversity may be due to the heterogeneity found in the arboreal habitat. Heterogeneity factors would include species diversity of plants and plant spider diversity; gradients of environmental factors such as light, wind humidity, temperature, etc. But abundance of species in this habitat would be automatically less because each microhabitat would be limited in terms of space. There would be more exposure to predators and environmental fluctuations. Sighting efficiency of the observer too would diminish with variations in the background (Figs.5 and 6).

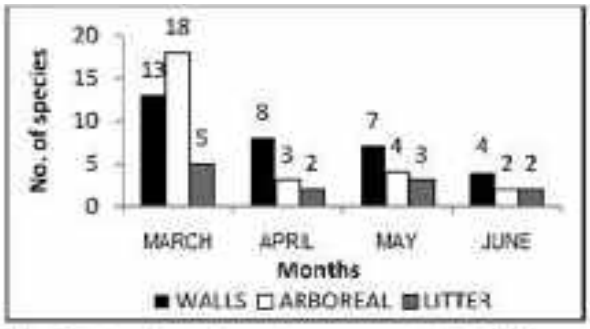

Fig. 5. Number of species per month in different habitats

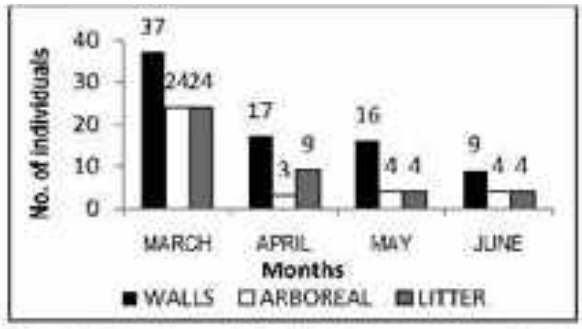

Fig. 6. Number of individuals per month in different habitats

Applying the same to litter habitat the reduced species diversity is attributed to sampling inadequacy and also to the homogeneity in the upper surface of the habitat. In the case of walls though there was high homogeneity in the overall habitat, small variations could lead to the formation of specialized niches both in terms of food and space. The factors attributing to such differences are basically distance from man-made light source and duration of the light being on, crevices in the walls; man-made microhabitats like wall hangings, cloth hangers, etc. There would also be more insect food especially near man made light sources and less exposure to predators, hence, high diversity and relatively medium abundance of species (Figs.5 and 6).

The alpha diversity indices calculated for different months show that the month of March had the maximum values for diversity indices such as Shanon's H, Evenness and Richness. Dominance was least in the month of March. The diversity indices declined along the gradient of months starting with March and ending with June while dominance increased (Table 3).

Table 3. Alpha diversity indices

Indices	March	Apr:	May	[illegible]	Pooled Values
[illegible]	[illegible]	[illegible]	[illegible]	[illegible]	[illegible]
[illegible]	[illegible]	[illegible]	[illegible]	[illegible]	[illegible]
[illegible]	[illegible]	[illegible]	[illegible]	[illegible]	[illegible]
[illegible]	[illegible]	[illegible]	[illegible]	[illegible]	[illegible]

In general, the pooled values for different diversity indices indicated medium diversity and low dominance (D=0.1064, H=2.802, e^H/S=0.4452, R=7.156). General observations and alpha diversity indices show that there was more diversity during the drier months. As rains increased both diversity and abundance decreased. This observation follows Rajashekar and Raghavendra[27] that the density and diversity of spiders corresponded to the occurrence of prey and that spiders are observed less during monsoons. As the

number of species decreased, dominance increased. This was mainly because lesser the number of species more equal the proportioning of resources. For all months both species diversity (S) and abundance (N) were significantly higher in mornings when compared to evenings (Figs. 7 and 8).

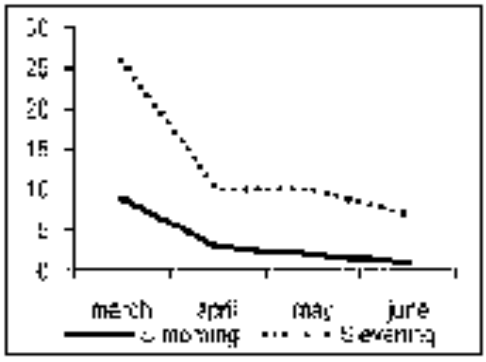

Fig. 7. Spider Diversity (S)- comparison morning and evening

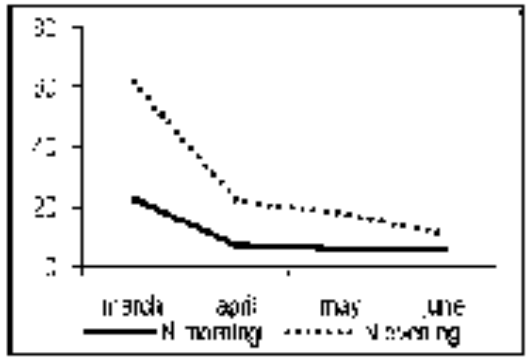

Fig. 8. Spider Abundance (N)- comparison morning and evening

Response to selected environmental parameters (temperature range, presence absence of rainfall, time of sunset and sunrise and photoperiod) was calculated using Spearman's rho. Species distribution was significantly positively correlated with the time of sunrise (r=-0.269; p=0.01; 2tailed;N=109) and significantly negatively correlated with photoperiod (r=-0.290,p=0.01; 2tailed;N=109). Further studies for longer periods of time are necessary to draw interpretations on the response of spiders to various ecological factors.

Studies have shown that spiders can categorize environmental conditions in habitats such as distinct plant architecture, litter depth and complexity [2, 4, 5, 6]. Hence study of spiders is both taxonomically and ecologically rewarding. It can also help in formulating land management practices and in measuring the ecological health of a habitat.

Our study which is the second[28] of its kind from the study area indicates promising potential in studying the ecological aspects of spider community organisation in a human inhabited environment which may offer complex and derived niches. That this time bound, short term study documented the presence of above 9% of Kerala's spider biodiversity shows the importance of intensive study in small study areas. Irrespective of natural or man-made habitats, awareness about biodiversity has to be generated and spread to design scientific conservation and management plans. Long term studies in small study areas which focus on the change in species composition especially in the face of climate change is the need of the hour.

Acknowledgements

We thank the Principals and Heads of the Department of Zoology, Mar Thoma College, Thiruvalla and St.

Thomas, College, Thrissur for permission to use the laboratory and other facilities. We thank Dr. P.A. Sebastian, S.H. College, Thevara, for help with identification of specimens.

References

1. Rossi J.P., van Halder I., 2010. Towards indicators of butterfly biodiversity based on a multiscale landscape description. Ecological Indicators. 10, 452–458.
2. *Wise D.H., 1993. Spiders in Ecological Webs. Cambridge University Press, Cambridge, U.K.
3. Topping C. J., Lovei G. L., 1997. Spider Density And Diversity In Relation To Disturbance In Agroecosystems In New Zealand, With A Comparison To England. New Zealand Journal of Ecology. 21(2), 121-128.
4. Halaj J., Ross D.W., Moldenke A.R., 1998. Habitat structure and prey availability as predictors of the abundance and community organization of spiders in Western Oregon forest canopies. Journal of Arachnology. 26,203–220.
5. Noel N. M., Finch O.D., 2010. Effects of the abandonment of alpine summer farms on spider assemblages (Araneae). J Insect Conserv. doi:10.1007/s10841-010-9272-8
6. Rubio G.D., Corronca J.A., Damborsky M.P., 2008. Do spider diversity and assemblages change in different contiguous habitats? A case study in the protected habitats of the Humid Chaco Ecoregion, Northeast Argentina. Environ Entomol.37,419–430.
7. Kremen C., Colwell R.K., Erwin T.L., Murphy D.D., Noss R.F., Sanjayan M.A., 1993. Terrestrial arthropod assemblages: their use in conservation planning. Conserv Biol. 7, 796–808
8. Maya-Morales J., Ibarra-Núñez G., León-Cortés J. L., Francisco I., 2012. Understory spider diversity in two remnants of tropical montane cloud forest in Chiapas, Mexico. Journal of Insect Conservation. 16, 25-38.
9. Sebastian P.A., Mathew M.J., Beevi S.P., Joseph J., Biju C.R., 2005. The spider fauna of the irrigated rice ecosystem in central Kerala, India across different elevational ranges. The Journal of Arachnology. 33, 247-255.
10. Sugumaran M. P., Ganeshkumar M., Ramasamy K., 2005. Biodiversity of spiders in Western Ghats of Tamil Nadu. – Entomon. 30 (2), 157-163.
11. Sebastian P.A., Murugesan S., Mathew M.J., Sudhikumar A.V., Sunish E., 2005. Spiders in Mangalavanam, an ecosensitive mangrove forest in Cochin, Kerala, India (Araneae). European Arachnology (Deltshev, C. & Stoev, P., eds) Acta zoologica bulgarica, Suppl. No. 1,pp. 315-318.
12. Sudhikumar A.V., Mathew M.J., Sunish E., Sebastian P.A., 2005. Seasonal variation in spider diversity in Kuttanad rice agroecosystem, Kerala, (Araneae). Acta zool. Bulg., 1, 181-190.
13. Sivaperuman C., Easa P. S., Swetharanyam S., 2002. Preliminary studies on spider diversity and their webs in selected sacred groves in Kerala. JBNHS.99(1), 144.
14. Sudhikumar A.V., Mathew M.J., Sunish E., Murugesan S., Sebastian P.A., 2005. Preliminary studies on the spider fauna in Mannavan shoala forest, Kerala, India (Araneae). European Arachnology (Deltshev, C. & Stoev, P., eds) Acta

zoologica bulgarica. Suppl. No. 1, 319-327.

15. Pocock R.I., 1900. The Fauna of British India including Ceylon and Burma: Arachnida. Taylor and Francis, London.
16. Platnick N. I., 2006. The world spider catalog, version 7.0. American Museum of Natural History.URL:http://research.amnh.org/entomology/spiders/catalog/ index.html.
17. Sebastian P.A., Sudhi A.V., 2006. Spiders of South India URL:http//www.southindianspiders.com. Division of Arachanology, Department of Zoology, Sacred Heart College, Thevara Kochi.,
18. Sebastian P.A., Peter K.V., 2009. Spiders of India. University Press India Pvt. Ltd. Hyderabad.
19. Heyer W.R., Maureen A.D., Mc Diarmind R.W., Hayek L.A.C., Foster M.S. (Eds.), 1994. Measuring and monitoring biological diversity; Standard methods for Amphibians. Smithsonian Institution.
20. *Uetz G.W., 1991. Habitat structure and spider foraging. In Bell S.S., McCoy, E.D., Mushinsky, H.R. (Eds.), Habitat Structure: The Physical Arrangement of Objects in Space. Chapman and Hall, London, U.K.
21. Uetz G.W., Halaj J., Cady A. B., 999. Guild structure of spiders in major crops. - Journal of Arachnology. 27, 270-280.
22. Jayaraman K., 2001. A handbook of statistical analysis in forestry research. KFRI.
23. Magurran A. E., 1988. Ecological diversity and its measurements. Chapman and Hall, London.
24. Siliwal, M., Molur S., Biswas B. K., 2005. Indian spiders (Arachnida: Araneae): updated checklist 2005. Zoo's Print Journal. 20, 1999-2049.
25. Devy S. M., Davidar P., 2001. Response of wet forest butterflies to selective logging in Kalakad – Mundanthurai Tiger Reserve: Implications for Conservation. Current Science. 80, 400-405.
26. Padhye A.D., Dahanukar N., Paingankar M., Deshpande M., Deshpande D., 2006. Season and Landscape wise distribution of Butterflies in Tamhini, Northern Western Ghats, India. Zoos' Print Journal. 21(3), 2175-2181.
27. Rajashekar K. P., Raghavendra N., 2003. An overview of spider diversity in India. In: ENVIS Bulletin: Wildlife and protected areas, Conservation of rainforests in India. Eds. Gupta A.K., Kumar A., Ramakantha V., 4(1), pp 121- 128.
28. Vincent V. V., 2004. Taxonomic studies of a few spider species of Tiruvalla taluk. B.Sc. Dissertation submitted to MG University.

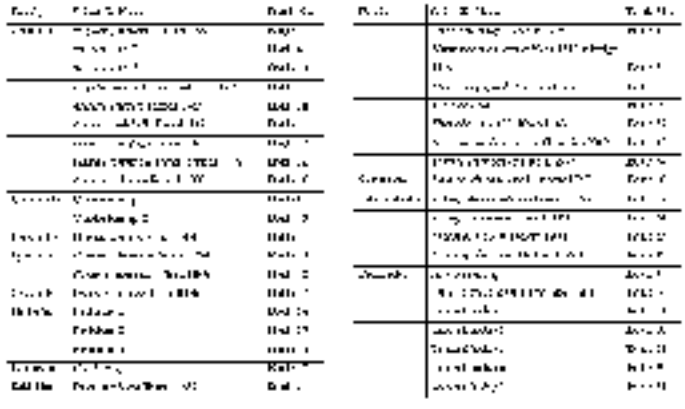

Scientia
Vol.9, No. 1, Jan - Dec. 2013, pp155-159
ISSN : 0976 - 8289

A study on the sintering temperature and dielectric properties of TiO_2

Tony Joseph[1] Arun Bose A[1] and Anlin Lazar K[2]

[1]Department of Physics, Govt. Victoria College, Palakkad, Kerala, India.
[2]Department of Physics, Mercy College, Palakkad, Kerala, India.

Abstract

Dense samples of TiO_2 were prepared by solid state sintering technique. Sintering temperature has been optimised by studying the variation of density with temperature. Phase identification has been performed with the help of powder X-ray diffraction technique. The dielectric properties at radio frequencies were measured using a LCR meter by the capacitor method. It was observed that sintered TiO_2 have high dielectric constant and poor loss coefficient. The conductivity of sintered TiO_2 measured suggest that TiO_2 might be in the semiconducting state.

Key words: solid state sintering, XRD, dielectric constant, dielectric loss, porosity.

Introduction

Materials having different dielectric constant (ε_r) have a wide range of application in the field of wireless communication. Low dielectric constant materials are essential for substrate applications, whereas very high dielectric constant is useful for applications as gate dielectrics and passive components in microelectronic technology.[1,2] Medium dielectric constant materials are needed for dielectric resonators (DRs) for applications as filters, duplexers, oscillators and antennas in highly miniaturized electronic devices.[3,4] There are also other important parameters like dielectric loss tangent (tan δ) and temperature coefficient of dielectric constant (τ_ε). tan δ indicates the energy loss in a dielectric medium when an alternating electric field is applied. τ_ε indicates the variation of dielectric constant of the material with temperature.[5,6]

Several dielectric resonator materials containing Ti such as $Ba_2Ti_9O_{20}$, $MgTiO_3$–$CaTiO_3$, (Zr, Sn)TiO_4, BaO–PbO–Nd_2O_3–TiO_2 etc. with ε_r values ranging from 20 to 150 have been developed for use in various applications.[5] Therefore TiO_2 is an important material in the field of electronic and wireless communication industry. TiO_2 exists in three forms: rutile, brookite, and anatase. Brookite and anatase convert irreversibly to rutile in the temperature range of 700°–920°C. Rutile has a tetragonal structure and also is a semiconductor under certain oxidation states. Sintering temperatures of up to 1500°C are required to attain dense samples of rutile for powders with particle sizes of 0.2–3 μm, although lower sintering temperatures are possible in much-finer powders. In this study, the sintering behaviour of TiO_2 is investigated along with its dielectric properties at radio frequency range. If sintering occurs in an air atmosphere or under low oxygen partial pressure, a slight reduction of TiO_2 occurs. Problems that are associated with titanium-containing ceramics (including reduction) have been highlighted in various

**Corresponding author, Email: shijith.pp@gmail.com*

publications.7-12

Materials and methods

Dense samples of TiO2 were prepared using solid state sintering technique, starting from TiO2 powder (Aldrich Chemicals). The powder is mixed with 6wt% of PVA (molecular weight 22,000, BDH Lab Suppliers), and were pressed into disks of about 11 mm in diameter and ~1 mm in height under a pressure of about 100 MPa. The green compacts were initially fired at a rate of 3 ?C/min up to 600 ?C and then at a rate of 12 ?C/min up to the sintering temperature. An intermediate soaking at 600 ?C for 30 minutes was given to expel the binder. After cooling from the sintering temperature to 1000 ?C at a rate of 2?C/min, the ceramics were cooled inside the furnace naturally. The sintering was carried out at different temperatures in the range 800 – 15000C for 2 h in order to attain maximum density for all the pellets. The temperature corresponding to maximum density has been chosen as the optimized sintering temperature of the sample. The density of the samples was measured by Archimedes method. The structure of the powdered sample is studied by X-ray diffraction using CuKα radiation (Philips X-Ray Diffractometer). The radio-frequency (upto 3 MHz) dielectric properties were measured by a LCR meter (Hioki 3532-50, Japan). This is done by the capacitor method, in which the sample is made into a parallel plate capacitor by pasting Ag on both sides and by connecting Cu leads.

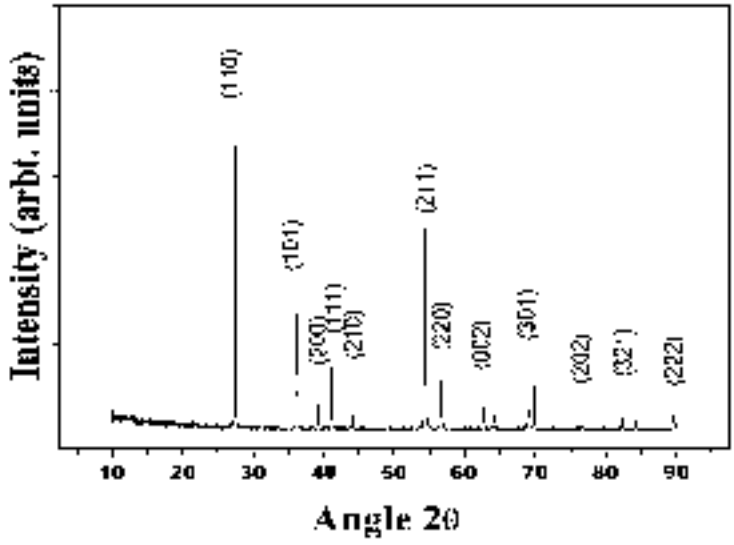

Fig. 1. Powder X-ray diffraction pattern of heat treated TiO_2

The x-ray diffraction pattern of TiO_2 is shown in Fig. 1. The diffraction pattern of TiO_2 is indexed based on ICDD file card no 89-4920. All recognizable reflection peaks could be readily indexed to the tetragonal structure of rutile having lattice parameters of a=4.584(2) ? , c=2.953(1) ? , and belonging to the space group $P4_2/mnm$ (136). Using the lattice parameters, the theoretical density can be calculated, which, in this

case, is found to be 4.276 g/cm^3. The most intense reflection is obtained from the (110) plane and the next one from (211) plane.

Optimization of sintering temperature

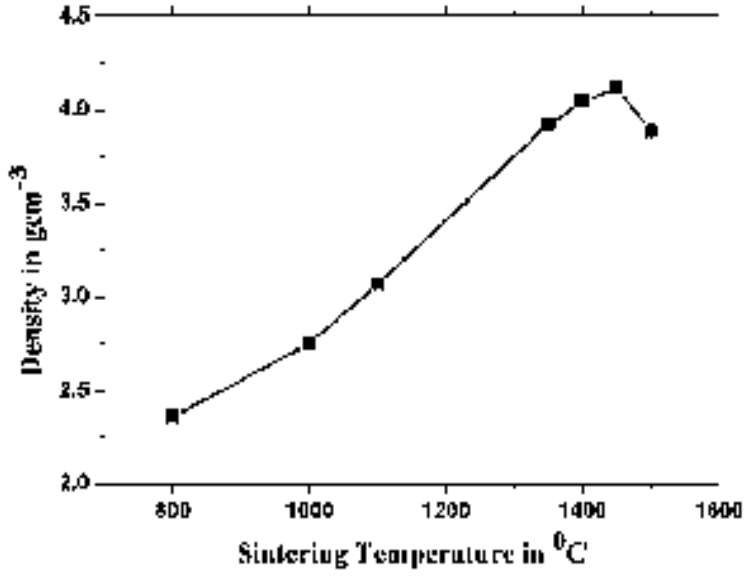

Fig.2. Variation of density of sintered TiO_2 with sintering temperature

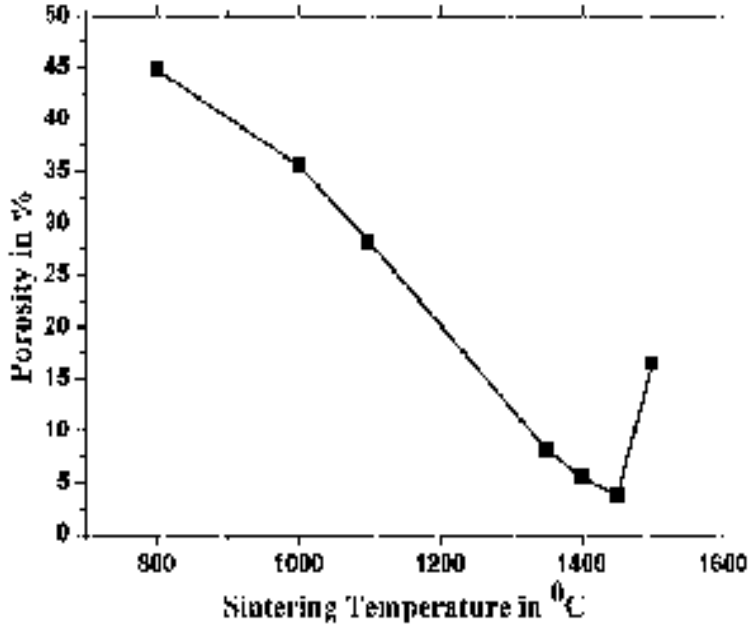

Fig. 2 represents the variations of the density with sintering temperature. The density of TiO_2 is found to be increased with sintering temperature. The increase in sintering temperature enhances grain growth, which results in the elimination of porosity and hence an improvement in density.

Fig. 3. Variation of porosity with sintering temperature

The highest density is achieved of TiO2 is 4.1159 g cm-3, when sintered 1450 0C/2h. It corresponds to a densification of 96.25% of the theoretical value. Further increasing in sintering temperature causes a decreasing density of TiO2. Fig. 3 shows the variation of porosity as a function of sintering temperature. The porosity in the material was calculated by the following expression

$$\frac{(\rho_{th} - \rho_m)}{\rho_{th}} \times 100$$

where ? and ?_m are theoretical and measured densities, respectively. The theoretical density of rutile TiO2 is 4.276 g cm-3.The porosity of TiO2 decreases from 44.8% at 800 0C and reaches a minimum value of 3.74% at a sintering temperature of 1450 0C. Therefore the optimized value of sintering temperature of TiO2 is 1450 oC/2h. Further increase in sintering temperature, however, increases the porosity.

Dielectric properties at radiofrequencies

The dielectric constant of TiO2 as a function of temperature is shown in Fig.4. The dielectric constant increases with sintering temperature and reaches a maximum value of 154.3 at a sintering temperature of 1450oC and thereafter it decreases. The increase in the dielectric constant with sintering temperature can be related to the decrease in the porosity of the samples at 1450oC. Air has r =1, which is very low compared to the dielectric constant of TiO2 phase. Therefore minimum value of porosity corresponds to maximum value of dielectric constant. Usually it is very difficult to obtain the TiO2 samples with 100% densification and hence a correction for porosity is always necessary. Here it is assumed that the material consists of two phases (TiO2 and air) with different values of dielectric constant. The following equation is used for porosity correction of dielectric constant of material

$$\varepsilon_m = \varepsilon_c\left(1 - \frac{3P(\varepsilon_c - 1)}{2\varepsilon_c + 1}\right)$$

where ?_m is the measured ?_r , ?_c is the corrected ?_r and P is the fractional porosity.13 The corrected value of dielectric constant at a sintering temperature of 1450 oC is 162.74. The frequency dependence of dielectric constant (dielectric constant) of sintered TiO2 is shown in Fig. 5. The dielectric constant decreases with frequency as shown in the figure. Relaxation effects are associated with permanent and induced molecular dipoles.5 At low frequencies the field changes slowly enough to allow dipoles to reach equilibrium before the field has measurably changed. Hence the polarization and corresponding dielectric constant will be high. For frequencies at which dipole orientations cannot follow the applied field due to the viscosity of the medium, the polarization will decrease, which decreases the dielectric constant. The absorption of the field's energy also leads to energy dissipation. The mechanism of dipoles relaxing is called dielectric relaxation and for ideal dipoles is described by classic Debye relaxation.

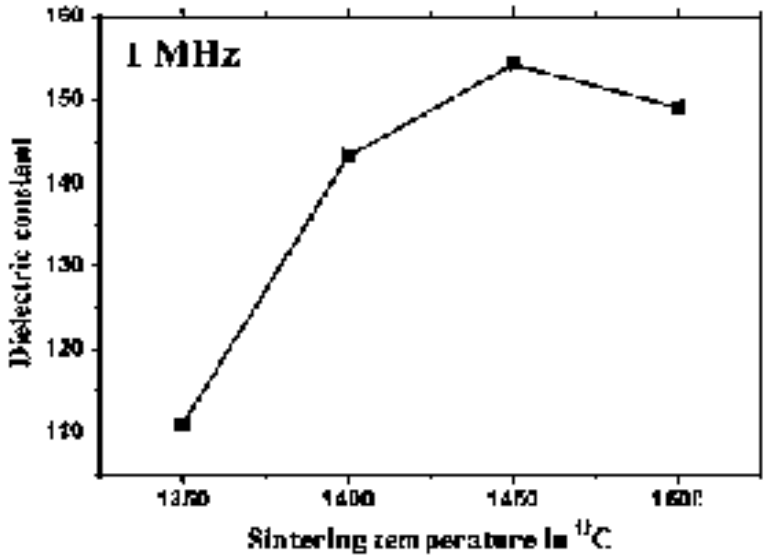

Fig. 4 Variation of dielectric constant with sintering temperature

At low frequencies the effect of interfacial polarization is dominant, which is due to the polarization of free charges accumulated at the interfaces of the samples. As frequency increases, the effect of interfacial polarization decreases leading to an overall degradation of dielectric constant.

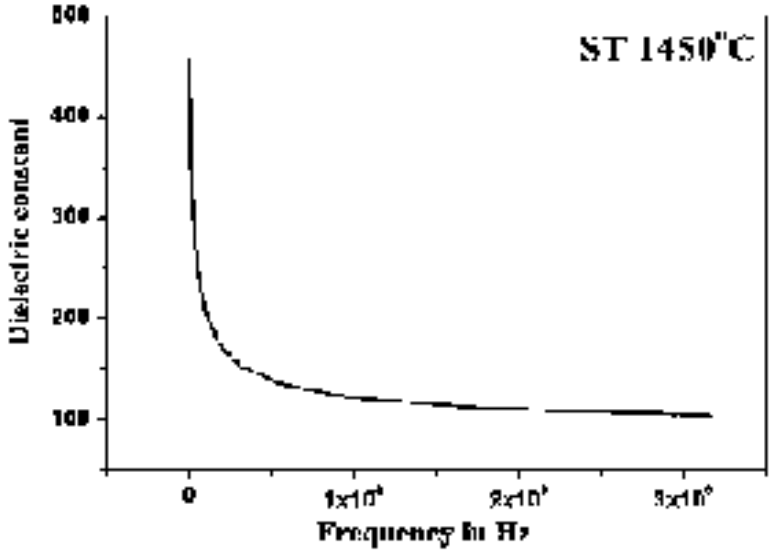

Fig.5. Variation of dielectric constant with frequency of sintered sample at 1450^{0}C

The dielectric loss tangent of the sample sintered at 1450 $^{\circ}$C is found to be 0.13, whereas the loss tangent of dielectrics is of the order of ~10^{-2} to 10^{-3}. The conductivity of TiO_2 sintered at 1450 $^{\circ}$C is found to be 5.8 × 10^{-5}S/cm, which is of the order of semiconductors. If sintering occurs in an air atmosphere or under low oxygen partial pressure, a slight reduction of TiO_2 occurs. Using standard Kroger–Vink notation, this

reduction can be described principally in terms of either the formation of oxygen vacancies (reaction (1)), Ti^{4+} interstitials (reaction (2)), Ti^{3+} interstitials (reaction (3)), or oxygen vacancies and Ti^{3+} species in octahedral lattice sites (reaction (4)):

$$2O_O^x \Leftrightarrow 2V_O^{\cdot\cdot} + 4e' + O_2 \quad \ldots\ldots(1)$$

$$Ti_{Ti}^x + 2O_O^x \Leftrightarrow Ti_i^{\cdot\cdot\cdot\cdot} + 4e' + O_2 \quad \ldots\ldots(2)$$

$$Ti_{Ti}^x + 2O_O^x \Leftrightarrow Ti_i^{\cdot\cdot\cdot} + 3e' + O_2 \quad \ldots\ldots(3)$$

$$2Ti_{Ti}^x - O_O^x \Leftrightarrow 2Ti_{Ti}' + V_O^{\cdot\cdot} + \frac{1}{2}O_2 \quad \ldots\ldots(4)$$

Therefore the TiO_2 samples prepared in this case shows the conductivity of semiconductors. It is reported that metal oxides, such as TiO_2, NiO, and Cr_2O_3, have semiconducting properties.[14,15]

Conclusions

The sintering temperature of TiO_2 was optimized to get maximum density of 4.12 g cm^{-3}, which corresponds to a densification of 96.25 %. The optimized sintering temperature was found to be 1450 ^oC/2h. The X-ray diffraction pattern indicates that, the material has a tetragonal structure of rutile and belongs to the space group $P4_2/mnm$ (136). The dielectric constant at 1 MHz has a maximum value of 154.3 at the optimized sintering temperature of 1450 ^oC/2h. A correction for porosity has also been performed, which is 162.7. It represents the dielectric constant of a 100% dense sample. The dielectric loss tangent of the sample at 1 MHz is found to be 0.13, which is quite unusual for a dielectric material. The conductivity of the sample measured suggests the possibility of a semiconducting phase formation.

Acknowledgement

The authors wish to acknowledge Dr. M.R. Anantharaman, Dept. of Physics, CUSAT, Cochin and Dr. M.T. Sebastian, Materials Division, NIIST (CSIR), Trivandrum for their help and support during the preparation and characterization of the samples.

References

1. Kajfez K., Guillon P., 1986. *Dielectric resonators*, Artech House, Norwood, Massachusetts.
2. Trinogga L. A., Kaizhou G., Hunter J. C., 1991. *Practical Microstrip Circuit Design*, Ellis Horwood, Chichester, UK.
3. Roberts G.L., Cava R.J., Peck W.F., Krajewski J.J., 1997. **Dielectric properties of Barium Titanium Niobates.** *J. Mater. Res.* 12, 526-530.
4. Kingon A.I., Maria J.P., Streiffer S.K., 2000. Alternative dielectrics to silicon dioxide for memory and logic devices. *Nature*. 406, 1032-1038.
5. Sebastian M. T., 2008. *Dielectric materials for wireless communication*, Elseiver Publishers, Oxford, U.K.
6. Joseph T and Sebastian M. T., 2010. Microwave dielectric properties of $(Sr_{1-x}A_x)_2(Zn_{1-x}B_x)Si_2O_7$ ceramics (A=Ca,Ba and B=Co, Mg, Mn, Ni). *J. Am. Ceram. Soc.* 93, 147–154

7. O'Bryan H. M., Thomson J., and Plourde J. K., 1974. A new BaO–TiO_2 compound with temperature-stable high permittivity and low microwave loss. *J. Am. Ceram. Soc.* **57,** 450–53.

8. O'Bryan H. M., Thomson J., and Plourde J. K., 1978. Effects of chemical treatment on loss quality of microwave dielectric ceramics. *Ber. Dtsch. Keram. Ges.* **55,** 348–51.

9. O'Bryan H. M., and Thomson J., 1983. $Ba_2Ti_9O_{20}$ Phase Equilibria. *J. Am. Ceram.Soc.* **66,** 66–68.

10. O'Bryan H. M., 1987. Identification of surface phases on $BaTiO_3$–TiO_2 ceramics. *Am. Ceram. Soc. Bull.* **66,** 677–80.

11. Nomura S., Tomaya K., and Kaneta K., 1983. Effect of Mn doping on the dielectric properties of $Ba_2Ti_9O_{20}$ ceramics at microwave frequencies. *Jpn. J. Appl. Phys.* **22,** 1125–28.

12. Negas T., Yeager G., Bell S., Coats N., and Minis I., 1993. $BaTi_4O_9$/$Ba_2Ti_9O_{20}$-based ceramics resurrected for modern microwave applications. *Am. Ceram. Soc. Bull.* **72,** 80–89.

13. Penn S. J., Alford N. M., Templeton A., Wang X., Xu M., Reece M. and Schrapel K., 1997. Effect of porosity and grain size on the microwave dielectric properties of sintered Alumina. *J. Am. Ceram. Soc.* 80, 1885-1888.

14. Kubaschewski O. and Hopkins B.E., 1967. *Oxidation of metals and alloys*, second ed. Butterworths, London.

15. N. Birks N. and Meier G. H., 1983. *Introduction to high temperature oxidation of metals*, Edward Arnold, London.

SCIENTIA
A National Science Journal

CONTENTS